



DWh[e[a` aXfZW5a` UWbfgS^? aVW^  
aXfZW=dSX'S 9WafZWd\_ S^EkefW\_



LV-2015-040



# Revision of the Conceptual Model of the Krafla Geothermal System



ÍSOR-2015/012, Vatnaskil 15.03

Project no.: 14-0200

October 2015



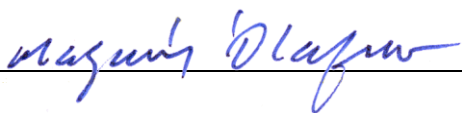
**Key Page****LV report no:** LV-2015-040 **Date:** October 2015**Number of pages:** 111 **Copies:** 8 **Distribution:**  On [www.lv.is](http://www.lv.is)  
 Open  
 Limited until**Title:** Revision of the Conceptual Model of the Krafla Geothermal System**Authors/Company:** Tobias Björn Weisenberger, Guðni Axelsson, Andri Arnaldsson, Anett Blischke, Finnbogi Óskarsson, Halldór Ármannsson, Hanna Blanck, Helga Margrét Helgadóttir, Jean-Claude C. Berthet, Knútur Árnason, Kristján Ágústsson, Sigríður Sif Gylfadóttir and Valdís Guðmundsdóttir**Project manager:** Egill Júlíusson (LV) Magnús Ólafsson (ÍSOR)**Prepared for:** Prepared by Iceland GeoSurvey (ÍSOR) for Landsvirkjun.**Co operators:** Vatnaskil**Abstract:**

This report presents an update of a conceptual model of the Krafla geothermal system from 2009. New data on seismic activity, chemical content (including tracer tests), mass/energy production and reservoir conditions are combined with existing and updated data from previous geological and geophysical studies to revise the conceptual model. Stratigraphic and alteration models have been updated and seismic activity correlated with structures seen in geophysical data and the production/-rejection pattern. Fluid chemistry data reflects the complex hydrological character of the system and chemical patterns are used to revise the classification of Krafla into specific subareas which is supported by a well classification based on changes in well output with time. The revised conceptual model provides the basis of a planned, detailed numerical modal of the Krafla geothermal system.

**Keywords:**

Krafla, conceptual model, geology, seismic activity, geophysical data, fluid chemistry, physical conditions, subareas

**ISBN no:****Approved by Landsvirkjun's  
project manager**

Project manager's signature 	Reviewed by BS
--	-------------------

## Ágrip

Í skýrslunni er fjallað um uppfærslu hugmyndalíkans af jarðhitakerfinu í Kröflu, sem síðast var uppfært 2009. Ný gögn um skjálftavirkni, efnainnihald (þ.m.t. ferilprófanir), massa-/orkuvinnslu og hita- og þrýstingsástand eru tengd tiltækum og uppfærðum gögnum úr eldri jarðfræði- og jarðeðlisfræðirannsóknnum til að uppfæra hugmyndalíkanið. Jarðlaga- og ummyndunarlíkön hafa verið uppfærð og tengsl skjálftavirkni við jarðeðlisfræðileg líkön auk vinnslu/niðurdælingar skoðuð. Efnainnihald jarðhitavökva endurspeglar flókna vatnafræði kerfisins og breytileiki í efnainnihaldi er notaður til að endurskoða flokkun Kröflu í undirsvæði, sem er jafnframt studd af flokkun borholna á grundvelli breytinga á afköstum þeirra með tímanum. Endurskoðað hugmyndalíkanið verður grunnur að flóknu númerísku reiknilíkani sem fyrirhugað er að gera fyrir Kröflu-kerfið.

# Table of contents

<b>1</b>	<b>Introduction.....</b>	<b>11</b>
<b>2</b>	<b>Background and earlier conceptual models.....</b>	<b>12</b>
2.1	Historical background.....	12
2.2	Conceptual model.....	19
2.2.1	Conceptual and numerical models before 2009.....	20
2.2.2	The 2009 conceptual model.....	20
<b>3</b>	<b>Geological overview.....</b>	<b>23</b>
<b>4</b>	<b>Stratigraphy and alteration in Krafla.....</b>	<b>24</b>
4.1	Stratigraphy.....	24
4.1.1	Stratigraphic profiles in the central part of the Krafla caldera.....	25
4.1.2	Stratigraphic profile by the southern edge of the Krafla caldera.....	28
4.2	Alteration.....	29
<b>5</b>	<b>Seismic activity.....</b>	<b>32</b>
5.1	Seismicity October 2013 to October 2014.....	32
5.2	Earthquake distribution.....	34
5.3	Vp/Vs velocity ratio.....	34
<b>6</b>	<b>Geophysics.....</b>	<b>36</b>
6.1	Gravity.....	36
6.2	Resistivity.....	39
<b>7</b>	<b>Chemical composition of reservoir liquid.....</b>	<b>42</b>
7.1	Data set.....	42
7.2	Subarea division.....	43
7.3	Reference temperature.....	44
7.4	Deep liquid composition.....	44
7.5	Subarea characteristics.....	47
7.5.1	Leirbotnar.....	47
7.5.2	Vítismór.....	48
7.5.3	Leirhnjúkur.....	48
7.5.4	Suðurhlíðar.....	48
7.5.5	Vesturhlíðar.....	50
7.5.6	Hvíthólar.....	50
7.5.7	Sandabotnar.....	50
7.6	Origin of recharge to the Námafjall Krafla area.....	57
7.7	Parameters controlling fluid flow.....	58
<b>8</b>	<b>Reservoir conditions and production analysis.....</b>	<b>59</b>

8.1	Temperature conditions .....	59
8.2	Hypothetical modelling of Krafla temperature conditions .....	61
8.3	Enthalpy and production .....	64
8.4	Simple lumped parameter modelling .....	68
8.4.1	Leirbotnar.....	69
8.4.2	Hvíthólar K-21.....	71
8.5	Analysis of production well output.....	72
8.5.1	Estimating well output decay .....	72
8.5.2	Total output decay.....	72
8.5.3	Steam output decay .....	73
8.6	Simulation of geothermal wells .....	78
<b>9</b>	<b>Tracer test results.....</b>	<b>80</b>
<b>10</b>	<b>Summarized results .....</b>	<b>81</b>
10.1	Major new findings since 2009 .....	81
10.2	Main aspects of the revised conceptual model of the Krafla system .....	83
10.3	Conclusions and recommendations .....	86
<b>11</b>	<b>References.....</b>	<b>88</b>
	<b>Appendix.....</b>	<b>99</b>

## List of tables

Table 1.	<i>Wells in the Krafla area.</i> .....	18
Table 2.	<i>Average temperatures and enthalpies for individual wells in the Krafla geothermal system.</i> .....	43
Table 3.	<i>Average deep liquid composition.</i> .....	49
Table 4.	<i>Krafla wells. General trends and average values for subareas.</i> .....	56
Table 5.	<i>Results of the lumped parameter modeling of pressure and production data from Leirbotnar and Hvíthólar.</i> .....	70
Table 6.	<i>Preliminary sets of <math>\alpha_0</math>, <math>\beta_0</math>, <math>\gamma_0</math>, <math>\delta_0</math>, <math>\alpha_1</math>, <math>\beta_1</math>, <math>\gamma_1</math> and <math>\delta_1</math> for the producing wells in Krafla.</i> .....	79

## List of figures

Figure 1.	<i>Historic overview of the Krafla geothermal power plant in the Krafla geothermal system.</i> .....	12
Figure 2.	<i>Geological map of the Krafla area.</i> .....	14
Figure 3.	<i>Legend to geological map</i> .....	15
Figure 4.	<i>Map of the Krafla well-field area showing tectonic features, different well-fields and individual wells.</i> .....	16
Figure 5.	<i>Aerial photo of the Krafla well-field area showing well and subarea locations.</i> .....	17
Figure 6.	<i>Legends for stratigraphic units and detailed well lithology in Figure 7 to Figure 10.</i> .....	26

Figure 7. Stratigraphic cross section from W to E through Leirhnjúkur, Vítismór, Leirbotnar and Suðurhlíðar. ....	26
Figure 8. Stratigraphic cross section from NW to SE through Vítismór, Hveragil and Suðurhlíðar. ....	27
Figure 9. Stratigraphic cross section from W to E through Vítismór and Hveragil. ....	27
Figure 10. Stratigraphic cross section from E to W through Vestursvæði, Hvíthólar and Sandabotnar .	28
Figure 11. Alteration cross section from W to E through Vítismór, Leirbotnar, and Suðurhlíðar. ....	30
Figure 12. Alteration cross section from NW to SE through Vítismór and Suðurhlíðar. ....	30
Figure 13. Alteration cross section from W to E through Vítismór and Vesturhlíðar. ....	31
Figure 14. Alteration cross section from W to E through Vestursvæði, Hvíthólar, and Sandabotnar. ....	31
Figure 15. Earthquake locations and E-W and N-S sections. ....	32
Figure 16. Depth distribution of earthquakes on cluster a) to e). ....	33
Figure 17. Vp/Vs ratio in Krafla and surrounding crust. ....	35
Figure 18. De-trended Bouguer gravity map (mgals) of the Krafla volcano. ....	36
Figure 19. Lithological section based on wells, from north to south within the Krafla caldera . ....	38
Figure 20. Faults and fissures in the Krafla fissure swarm and eruptive fissures and craters . ....	39
Figure 21. Resistivity at 200 m a.s.l. based on TEM soundings. ....	40
Figure 22. Elevation (km above sea level) of the upper boundary of deep conductors in the Krafla volcanic complex as seen by 1D inversion. ....	41
Figure 23. Resistivity at 1.25 km b.s.l. in the Krafla volcanic complex according to 3D inversion of MT. ....	42
Figure 24. Correlation of calculated temperatures by using different geothermometers . ....	45
Figure 25. Silica content of discharge from the excess enthalpy wells against discharge enthalpy. ....	46
Figure 26. Evolution of pH in the deep liquid. ....	51
Figure 27. Concentration of silica in the deep liquid. ....	51
Figure 28. Concentration of boron in the deep liquid. ....	52
Figure 29. Concentration of hydrogen in the deep liquid. ....	52
Figure 30. Concentration of carbon dioxide in the deep liquid. ....	53
Figure 31. Concentration of hydrogen sulfide in the deep liquid. ....	53
Figure 32. Concentration of chloride in the deep liquid. ....	54
Figure 33. Concentration of fluoride in the deep liquid. ....	54
Figure 34. Concentration of sulphate in the deep liquid. ....	55
Figure 35. Concentration of calcium in the deep liquid. ....	55
Figure 36. Concentration of sodium in the deep liquid. ....	56
Figure 37. Proposed groundwater flow to the Námafjall and Krafla geothermal systems . ....	57
Figure 38. A WNW-ESE cross-section through the temperature model for the Krafla system. ....	60
Figure 39. A NW-SE cross-section through the temperature model for the Krafla system. ....	60
Figure 40. A WNW-ESE cross-section through the temperature model for the Krafla system . ....	61
Figure 41. Thermo-hydraulic state of a geothermal system 3000 years after emplacement of an 800 m wide “dike” intrusion extending up to 2.45 km below surface. ....	63

Figure 42. Average total mass production per year and weighted yearly mean enthalpy for all Krafla production wells.....	65
Figure 43. Hvíthólar average mass production per year and weighted yearly mean enthalpy .....	65
Figure 44. Leirbotnar lower system average mass production per year and weighted yearly mean enthalpy.....	66
Figure 45. Leirbotnar upper system average mass production per year and weighted yearly mean enthalpy.....	66
Figure 46. Suðurhlíðar average mass production per year and weighted yearly mean enthalpy.....	67
Figure 47. Vesturhlíðar average mass production per year and weighted yearly mean enthalpy.....	67
Figure 48. Vítismór average mass production per year and weighted yearly mean enthalpy.....	68
Figure 49. Pressure and production data for Leirbotnar;.....	70
Figure 50. Pressure and production data for Hvíthólar .....	71
Figure 51. The estimated total output decay in % per year for 20 wells in the Krafla caldera. ....	73
Figure 52. Total output decay plotted against feed zone depth in the wells analyzed in this section. ....	74
Figure 53. The estimated steam output decay in % per year for 20 wells in the Krafla caldera. ....	75
Figure 54. Steam output decay plotted against feed zone depth in the wells analyzed in this section. ....	75
Figure 55. Total output decay of selected wells mapped onto the surface of the Krafla geothermal field. .	76
Figure 56. Steam decay of selected wells mapped onto the surface of the Krafla geothermal field. ....	77
Figure 57. The well-head pressures calculated by WellSim are fitted at constant enthalpy to find $a_0$ and $b_0$ for a given enthalpy.....	78
Figure 58. Regression analysis of $a_0$ and $b_0^2$ versus enthalpy used to determine $\alpha_0$ , $\beta_0$ , $\gamma_0$ and $\delta_0$ for well K-31.....	80

## List of figures in Appendix

Figure A 1. Enthalpy vs. time of each well included in this study in Vítimór. ....	99
Figure A 2. Enthalpy vs. time of each well included in this study in Vesturhlíðar.....	99
Figure A 3. Enthalpy vs. time of each well included in this study in Suðurhlíðar.....	100
Figure A 4. Enthalpy vs. time of each well included in this study in Leirhnjúkur. ....	100
Figure A 5. Enthalpy vs. time of each well included in this study in Leirbotnar. ....	101
Figure A 6. Enthalpy vs. time of each well included in this study in Hvíthólar. ....	101
Figure A 7. Enthalpy, output and steam decay in well K-5. ....	102
Figure A 8. Enthalpy, output and steam decay in well K-8. ....	102
Figure A 9. Enthalpy, output and steam decay in well K-9. ....	103
Figure A 10. Enthalpy, output and steam decay in well K-14. ....	103
Figure A 11. Enthalpy, output and steam decay in well K-15. ....	104
Figure A 12. Enthalpy, output and steam decay in well K-16A.....	104
Figure A 13. Enthalpy, output and steam decay in well K-17. ....	105
Figure A 14. Enthalpy, output and steam decay in well K-19. ....	105
Figure A 15. Enthalpy, output and steam decay in well K-10. ....	106

Figure A 16. *Enthalpy, output and steam decay in well K-21.* ..... 106

Figure A 17. *Enthalpy, output and steam decay in well K-22.* ..... 107

Figure A 18. *Enthalpy, output and steam decay in well K-24.* ..... 107

Figure A 19. *Enthalpy, output and steam decay in well K-30.* ..... 108

Figure A 20. *Enthalpy, output and steam decay in well K-31.* ..... 108

Figure A 21. *Enthalpy, output and steam decay in well K-32.* ..... 109

Figure A 22. *Enthalpy, output and steam decay in well K-33.* ..... 109

Figure A 23. *Enthalpy, output and steam decay in well K-34.* ..... 110

Figure A 24. *Enthalpy, output and steam decay in well K-36.* ..... 110

Figure A 25. *Enthalpy, output and steam decay in well K-37.* ..... 111

Figure A 26. *Enthalpy, output and steam decay in well K-40.* ..... 111



# 1 Introduction

This report presents the results of a revision of the conceptual model of the Krafla geothermal system in NE-Iceland carried out in preparation for the development of a new numerical reservoir model of the system. The revision has been carried out by ÍSOR (Iceland GeoSurvey) and Vatnaskil Consulting Engineers (Vatnaskil), under a contract between Landsvirkjun on one hand and ÍSOR and Vatnaskil on the other. A comprehensive upgrading of the conceptual of the Krafla geothermal system was carried out during 2007–2009 (Mortensen et al., 2009a), which provides the basis for the present revision. Additional information on the Krafla system has been gathered since then, both through additional geo-scientific research and through monitoring the output of production wells and the response of the geothermal system to that production. Special emphasis has been placed, in the present work, on aspects of the conceptual model, which are relevant for the planned numerical reservoir model.

The first complete conceptual model of the Krafla geothermal system was presented in 1977, at the time the Krafla power plant started operating (Stefánsson et al., 1977). That model was based on limited exploration data as well as data from the first 11 wells drilled. Up to 2009, when the latest conceptual model revision was completed, the conceptual model was revised a few times, mainly based on the results of drilling and production monitoring. This was done systematically in conjunction with the development of numerical reservoir models of Krafla during the last two decades of the 20<sup>th</sup> century.

Numerical models of the Krafla geothermal system have been set up during four occasions, prior to the one now being prepared. The first model was developed in the early eighties by Böðvarsson et al., (1982, 1984). It was developed as two separate models; a natural state model and a production model, and was quite simple in comparison to present-day numerical models as numerical modeling of geothermal system was then a new approach in geothermal reservoir engineering. In the late eighties a two-dimensional model of the Hvíthólar subarea of Krafla was developed, which was a few years later expanded to a 3-dimensional numerical model (Tulinus and Sigurðsson, 1988, 1991). The most complex numerical model of Krafla developed to date was developed during 1996–1999, being a 3-dimensional model covering the whole Krafla geothermal system (Björnsson et al., 1997).

This report starts out by reviewing the development history of Krafla along with the general aspects of conceptual model development and the main features of the 2009 conceptual model of Krafla (chapter 2). Following that (chapter 3) a geological overview of the Krafla volcanic and geothermal system is given. Chapters 4–9 present the results of re-evaluation of older data and interpretation of new data, separately for each scientific discipline involved in geothermal research in Krafla. The report is concluded by a summary of new findings and synopsis of the main aspects of the new revision of the conceptual model of the Krafla geothermal system.

## 2 Background and earlier conceptual models

### 2.1 Historical background

The Krafla region has long been known for the volcanic and geothermal activity. The first geothermal research study was conducted in 1969 (Björnsson, 1969) (Figure 1). Preliminary results were published by Guðmundsson et al. (1971) who investigated an area of 280 km<sup>2</sup>, with main emphasis on the examination of the Krafla and Námafjall areas. Aeromagnetic maps were produced and the geothermal system was estimated to be at temperature of 200–300 °C. During 1971 and 1972 resistivity surveying was conducted (Guðmundsson et al., 1971; Karlsdóttir et al., 1978).

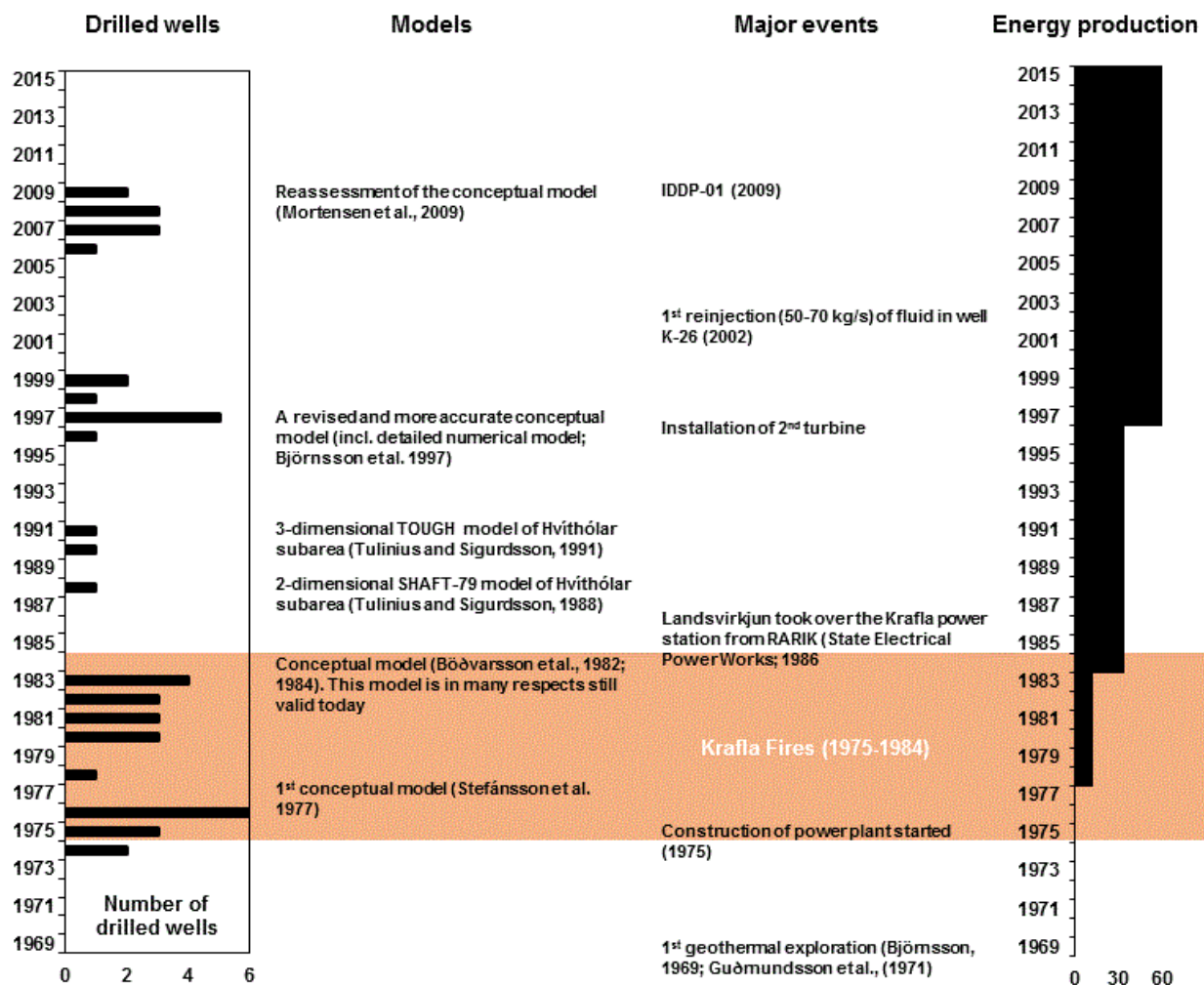


Figure 1. Historic overview of the Krafla geothermal power plant in the Krafla geothermal system.

During the next few years, Krafla became a benchmark in the domestic power industry when major protests arose against the expansion of the Laxá power station. The Laxá idea was waved, but search began for alternative energy production in northeast Iceland. Therefore, the Krafla area was selected for the first major electrical geothermal power plant in Iceland. The first two exploration wells were drilled down to 1200 m depth in 1974 and production drilling began a year later. In the same year, the National Energy Authority (Orkustofnun) published the results of the exploratory drilling (Sæmundsson et al., 1975). It was the first data collection for the geothermal reservoir in Krafla with respect to the decision to build a 60 MW<sub>e</sub> geothermal power plant. Construction of the power plant and production drilling started in 1975 and concurrently the 1975–1984 Krafla volcanic episode (Krafla Fires) started. Ongoing construction, exploration and drilling took place during the following years, in the shadow of the Krafla fires. Six production wells were drilled in 1976, and borehole- and surface exploration continued. Important knowledge of the reservoir was revealed in the Leirbotnar area, which could apparently be divided into two systems (upper and lower) with different production characteristics (Stefánsson et al., 1977).

In 1978, electricity generation began with an initial production of 7 MW<sub>e</sub> and an additional steam well was drilled. Because of problems due to the influence of the volcanic activity on steam production, extensive studies on the fumarolic steam flow at Krafla were carried out. Samples were taken from almost all steam vents and natural outflows.

The research results indicated changes in the proportion of magmatic gases in steam in the Krafla area (Gíslason et al., 1978; Ármannsson et al., 1981). This applied to the Leirbotnar subarea (including Vítismór) whereas in Hvíthólar and Sudurhlíðar no magmatic gas influence appeared. During 1980–1983, 13 wells were drilled, two of which were directional wells. A year later, one of two generators in Krafla was finally operated at full 30 MW<sub>e</sub>. In early 1986, Landsvirkjun took over the Krafla power station from RARIK (State Electrical Power Works).

Maintenance and minor exploration continued the following years, and during 1990–1993 a new investigation period began. Two new wells (K-25 and K-26) were drilled, to examine whether conditions in the deep parts of the geothermal system Leirbotnar/Vítismór had improved and resistivity surveying was conducted (TEM method). In spite of the diminishing effect of magmatic gas within the geothermal system, a decision was made in 1996 to proceed with the development of the Krafla power plant, and the second generator was set up to double the performance of the power plant. Drilling to provide steam for the second generator began during the second half of 1996, and in 1999 drilling of eight production wells was completed. The drilling results were overall good and the Krafla power plant was fully operational in 1999. In 2000 it was decided to conduct TEM resistivity measurements for the whole Krafla area. At the same time, plans involving the expansion of the Krafla power plant by 40 MW<sub>e</sub> were initiated. However, the project was put on hold because there was no need for the additional energy to power the economy at the time.

A milestone in the operation of Krafla occurred in 2002 when reinjection (50–70 kg/s) of fluid down to more than 2000 m depth in borehole K-26 was initiated. The same year, scale inhibitor equipment was inserted in well K-28.



# KRAFLA

## JARÐFRÆÐIKORT / GEOLOGICAL MAP

### SKÝRINGAR / LEGEND



### STADSETNINGARKORT / KEYMAP



Tilvísun korta: Kristján Samundsson  
Krafla Jarðfræðikort, 1:25.000  
Landsvirkjun og lösmælar orkusamráðgjafi.  
Útgefandi: Landsvirkjun og lösmælar orkusamráðgjafi.  
Höfundur: Kristján Samundsson.  
Kortgerð: Guðrún Siglífur Jónsdóttir.  
Úrnið í landfræðilegu upplýsingakerfi (ArcInfo),  
Gisværktúla Landsvirkjun og lösmælar orkusamráðgjafi.  
Útgefið: 2008

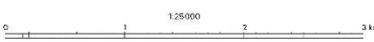
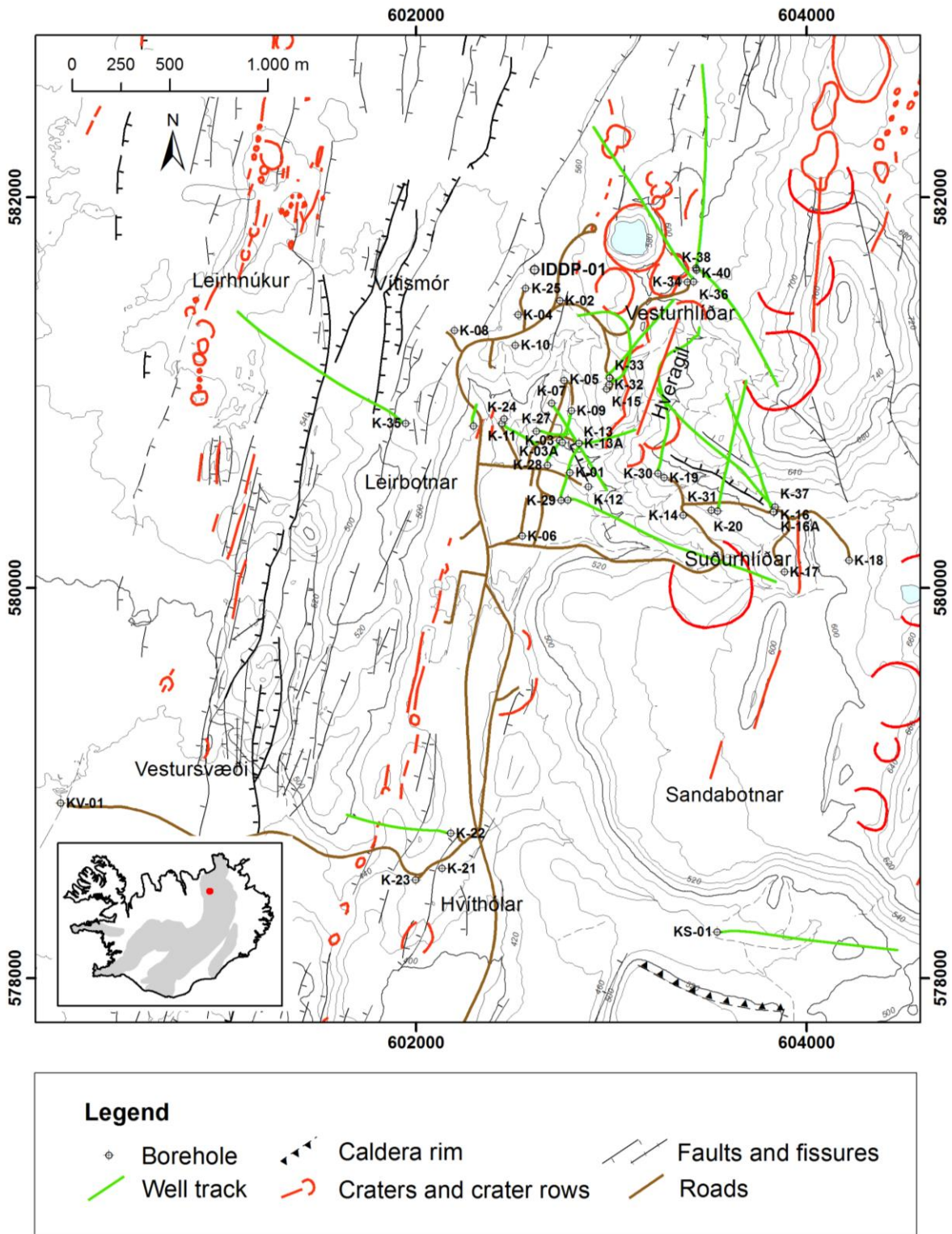


Figure 3. Legend to geological map (Figure 2).



**Figure 4.** Map of the Krafla well-field area showing tectonic features, different well fields and individual wells.

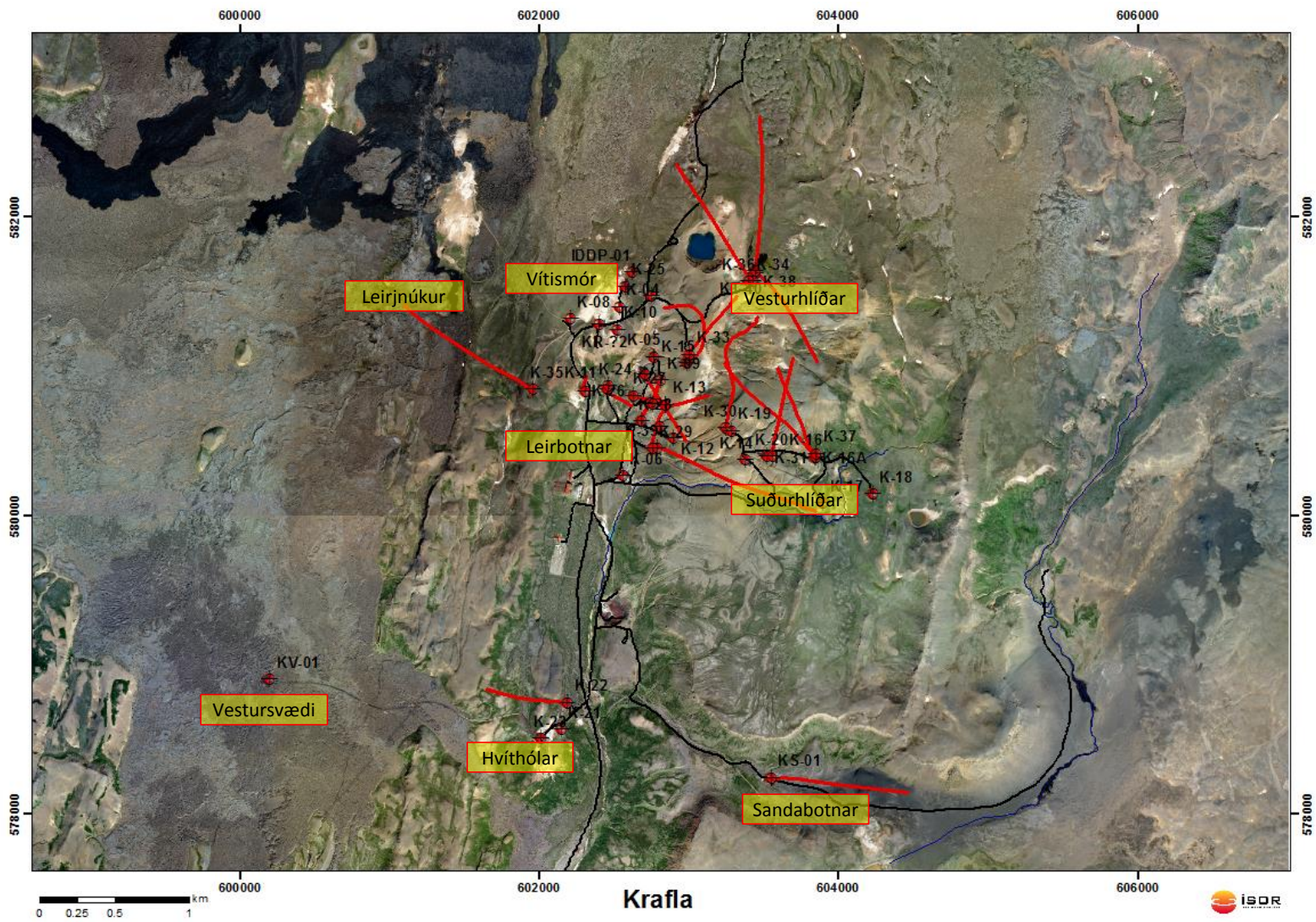


Figure 5. Aerial photo of the Krafla well-field area showing well and subarea locations.

**Table 1. Wells in the Krafla area.**

Well-name	ID no	Well field	Year	x	y	z	Total depth	Anchor casing	Production casing	Liner	Design	Condition	Additional Information
K-01	58001	Leirbotnar	1974	602789	580590	482	1138	80	227.5	1132.5	vertical	abandoned	
K-02	58002	Vítismór	1974	602736	581470	553.5	1204		299	910.5	vertical	abandoned	
K-03	58003	Leirbotnar	1975	602734	580753	499.8	1720	114.2	604.2	1671.1	vertical	abandoned	
K-03A	58103	Leirbotnar	1983	602748	580744	499.9	985	331.9	663.4		vertical	offline	possible reinjection well
K-04	58004	Vítismór	1975	602524	581397	549	2000	113.4	593.6		vertical	abandoned	
K-05	58005	Leirbotnar	1975	602760	581068	523	1299	114.4	642.9		vertical	in production	
K-06	58006	Leirbotnar	1976	602544	580265	464.5	2000	142.3	576.2	1936.3	vertical	offline / monitoring	could be used for production
K-07	58007	Leirbotnar	1976	602694	580944	509	2165	276	808.9	2106.2	vertical	abandoned	
K-08	58008	Vítismór	1976	602196	581317	535	1658	141.9	537	1645.9	vertical	abandoned	
K-09	58009	Leirbotnar	1976	602796	580906	522	1280	274.9	1074	1264	vertical	offline	1977 deepened 163 m to 1264; 1982 redrilled to 1280 m
K-10	58010	Vítismór	1976	602510	581242	542	2082	275.3	805.5	2060	vertical	abandoned /- monitoring	
K-11	58011	Leirbotnar	1976	602440	580841	483.2	2217	275	788.4	2193.5	vertical	offline /- monitoring	
K-12	58012	Leirbotnar	1978	602883	580516	487	2222	282.8	985.3	2213.8	vertical	abandoned	
K-13	58013	Leirbotnar	1980	602834	580739	505	2050	279.1	1057.9	2018	vertical	blocked	side tracking
K-13A	58113	Leirbotnar	1983	602834	580739	505	1780			1698.5	directional	in production	
K-14	58014	Suðurhlíðar	1980	603367	580371	571.1	2107	206.5	699.1	2094.9	vertical	in production	
K-15	58015	Leirbotnar	1980	602975	581017	571	2097	290.2	1086.6	2093.3	vertical	offline	
K-16	58016	Suðurhlíðar	1981	603829	580387	609.3	1981	201.3	662.1	1946.4	vertical	blocked	side tracking
K-16A	58116	Suðurhlíðar	1997	603829	580387	609.3	2191		662.1	2171.8	directional	in production	
K-17	58017	Suðurhlíðar	1981	603886	580081	593.1	2190	201.3	685.3	1958.9	vertical	in production	
K-18	58018	Suðurhlíðar	1981	604217	580140	611	2215	193.3	662.6		vertical	offline / monitoring	
K-19	58019	Suðurhlíðar	1982	603270	580564	584.2	2150	195.1	642.1	2004.8	vertical	in production	
K-20	58020	Suðurhlíðar	1982	603544	580392	584.4	1823	206.3	641.3	2020.4	directional	in production	
K-21	58021	Hvithóll	1982	602134	578563	448.2	1200	23.5	281.4	1035.6	vertical	in production	repair in 1984 with 9 5/8" casing and liner
K-22	58022	Hvithóll	1983	602177	578743	446.9	1876	150.3	558.6	1845.9	directional	offline	
K-23	58023	Hvithóll	1983	601997	578504	446.1	1968	186	529.7		vertical	blocked	
K-24	58024	Leirbotnar	1988	602439	580861	483.2	1400	54.9	405.6	1196.2	vertical	in production	
K-25	58025	Vítismór	1990	602562	581533	549.9	2105	389.4	1144.6	2089	vertical	blocked	Cement and drillpipes at ~1150 m depth.
K-26	58026	Leirbotnar	1991	602295	580829	490	2127	417.9	1199.8	2114.4	vertical	reinjection	
K-27	58027	Leirbotnar	1997	602616	580802	486.2	1771	376.3	1093.8	1744.5	vertical	in production	
K-28	58028	Leirbotnar	1996	602673	580628	475.3	1003	2.8	55.8	973.5	vertical	offline	
K-29	58029	Leirbotnar	1997	602744	580447	471.1	2103	388.6	997.2	2076	directional	blocked	
K-30	58030	Suðurhlíðar	1997	603238	580584	584.2	2054	280.6	804.6	1787	directional	in production	
K-31	58031	Suðurhlíðar	1997	603511	580397	584.6	1440	294	780	1387	vertical	in production	
K-32*	58032	Vítismór	1998	602988	581039	571.8	1875	286	1069.5	1832	directional	in production	
K-33	58033	Vesturhlíðar	1999	602990	581074	571.8	2011	307.8	1103.3	1869	directional	in production	
K-34	58034	Vesturhlíðar	1999	603390	581566	603.1	2002	365	1021	1984.8	vertical	in production	
K-35	58035	Leirhnjúkur	2007	601951	580842	538.7	2508	261.3	1286.1	2480.3	directional	offline	
K-36†	58036	Vesturhlíðar	2007	603420	581567	604.4	2501	289.6	1102.9	2432.6	directional	in production	Cemented up to ~1700 m
K-37	58037	Suðurhlíðar	2008	603838	580416	609.3	2194	228.8	759.4	2186	directional	in production	
K-38‡	58038	Vesturhlíðar	2008	603435	581626	605	2700	299.3	1038.4	2640.4	directional	in production	
K-39	58039	Suðurhlíðar	2008	602777	580451	471	2865	289	973.3	2614.4	directional	reinjection	Cemented up to ~2612 m, blocked at ~1600 m
K-40	58040	Vesturhlíðar	2009	603433	581638	607	1468	300.9	999	1366	directional	in production	
KV-01	58701	Vestursvæðið	2006	600184	578899	475	2894	278.4	795.9	2878.2	vertical	offline	
KS-01	58801	Sandabotnar	2007	603541	578238	473	2502	272.2	891.7	2445.2	directional	offline	
IDDP-01	28501	Vítismór	2009	602607	581630	549	2104	791.5	1958.2	2080	vertical	reinjection	

\* was classified into subarea Vítismór-Vesturhlíðar by Mortensen et al. (2009a)

† was classified into subarea Vítismór by Mortensen et al. (2009a)

‡ was classified into subarea Vítismór-Vesturhlíðar by Mortensen et al. (2009a)

## 2.2 Conceptual model

A conceptual model is a descriptive or qualitative model of a geothermal system that incorporates the essential physical features of the system and is capable of matching the salient behavior or characteristics of interest to the modeler (Grant et al., 1982).

In general, this model estimates the heat content of the reservoir system, the upward flow of geothermal fluids and the total flow in the system. A conceptual model is a model made of the composition of concepts, which are used to help people know, understand, or simulate a subject the model represents. In order to make the conceptual model of a geothermal system it is necessary to screen all available data, and data interpretation, and view them in their context. The following key data, available for Krafla, are used in the construction and revision of the corresponding conceptual model Mortensen et al. (2009a).

- Surface geology, including data about the geology, geothermal manifestations and structures.
- Geophysical measurements, in particular resistivity surveying by TEM and MT methods, and in addition magnetic and gravity measurements.
- Chemical composition of liquid water and steam from natural manifestations.
- Locations of micro-earthquakes
- Borehole geology.
- Temperature and pressure measurements from wells and information on the main feed zones in each well.
- Well tests, e.g. injection and discharge test data.
- Changes of pressure and temperature in the geothermal system during utilization.
- Chemical compositions of well fluids and their changes over time in response to utilization.
- Effects on energy reserves and utilization life time.

The main features of a conceptual model of the geothermal system are intended to show the following:

- Geology of individual stratigraphic layers in the region, possible fractures, faults and other structures that may affect the flow of fluids in the geothermal system.
- Initial temperature and pressure conditions.
- Variations within the system based on the chemical content of liquid and steam, and other factors.
- Location of inflow into the geothermal system, upflow and outflow zones.
- Area size and thickness.
- Assessment of reservoir permeability, porosity and other related factors.
- Boundary conditions for mathematical model.
- The effect of reinjection into the geothermal system and on its utilization.

### **2.2.1 Conceptual and numerical models before 2009**

Conceptual models of the Krafla reservoir and geothermal system, respectively have been presented several times since the investigation of the area began. Stefánsson et al. (1977) presented the first conceptual model of the geothermal system. The model was based on limited data (temperature distribution), mainly surface exploration studies and the results of the first eleven wells drilled in the area (Stefánsson, 1980, 1981). The next conceptual model by Böðvarsson et al. (1982, 1984) gave a clearer picture of the geothermal system east and west of Hveragil. This model is in many respects still valid today. In 1988 a two-dimensional SHAFT-79 model of the Hvíthólar subarea in Krafla, which includes wells K-21, K-22, and K-23 (Tulinus and Sigurðsson, 1988), was set up and during 1990–1991 a three-dimensional TOUGH model of the same area was created (Tulinus and Sigurðsson, 1991). A revised and more accurate conceptual model was presented in the context of a detailed numerical model of the geothermal system in 1996–1997 (Björnsson et al., 1997, 1998).

Besides the geothermal exploration in Krafla, an extensive and significant geological and volcanological research was carried out in the area following the Krafla Fires. This included research on the volcanic system, on the fissure system north and south of Krafla and on crustal deformation in the area (Johnson et al., 1980; Einarsson, 1991; Sæmundsson, 1991; Björnsson and Eysteinnsson, 1998). These studies have added more information and understanding on the type and nature of the Krafla geothermal system and geothermal systems in Iceland in general.

According to a previous volumetric resource assessment the Krafla geothermal system can generate energy of 590 PJ ( $\text{PJ} = 10^{15}\text{J}$ ), which corresponding to almost 380  $\text{MW}_e$  for 50 years or 190  $\text{MW}_e$  to 100 years (Pálmason et al., 1985).

### **2.2.2 The 2009 conceptual model**

The Krafla area is one of the larger geothermal areas in Iceland. It is an active volcanic system believed to host a relatively shallow magma chamber. The last volcanism occurred there during the Krafla Fires (1975–1984). More than 20 years passed since the first steps of development until the power plant reached full capacity of 60  $\text{MW}_e$ . A proposed increase in power generation corresponding to a 150 MW capacity required further exploration and drilling, which was mostly conducted up to 2009, including the exploration of new potential production areas. This required a reassessment of the conceptual model and a new geothermal assessment, which was presented by Mortensen et al. (2009a).

Location of the Krafla geothermal system within a caldera on the central plate boundary increases the likelihood of good rock permeability. However, the interaction of heat, pressure, and permeability causes variable conditions within the system. Various constraints affect the possible expansion, mainly the effects of magmatic gases, but also variable permeability, varying pressure drawdown and variable temperature.

In their report, Mortensen et al. (2009a) summarize their main findings and present a revision of the conceptual model of the geothermal system. The main parameters of the geothermal system were evaluated and the older volumetric assessment of the Krafla geothermal system was recalculated.

The main results of the volumetric assessment that neither takes into account the effects of variable permeability, induced inflow due to pressure drawdown, nor existing chemical and technical difficulties while utilizing the deeper parts of the system:

- The size of the geothermal area was estimated to be 48 km<sup>2</sup> according to resistivity measurements, but as drilling has shown that parts of the system have cooled down; the net size of the area was estimated to be 40 km<sup>2</sup>.
- Based on these dimensions, estimated rock temperature, reservoir thickness, and other factors, the recoverable geothermal energy above 170 °C down to 3 km depth within the geothermal system was estimated in the range from 1.5 EJ (10<sup>18</sup> J or 10<sup>9</sup> GJ) up to 4.5 EJ (90% confidence interval).
- Given a 12% efficiency of electrical energy production, the capacity of the reservoir was estimated in the range of 120–350 MW<sub>e</sub> (90% probability range) for 50 years.

The results of the geothermal assessment indicated that sufficient energy was present in the geothermal system to meet the planned expansion of the Krafla power station at the time. If excessive utilization is conducted temporarily in the area, it will subsequently reduce the sustainable utilization.

Although a great amount of energy exists in the geothermal system various limitation exist, as the utilization experience of the past few decades has shown, for which no technical solutions have been found yet. These mainly include the impact of “magmatic gases” (acidic gases) but also include variations in permeability, pressure drawdown and temperature in the different subareas. Good productivity has been limited to certain parts of the geothermal system, i.e. Leirbotnar, Vítismór, Suðurhlíðar, Vesturhlíðar, and Hvíthólar. Because of the planned expansion of the plant, other areas have also been investigated, especially Sandabotnar, Leirhnjúkur, and finally Vestursvæðið. Following conclusions have been drawn regarding further utilization of these areas:

- In the upper Leirbotnar and Vítismór fields pressure had dropped slightly up to 2009, or about 3–7 bar since utilization began. This indicates that the upper system in these zones can sustain increased production of low-pressure steam.
- There have been great changes (boiling due to pressure drop) in lower Leirbotnar and Vítismór reservoirs since energy production from the Krafla system began. It is believed that they are also not fully utilized. Drilling has shown that acidic geothermal fluids (mainly HCl) still prevent further geothermal utilization below 2000 m, to some extent, in these areas. It is therefore essential that a technical solution is found on how to utilize superheated and HCl-rich vapor. Two wells, K-39 and IDDP-1, have been drilled into magma, at ~2100 m in Vítismór and ~2500 m under Sandabotnafjall. It implies a certain risk, but so far 22 wells have been drilled down more than 2000 m depth in Krafla.
- In Suðurhlíðar pressure has dropped significantly up to 2009, probably about 20–30 bar in the center of the area. It is consistent with the performance of wells, which were declining in output steadily over time. In addition, the performance of new wells proved to be lower than the permeability of the wells suggested (K-31 and K-37). This is believed to be caused by the limited natural inflow into this part of the geothermal system. It does not seem possible to

increase production in the region, unless reinjection will be started, which will partly supplement natural inflow.

- In the decade up to 2009 the Vesturhlíðar subarea became one of the main production areas in Krafla. Limited information is available on pressure changes there, with the exception of well K-34, which did show a pressure decrease. Possible further utilization areas are believed to be located east and northeast under Mt. Krafla as well as in Hveragil. Vesturhlíðar is probably linked to some extent to Suðurhlíðar and reinjection in Suðurhlíðar could have a positive impact on the pressure conditions in Vesturhlíðar.
- Hvíthólar is limited by size as well as capacity. Since the pressure there had dropped by 20–25 bar in 2009 it is not considered possible to increase the output of the area significantly, but it could change if possible connections are found to other sub-areas.
- The presence of a hydrothermal system with good permeability and some production capability had been confirmed in Sandabotnar where MT measurements indicated heat and/or up-flow. This system, or sub-system, seems to stretch to the north along fractures and fissures according to surface and TEM-resistance measurements. It is therefore appropriate to examine in detail whether there is potential there for new wells. It is considered likely that fluids are suitable for utilization, as it is less likely that acidic fluids are present, because of the large distance from the Krafla magma chamber. It is also worth noting the potential connection of Sandabotnar to Hvíthólar in the west, along the rim of the Krafla caldera.
- It is appropriate to examine whether the Krafla utilization area may be expanded to the northern territory, i.e. the area north of Víti and between Krafla and Graddabungu. Analytical result of fluids from well K-38 showed still an influence of magmatic gases in this area. However, it would be appropriate to try to find permeable fractures near the volcanic fissures north of Mt. Krafla. With increasing distance from the postulated magma chamber, there will be reduced risk of acidic gases.
- A high temperature fracture system with good permeability has been confirmed by drilling, just south of Leirhnjúkur. The system there is still under the influence of magmatic gases at a depth below 2000 m. Above the proposed magma chamber, superheated and HCl-rich gases are likely, but exploration of the fissure north and south of Leirhnjúkur should result in lower magmatic gases. On the other hand, the probability of fissures that have cooled down increases to the north and south of Leirhnjúkur, as drilling in Vestursvæði has indicated. The area of Leirhnjúkur is proposed as another major up-flow zone in the geothermal system. According to resistivity measurements it may probably become one of the main utilization areas, after a technical solution has been found for utilizing or preventing the formation of acidic geothermal fluids. It has been pointed out that to the west of Leirhnjúkur, the area around Hvannstóð and Krókóttuvötn, may well be usable for utilization as resistivity measurements did indicate. A major geothermal alteration surface is found there, which has now been cooled. No drilling has been conducted there yet.
- In general, it should be pointed out that reinjection of fluids can play a key role in the development and utilization of the geothermal reservoir. Because of the great amount of energy present in the system, reinjection can help to retrieve some of this, as well as help to

maintain the pressure in the system. It was also considered worth pointing out the importance of energy efficiency, for example, with a binary energy cycle.

### 3 Geological overview

The Krafla central volcano is located within the neo-volcanic North-Iceland Rift Zone (Figure 2 and Figure 3). The volcano is approximately 20 km in diameter. The Krafla geothermal field is located in an eroded, collapsed and partly filled caldera  $8 \times 10$  km in diameter. A NNE–SSW oriented and 90 km long fissure swarm that marks the North Iceland Rift Zone bisects the caldera. Within the caldera a prominent NW–SE elongated geothermal area is present covering approximately 10 km<sup>2</sup> (Sæmundsson, 1991, 2008). The Krafla volcano is an active volcano with recurring volcanic episodes, which in the Holocene predominantly have been in the form of fissure eruptions. The volcanic activity has been centered in the eastern part of the fissure swarm during the past 3000 years occurring with a frequency of 300–1000 years (Sæmundsson, 1991). The caldera is largely filled by basaltic lavas and hyaloclastites. Rhyolites has erupted periodically in minor volumes forming subglacial rhyolitic ridges that are found mainly at or outside the margins of the caldera. Intermediate composition lavas are not abundant (Sæmundsson, 1991; Jónasson, 1994). Since 1974 extensive drilling for geothermal development have been performed in the Krafla caldera. This drilling reveals the extent of several active geothermal reservoirs and defines the subsurface geology (Kristmannsdóttir, 1978; Stefánsson, 1980, 1981; Ármannsson et al., 1987). Drilling has revealed a similar bimodal compositional distribution of the volcanic and plutonic rocks in the substrata (Guðmundsson, 1983d; Ármannsson et al., 1987). The postglacial, near-surface basaltic lavas are underlain by hyaloclastite erupted during the last glacial period (Guðmundsson, 1983). A second, older sequence of hyaloclastite is overlain and underlain by interglacial lavas down to about ~1,200 m, where intrusive rocks begin to dominate. Doleritic intrusions are abundant in the deeper parts of the reservoir, but felsic intrusions have been intersected in several drill holes (Guðmundsson, 1983; Ármannsson et al., 1987). Intrusions become more abundant and coarser grained at greater depth and include gabbros.

Volcanic activity and events affect the geothermal system renewing the heat supply. However, volcanic events can also cause temporary deterioration of the fluid source with excessive volcanic gas influx, as was experienced in part of the Krafla geothermal field during the Krafla Fires 1975–1984 (Guðmundsson, 2001). The Krafla geothermal area seems closely associated with a magma chamber, which is inferred to underlie Krafla Caldera at depths of 3–7 km based on observation of attenuation of S-waves during the Krafla Fires rifting episode (Einarsson, 1978). The extent of the geothermal system in Krafla is estimated to be ~40 km<sup>2</sup> (Mortensen et al., 2009a).

By 2014 a total of 46 exploration and production wells have been drilled in Krafla geothermal system (Table 1). The main well field is located in the eastern part of the caldera (Figure 4 and Figure 5) and through drilling, the volcanic structure at depth has been outlined as well as the physical conditions of the geothermal system (Stefánsson, 1981; Böðvarsson et al., 1984; Ármannsson et al., 1987). The geothermal area is divided into several subareas: Leirbotnar, Suðurhlíðar, Vesturhlíðar, Vítismór, Leirhnjúkur Sandabotnar, Vestursvæði, and Hvíthólar (Figure 4 and Figure 5).

## 4 Stratigraphy and alteration in Krafla

Since the last geological model of Krafla was made and published in 2009 (Mortensen et al., 2009a) only two wells has been completed and drilled (IDDP-1, K-40) adding limited data to the existing model. The stratigraphic and alteration models have now been incorporated into the 3D software Petrel. The Petrel model includes the stratigraphy from the following wells: KS-1, KV-1, K-4, K-8, K-10, K-18, K-19, K-21, K-22, K-24 to K-27, K-30 to K-40 and IDDP-1. Other wells have not been incorporated into the model since no computerized data on the stratigraphy is available. Clay alteration information (clay zones) from the following wells has also been incorporated: KS-1, KV-1, K-3 to K-26, K-28 to K-30, K-33 to K-35 and K-38.

Further work is needed to establish a more precise stratigraphic model of the Krafla area. Comprehensive petrographic analyses would strengthen the division between formations and connections made between them and stratigraphic columns from more wells need to be included in the model. Additional XRD analyses from the latest drilled wells would furthermore strengthen the conception of alteration zones in the area. Without XRD analyses the clay mineral classification is not sufficient and the appearance of actinolite (implying >280°C formation temperature) is not as well established.

Information on stratigraphy and alteration in the wells is based on research published in section-reports of the wells (Guðmundsson et al., 1981a, b; Friðleifsson et al., 1981a, b,; Friðleifsson and Sigvaldason, 1981; Friðleifsson and Stefánsson, 1981; Guðmundsson et al., 1982a, b, c; Steingrímsson et al., 1982; Guðmundsson et al., 1983a, b, c, e, f, g; Stefánsson et al., 1983; Guðmundsson et al., 1988a, b, c; Guðmundsson et al., 1990, Guðmundsson et al., 1990a, b; Guðmundsson et al., 1991a, b; Guðmundsson et al., 1992; Guðmundsson et al., 1996; Franzson et al., 1996; Guðmundsson et al., 1997a, b, c, d, e, f, g; Guðmundsson et al., 1998a, b, c; Franzson et al., 1998; Hjartarson et al., 1999; Guðmundsson et al., 1999a, b, c, d; Steingrímsson et al., 1999; Blischke et al., 2004; Gautason et al., 2006; Þórarinnsson et al., 2006a, b; Mortensen et al., 2007a, b, c; Guðmundsson et al., 2007a, b, c; Gautason et al., 2007a, b; Guðmundsson et al., 2008a, b; Gautason et al., 2008a, b, c, d; Sigurgeirsson et al., 2008; Gautason et al., 2009; Ingimarsdóttir et al., 2009a, b; Árnadóttir et al., 2009a, b, c; Sigurgeirsson et al., 2009; Mortensen et al., 2009b).

### 4.1 Stratigraphy

In the profiles presented in Figure 6 to Figure 10a number of wells contribute to the stratigraphy of the model itself as connections are made between all of the available wells. Only profiles of wells that are close to the trail of the cross sections are presented in the figures but other wells contribute to the drawing of the 3D profiles as well. This is the reason why the stratigraphy of each well does not match perfectly with the 3D stratigraphy of each cross section.

The connections made between stratigraphic units are usually based on either hyaloclastite formations at a similar depth or lava layers. In the 3D software Petrel the program assumes that there are layers with approximately constant thickness. This is not very practical for hyaloclastite units as they form mountains and ridges instead of spreading laterally. There are therefore some differences between the pictures in the current report when compared with the cross sections from the Mortensen et al. (2009a) report.

In the cross sections, the lithology from the wells where digital data was available is shown in each well profile. It becomes quite obvious that the lithology of the wells does not always follow the model's horizons (Figure 7 to Figure 10). This is caused by the deviation of the individual wells from the simplified trail of the assumed cross section. Omitted from the Petrel model are the locations of felsic and intermediate rocks, either extrusive or intrusive. Local formations are difficult to present properly in the software and more work is needed to show these in the cross sections. However, it is depicted in the lithology profiles of the wells themselves (see legend in Figure 6 and profiles in Figure 7 to Figure 10).

The stratigraphy of the central part of the Krafla caldera is discussed separately from the stratigraphy at the southern edge of the caldera as there are some differences. In both cases, it is possible to divide the lithology into two major formations; extrusive igneous rocks (hyaloclastite and lava piles) which dominate down to 400–1500 m below sea level (b.s.l.), after which intrusions dominate (Figure 7 to Figure 10).

#### **4.1.1 Stratigraphic profiles in the central part of the Krafla caldera**

The lithology in the central part of the Krafla caldera roughly consists of extrusive igneous rocks (hyaloclastite and lava piles), which dominate down to approximately 400–1000 m (b.s.l.) whereas basaltic intrusions dominate below that (Figure 7 to Figure 9). As seen in the profiles in Figure 4 and Figure 5, beneath Suðurhlíðar there is a prominent 200–400 m thick felsic intrusion. Felsic intrusions are not as prominent west of Hveragil and in the easternmost part of Suðurhlíðar (K-18). Thin, felsic or intermediate intrusions, however, occur at variable depths in Leirbotnar and Vítismór. Furthermore, it has been established that there is felsic magma at shallow depths in the crust since felsic magma has been reached twice by drilling, on the one hand in Suðurhlíðar (below 2500 m MD in well K-39) and on the other hand in Vítismór (at a little less than 2100 m MD in well IDDP-1). Beneath Suðurhlíðar there is, furthermore, up to 200–300 m thick pile of felsic intrusions at around 900–1400 m (b.s.l.) (Figure 7). Gabbroic intrusions follow at around 1300–1900 m (b.s.l.) in the wells in that area which is evident in the lithology profile of each well (K-18, K-19, and K-39). Felsic intrusions are not as prominent west of Hveragil and in the easternmost part of Suðurhlíðar (well K-18).

The lithology in well K-35, to the left in Figure 7, is somewhat different from what is seen in the wells in Leirbotnar as extrusive rocks dominate all the way down to 1200 m b.s.l. As explained in the last model (Mortensen et al., 2009a) the lower intensity of intrusions can, at least in part, be explained by the domination of vertical dykes which occur as thin adjacent dykes in directionally drilled wells. The wells in Leirbotnar and Vítismór are in most cases straight and if such wells cut an almost vertical intrusion, it can form a rather thick formation (even though it is a thin dyke). The stratigraphy in most of the wells in Leirbotnar and Vítismór is dominated by intrusions (>90%) below 400 m b.s.l. and one intrusion after the other is cut without apparent signs of extrusive rocks. This can in part be explained with the location of the wells in a close proximity to an eruption fissure and/or fissure/dyke swarms. To the north, in the Vesturhlíðar wells, the intrusion frequency is also low when compared to the wells in Leirbotnar and Suðurhlíðar (Figure 7 to Figure 9).

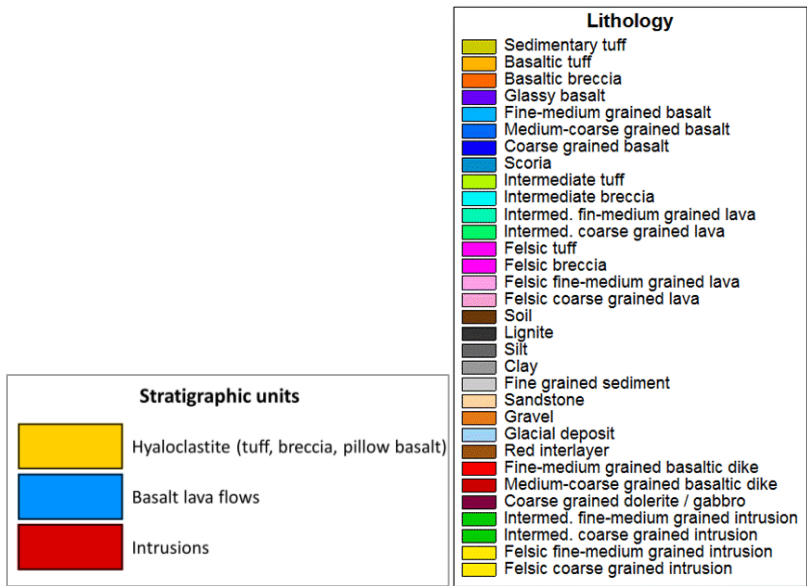


Figure 6. Legends for stratigraphic units and detailed well lithology in Figure 7 to Figure 10.

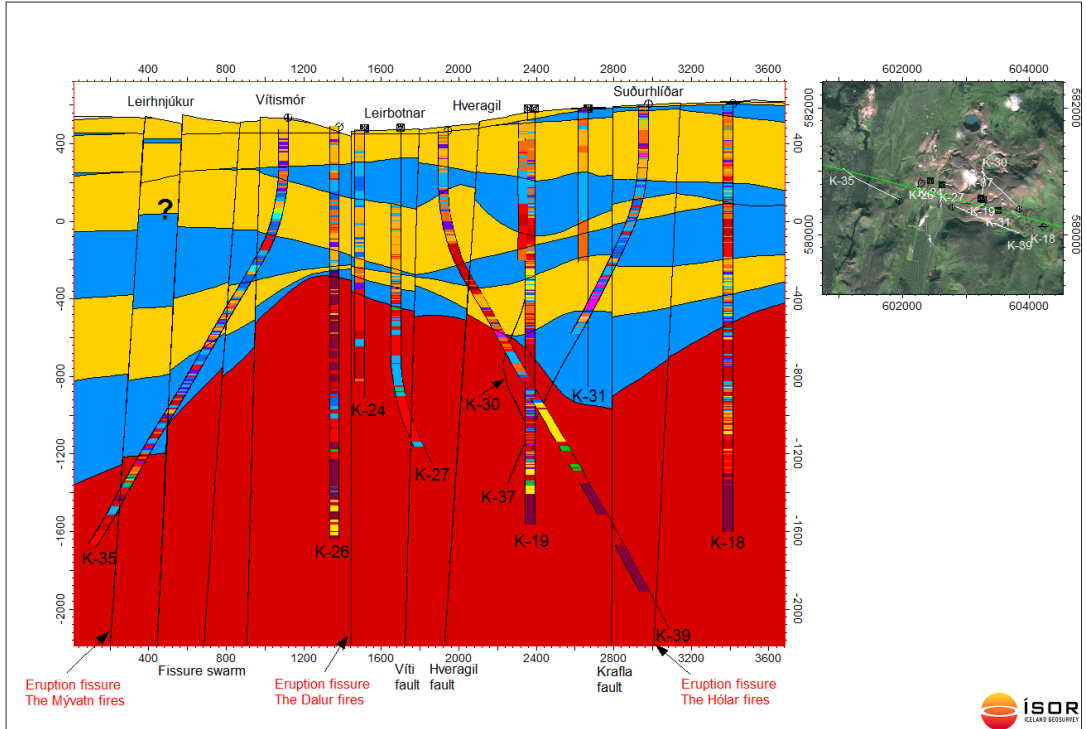


Figure 7. Stratigraphic cross section from W to E through Leirhnjúkur, Vítismór, Leirbotnar and Suðurhlíðar.

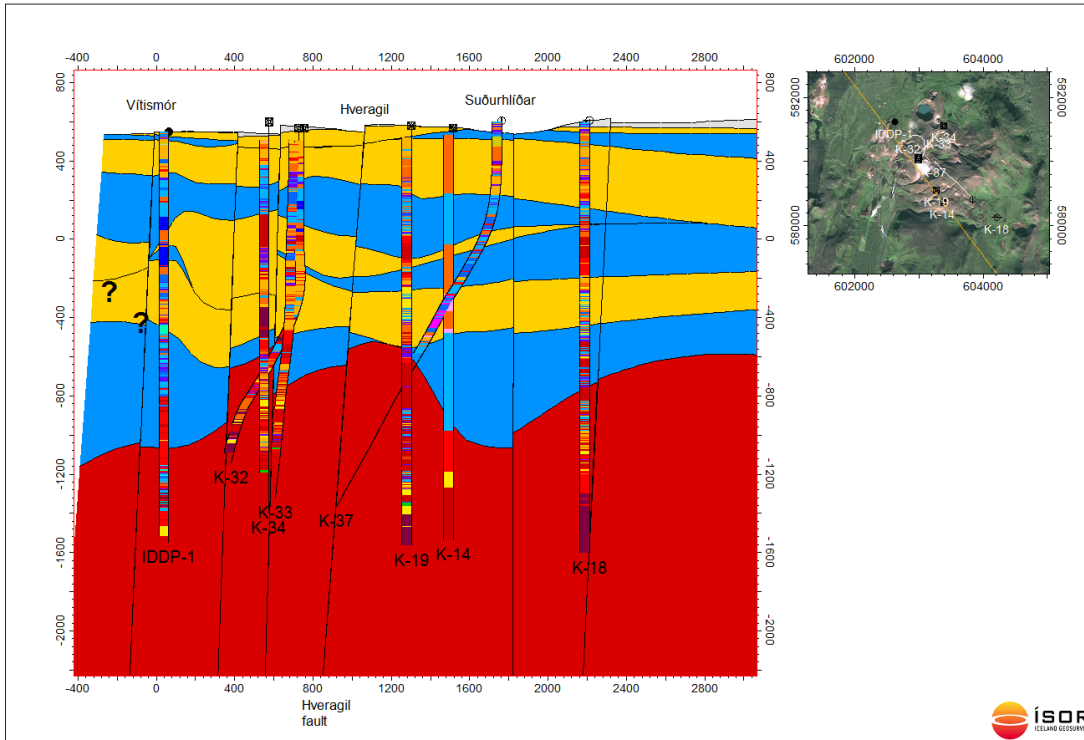


Figure 8. Stratigraphic cross section from NW to SE through Vitismór, Hveragil and Suðurhlíðar.

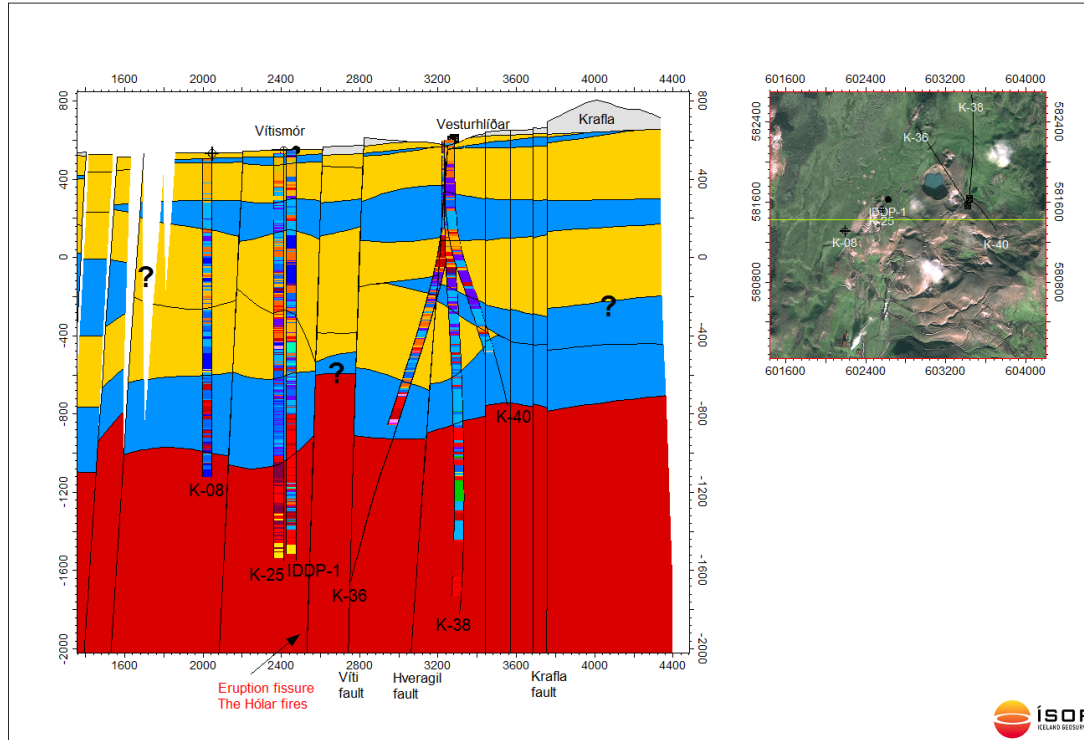
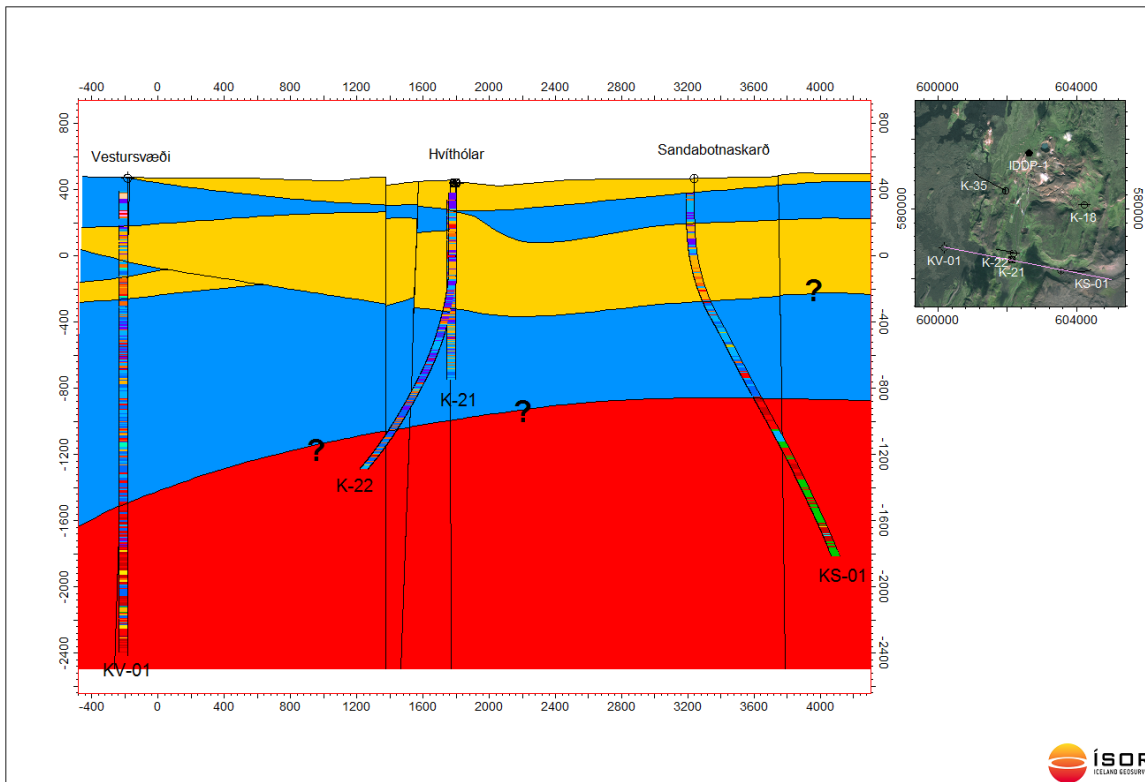


Figure 9. Stratigraphic cross section from W to E through Vitismór and Hveragil.



**Figure 10.** Stratigraphic cross section from E to W through Vestursvæði, Hvíthólar, and Sandabotnar.

#### 4.1.2 Stratigraphic profile by the southern edge of the Krafla caldera

E-W stratigraphic profile from the southern rim of the Krafla caldera is shown in Figure 10. Excluding an approximately 100 m thick lava pile hyaloclastite formations dominate down to 100–400 m b.s.l. and no prominent lava piles are noted in the hyaloclastite formations. Below the hyaloclastites lava piles dominate down to at least 1600 m b.s.l. (KV-1).

Intrusion frequency is lower in most of the wells by the southern edge of the caldera than in the central part (with the exception of KS-1 where intrusions dominate below 800 m b.s.l. The wells by Hvíthólar do not reach more than 1600 m b.s.l. and they have low intrusion frequency. The 3D model assumes, however, that there are intrusions below 1200 m b.s.l. although that is not the case in reality (Figure 10). This is because of interpolation between the wells, which affects the overall model. In well KV-1 in Vestursvæði, intrusions dominate below 1500 m b.s.l. while intrusion frequency is considerably higher in well KS-1 in Sandabotnar. In well KS-1 a thick unit of an intermediate intrusion (diorite or granodiorite) is present below 1200 m b.s.l. (based on cutting analysis). Excluding well KS-1 the proportion of intermediate or felsic formations is low by the caldera edge although thin felsic formations are seen towards the bottom in well KV-1 in the Vestursvæði area.

## 4.2 Alteration

Alteration has been mapped with depth in each well in the Krafla area. This has been done from cutting analyses as well as XRD analyses and in some cases petrographic analyses. In geothermal systems variable alteration minerals form, which are stable at prevailing temperatures and geothermal fluids at each time, a testament of a former temperature state as most of them remain stable even though the systems cooled down. Geothermal alteration in high temperature areas can be divided into alteration zones named after certain temperature dependent minerals. It is customary to use the following alteration zones in Iceland: zeolite-smectite, mixed layer clay, chlorite, chlorite-epidote and epidote-actinolite, and these zones define the highest prevailing temperatures in the area. Alteration zones in Krafla are presented in Figure 11 to **Figure 14**.

In addition to these alteration zones the disappearance of calcite (giving  $>290^{\circ}\text{C}$  alteration temperature) is presented in the last model (Mortensen et al., 2009a). This has not yet been incorporated into Petrel and is therefore not shown in Figure 11 to **Figure 14**. The information, however, is still valid. As there are no apparent changes in the alteration model from 2009, no detailed descriptions concerning the alteration will be made in this report.

As realized in former work in the area there is a divide in the alteration apparently marked by the Hveragil fault (Figure 11 to Figure 13). The area east of Hveragil, beneath Suðurhlíðar, reveals shallow high temperature alteration, reaching the chlorite-epidote zone at 200–300 m a.s.l. (Figure 11). No signs are of substantial cooling but fast changes in alteration suggest that formation temperature is close to boiling point beneath Suðurhlíðar (Mortensen et al., 2009a). Well K-18 in the easternmost part of Suðurhlíðar is, however, different to the rest of the Suðurhlíðar wells showing that increasing alteration is not as fast with depth in that area. As former work has revealed, this suggests that the eastern boundary of the geothermal system in Suðurhlíðar is near or that the system is deeper (e.g. Mortensen et al., 2009a). To the west of the Hveragil fault, in Leirbotnar, the zeolite-smectite zone is shallow but the other alteration zones are much deeper than east of Hveragil, except for the epidote-actinolite zone, which appears at a similar depth (Figure 11).

The alteration at the southern edge of the caldera is very variable in the three drilling areas (**Figure 14**). High temperature alteration is shallow in the Hvíthólar area whereas it is much deeper in both Vestursvæði and Sandabotnar. In Sandabotnar alteration increases very slowly but gradually with depth. In the Vestursvæði area alteration increases quite fast in the upper part of well KV-1 (from the smectite zone to the chlorite-epidote zone) whereas the epidote-actinolite zone appears quite deep down.

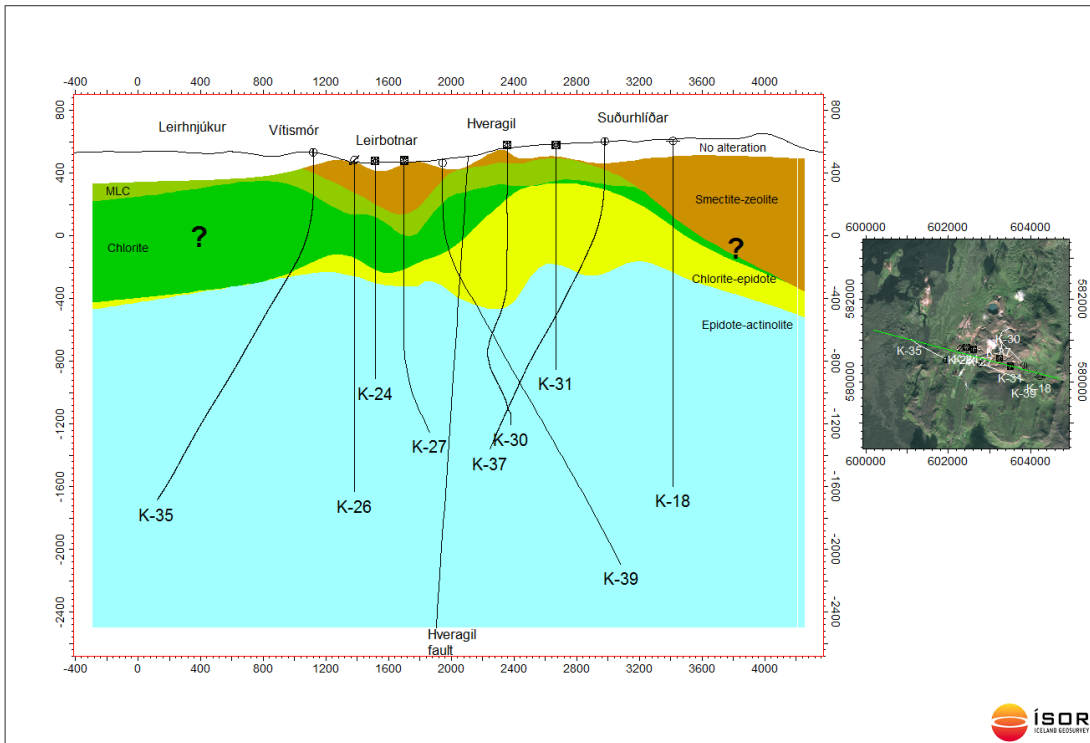


Figure 11. Alteration cross section from W to E through Vitismór, Leirbotnar, and Suðurhlíðar.

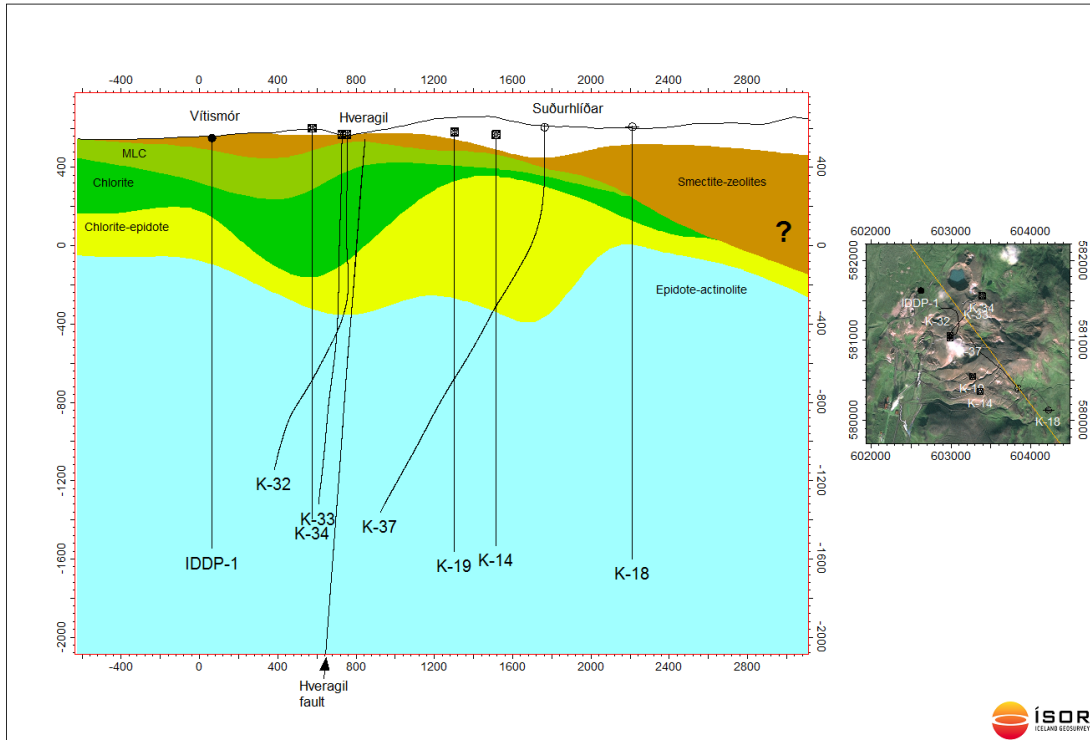


Figure 12. Alteration cross section from NW to SE through Vitismór and Suðurhlíðar.

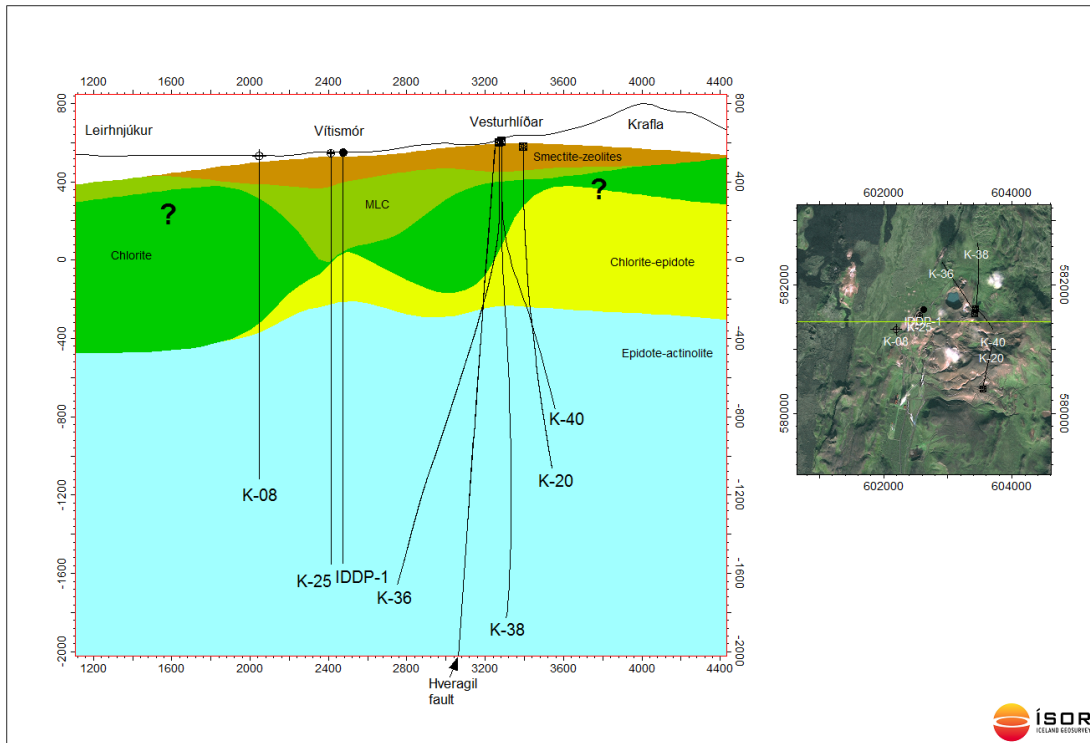


Figure 13. Alteration cross section from W to E through Vítismór and Vesturhlíðar.

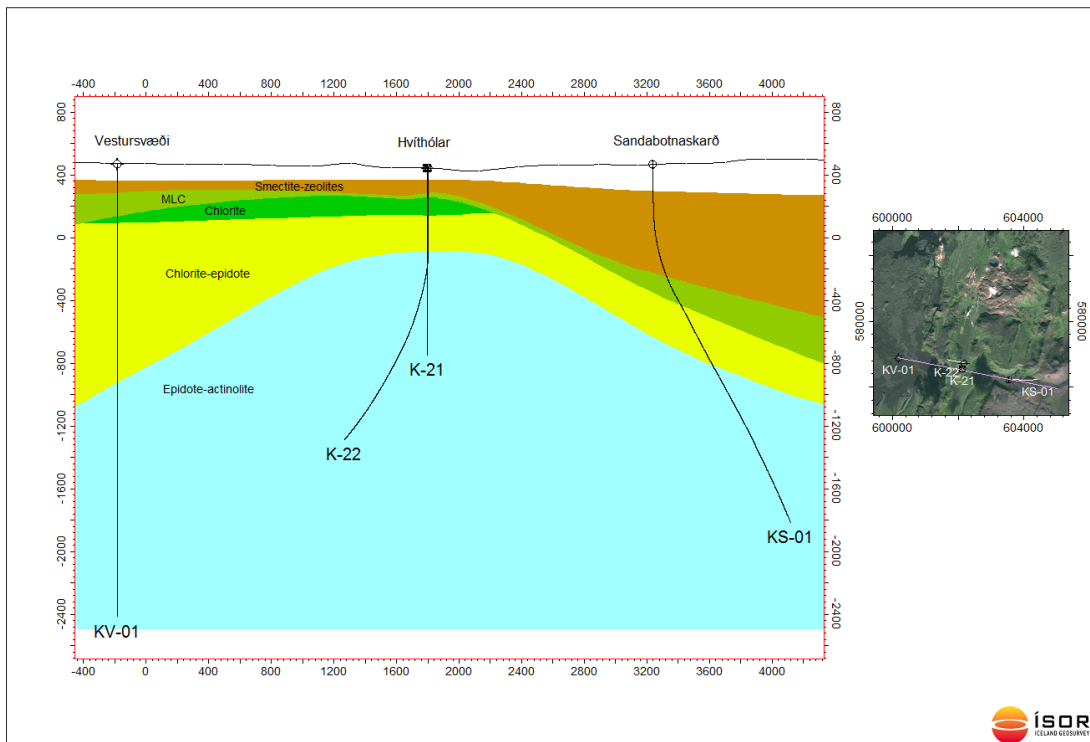
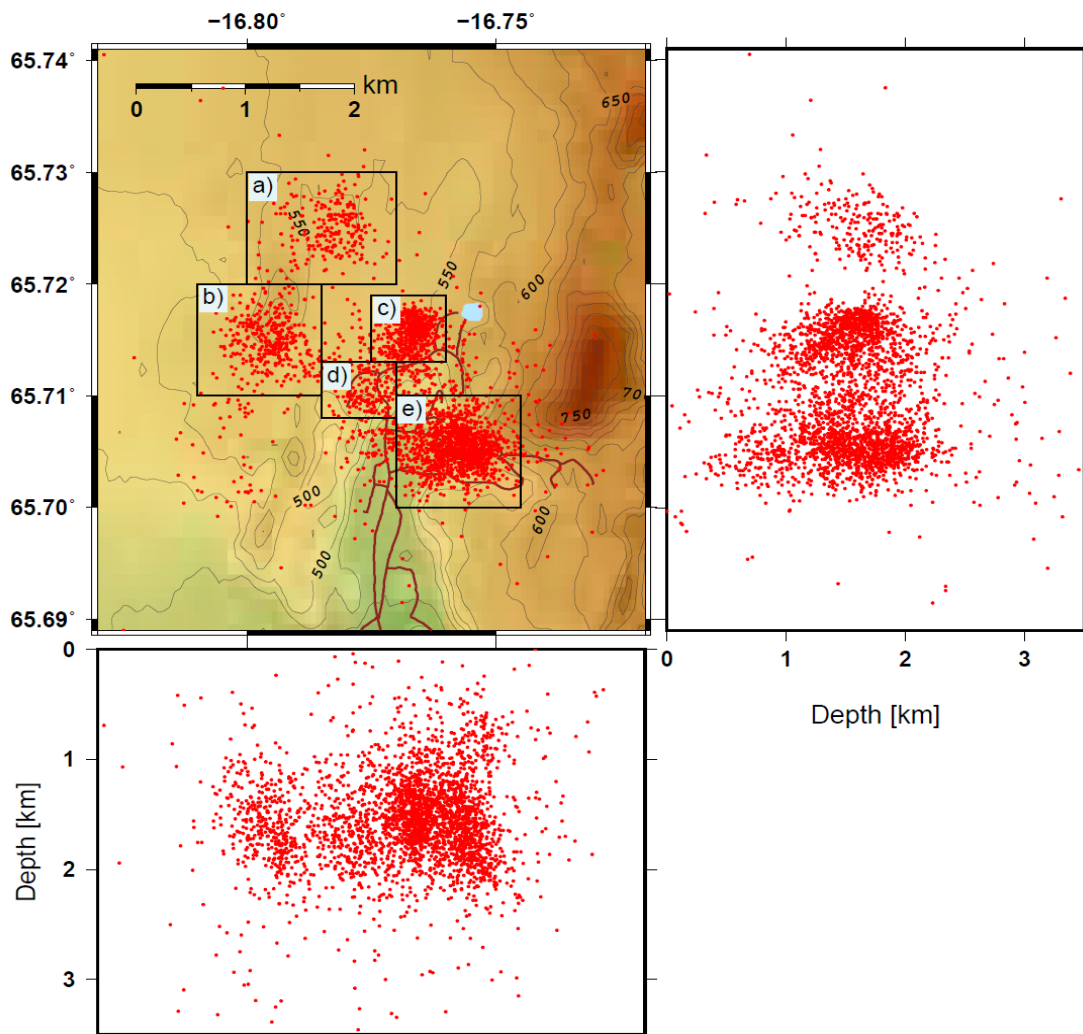


Figure 14. Alteration cross section from W to E through Vestursvæði, Hvíthólar, and Sandabotnaskarð.

## 5 Seismic activity

### 5.1 Seismicity October 2013 to October 2014

A network, currently consisting of 15 short period seismometers, is operated in the Krafla geothermal area to monitor the seismic activity within and around the geothermal system. Seismicity in the Krafla geothermal area is both of natural origin as well as induced by the geothermal production and reinjection. In the period from October 25, 2013, until October 31, 2014 a total of 3047 earthquakes were recorded.



**Figure 15.** Earthquake locations and E-W and N-S sections. The main activity occurs in five clusters. The largest cluster is associated with the main production area in Suðurhlíðar (e). The second cluster west of Víti lies in the area around the IDDP-1 well (c). Two clusters are NNE and SSW of Leirhnjúkur (a and b) and the smallest cluster just north of Rauðhóll, close to the reinjection well K-26 (d).

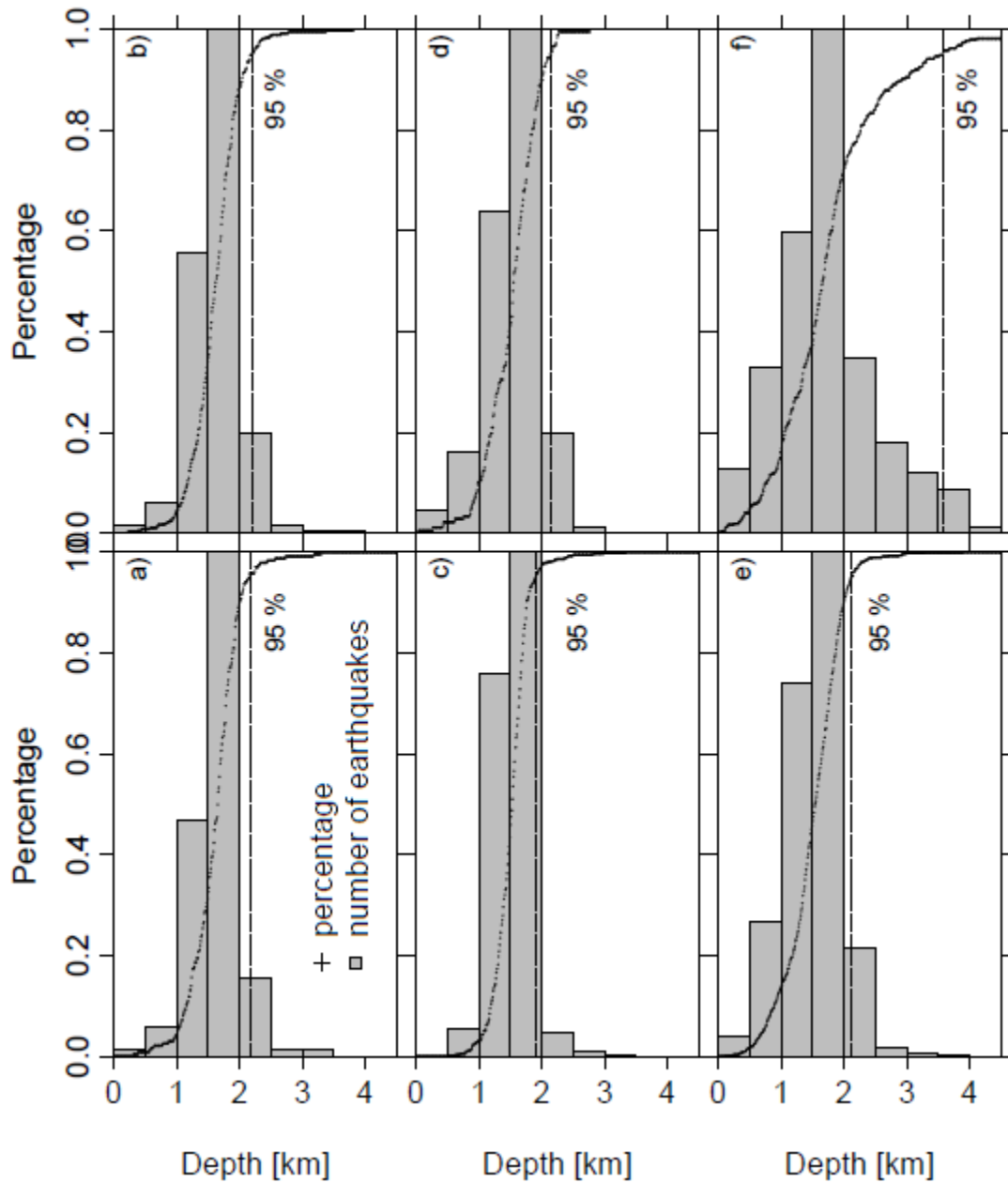


**Figure 16.** Depth distribution of earthquakes on cluster a) to e). In f) are all event summed up that do not lie inside any of those clusters but within the Krafla caldera. The number of earthquakes is normalized with the maximal number of earthquakes in one layer in the cluster and is represented by a gray column. The crosses show the cumulative number of earthquakes in percent of the total number of events in the cluster. The dashed line represents the maximal focal depth of 95 % of the events.

Their locations are shown in Figure 15. The seismic activity is variable as can e.g. be seen in the number of events per day. This number is subject to strong fluctuations both on a short and long time scale. The number varies between zero and 36 events per day with an average of 8.2. A comparison with local average wind velocities revealed a decrease in the number of recorded events with increasing wind velocities, reflecting reduced sensitivity of the network during windy periods.

## 5.2 Earthquake distribution

The distribution of the hypocenters suggests that the events occur in spatially separated clusters. Their location and classification is shown on (Figure 15). They are partly associated with the centers of natural activity (clusters a and b close to Leirhnjúkur), partly with centers of activity related to the operation of the Krafla power plant (injection), i.e. cluster c around the IDDP-1 well, cluster d at the injection borehole K-26, and cluster e under the main production area, which, is possibly related to reinjection in well K-39.

The depth distribution is similar in the different clusters, except for cluster c (Figure 16), where the earthquakes are somewhat shallower. In cluster c the ductile-brittle boundary (maximum focal depth of 95 % of the events) lies at about 1900 m depth. This is partly due to a considerable number of shallow earthquakes which are induced by the injection of fluids taking place in well IDDP-1 and these induced earthquakes bias the estimation of the brittle ductile boundary (Ágústsson et al., 2012; Blanck et al., 2014). In the other four clusters the boundary lies between 2100 and 2200 m (average 2160 m) depth. Analyzing the earthquakes outside of the clusters, but within the seismic network, shows different result. There the depth of the ductile-brittle boundary is about 1400 m deeper, or at about 3600 m depth. The ductile-brittle boundary is associated with a maximum temperature of 800°C (Ágústsson and Flóvenz, 2005). Extrapolation of laboratory measurements of non-glassy basalts predicts that the temperature at the brittle ductile boundary might occur at temperatures higher than  $550 \pm 100$  °C (Violay et al., 2012). However, in case of continental crust and more silicic crustal material, the brittle ductile boundary can be expected at temperatures even lower than 450°C (Chen and Molnar, 1983). This indicates the existence of shallow heat source(s) underneath the clusters in Krafla, which increase the local geothermal gradient.

## 5.3 $V_p/V_s$ velocity ratio

Detailed information on seismic velocity ratios is important to verify or improve existing velocity models. The Standard Wadati method (Wadati, 1928) to derive the  $V_p/V_s$  ratio of the crust makes use of the arrival times both of the p- and s-wave. The location of the events is not needed. The result of this method yields the average of the velocity ratio in the crust the waves travel through from the source towards the seismometers.

The  $V_p/V_s$  ratio derived for the Krafla area with the Standard Wadati approach is estimated as 1.680, which is unusually low (1.73 is the expected value for an ideal elastic medium) (Figure 17). Low velocity ratios are a common feature observed at shallow depths in geothermal areas (e.g. Walck, 1988; Julian et al., 1996; Muskin et al., 2013). They can be a consequence of high quartz content in granitic or andesitic rock (Christensen, 1996). Foulger et al., (1995) suggest mineral alteration or supercritical fluids as the cause. In Krafla, we have rhyolite and probably a steam

cap but steam in the pores reduces the bulk incompressibility of the rock and reduces the p-wave velocity. Both the rhyolite and possible steam cap could explain the low  $V_p/V_s$  ratio.

To compare the velocity ratio estimated for the Krafla geothermal system with the ratio outside the system 265 earthquakes that were recorded by the seismic network outside the geothermal area were used for the calculation of the  $V_p/V_s$  ratio of the surrounding crust. The  $V_p/V_s$  ratio outside of the Krafla system was estimated to equal 1.782 (Figure 17). It is in agreement with the results of studies on the Icelandic crust, which suggest values of about 1.75–1.79 (e.g. Brandsdóttir and Menke, 2008).

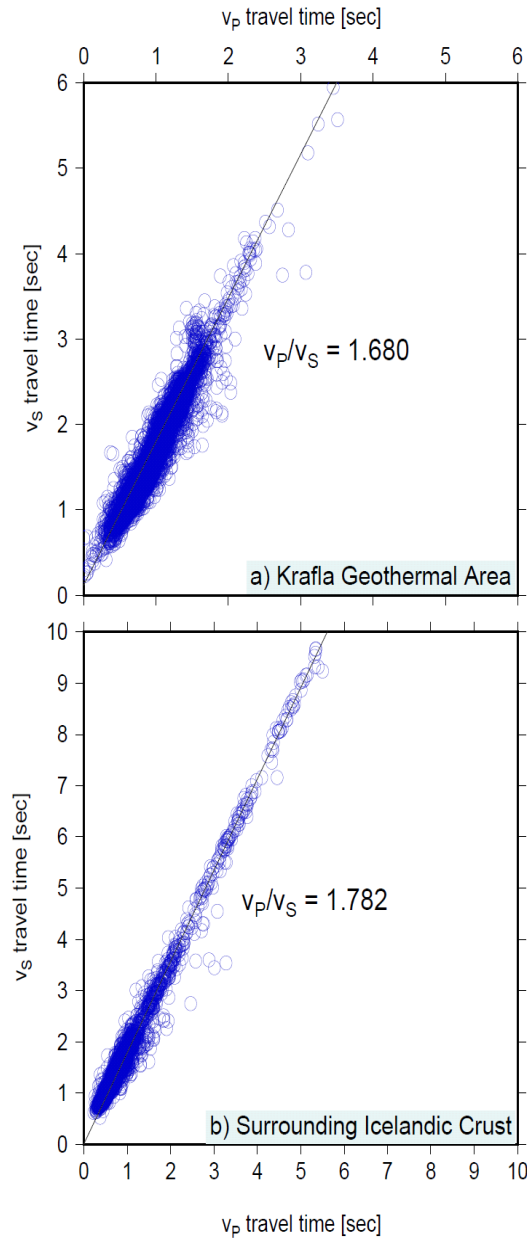


**Figure 17.**  $V_p/V_s$  ratio in Krafla and surrounding crust.

## 6 Geophysics

### 6.1 Gravity

In 1967 to 1984 an extensive gravity survey was carried out, covering the Krafla area and its surroundings (Johnsen, 1995). Figure 18 shows a de-trended (and hence relative) Bouguer gravity map of the Krafla volcano and its immediate surroundings based on these data.

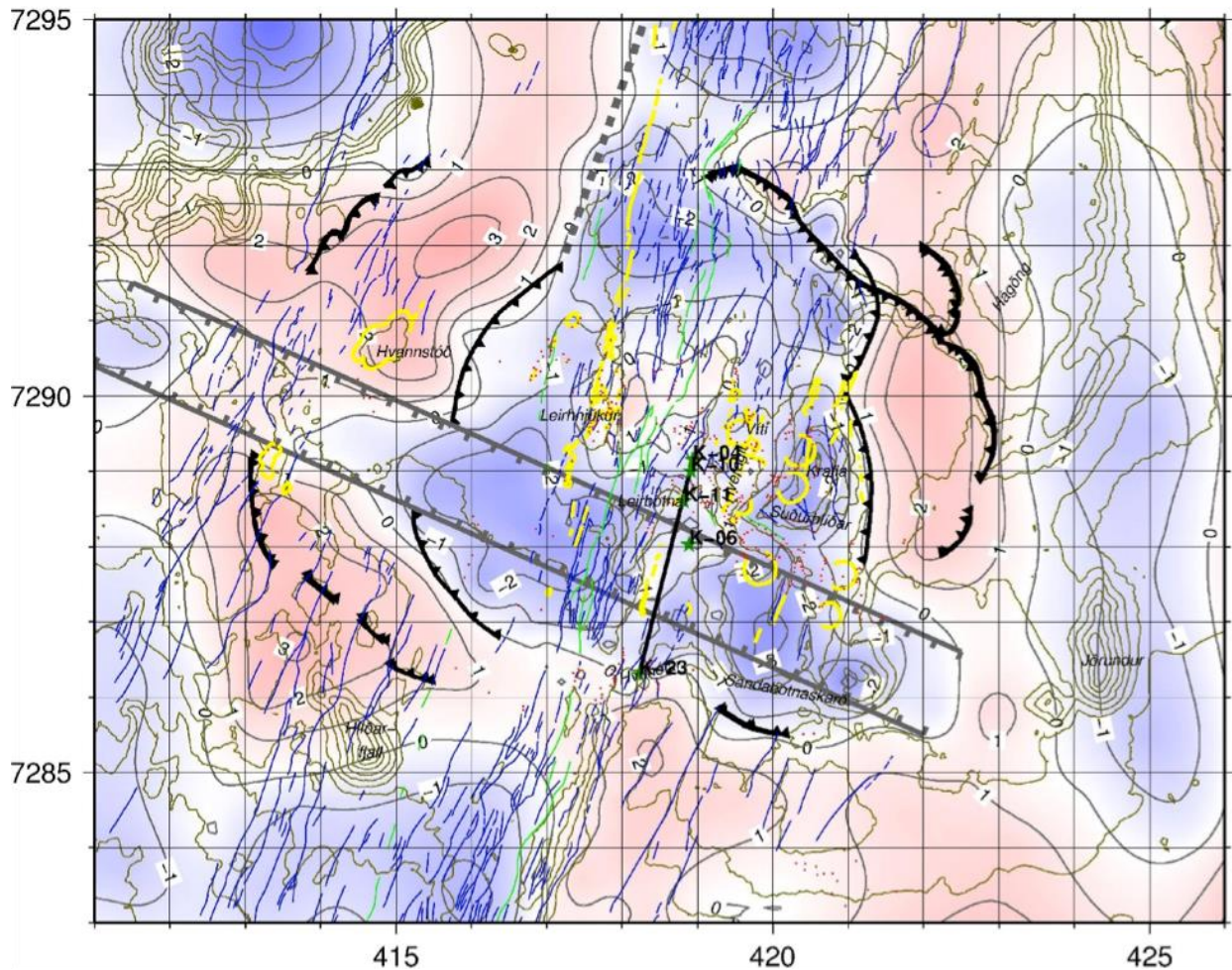


**Figure 18.** De-trended Bouguer gravity map (mgals) of the Krafla volcano. The rims of the outer caldera and the inferred buried inner caldera are shown (hatched black lines). An inferred ESE-WNW transform low gravity lineament is shown (gray fault lines) A linear density contrast in the fissure swarm to the north is also shown (gray broken line). The location of a lithological section in Figure 19 is shown (black line) and the wells on which it is based (green stars).

The figure shows that there is a relative gravity low within the caldera. Superimposed on the gravity low is a gravity high at Leirhnjúkur and towards Mt. Krafla. The caldera is bisected by two more or less linear gravity lows. One is along the part of the fissure swarm that was active in

the Krafla fires (bounded by green lines on Figure 18). The other is ESE-WNW trending from Mount Jörundur in the SE and to the valley Gæsadalur (SW of Gæsafjöll) in the NW. Where these anomalies would cut through the caldera rim, the rim is not visible.

The caldera is 110,000 years old (Sæmundsson, 1991) and if the spreading rate is assumed to be about 1.8–2.0 cm/year the total spreading since the formation of the caldera is about 2 km. Assuming that 75–100% of the spreading has been in the fissure swarm through the caldera, it should be torn apart by some 1.5–2.0 km. The gaps in the southern and northern caldera rims (as seen on surface) are about 3.5 to 4 km so parts of the rims have subsided and been buried.

The gaps in the eastern and western part of the caldera rim might be because it is buried there, but the fact that they are found where the caldera is cut through by low gravity anomalies strongly suggests that the caldera is torn apart by a low gravity lineament, filled with rocks of lower average density (more abundant hyaloclastite). Similar low gravity lineament (grabens) or trenches are known in transform zones in the north part and north off Iceland, where the crustal spreading is migrating westwards to the Kolbeinsey ridge. Lake Botnsvatn in the Húsavík transform is probably of similar origin as well as the Flatey sedimentary basin, which has its boundary faults with almost exactly the same strike as the gravity low in bisecting the Krafla caldera.

Figure 19 shows a lithological section across the inferred low gravity lineament (Ármansson et al., 1987). The wells on which the section is based and the location of the section is shown on Figure 18. The section shows a 600–700 m thicker pile of hyaloclastite with interbedded lava flows within the low gravity lineament (well K-6) than north of the low gravity lineament (wells K-4, K-8, and K-10). This lends support to the idea that the caldera is indeed bisected by an ESE-WNW low gravity lineament.

What sort of tectonics is responsible for this is not clear, but the most likely candidate is some “transform tectonics” where the spreading axis under Iceland is gradually adjusting westwards, towards the oceanic ridge north of the island. On a large scale, the northern volcanic zone has an arc shape, from NNE-SSW north of Vatnajökull, and progressively more N-S trending towards north and eventually having a slight NNV-SSE trend furthest to the north. If this reflects the deep crustal spreading, then the deep spreading around Krafla would be close to east-west, even though the spreading visible on the surface, in the fissure swarm, is somewhat south of due east.

The change in the spreading direction in the northern volcanic zone is probably also reflected locally around Krafla. A close look at the fissure swarm through Krafla reveals that south of the caldera(s) the fissures swarm trends about N22°E but about N4°E immediately north of the caldera(s) (). Recent GPS measurements show that in both cases the crustal spreading is perpendicular to the faults and fissures (pers. comm., Vincent Drouin and Freysteinn Sigmundsson, Institute of Earth Sciences, University of Iceland, September 2015). This would lead to an opening component along the fissure swarm within the volcano of about 0.3 times the spreading to the north and south.

In Figure 18, several structural features are visible. There are gravity highs at and inside the caldera rim in the southwest, northwest and east. These high gravity anomalies are bounded by steep gradients towards a gravity low in the center of the caldera, which is filled with less dense

rocks. In the eastern part of the caldera the gradient coincides with arc like eruptive fissures from Hólseidar, about 2000 years ago (Sæmundsson, 1991). Some might like to argue that the high gravity at and inside the caldera rim is due to dense intrusions, but the steep gradients clearly show that the density contrasts are at shallow depth. This suggests that there is another buried caldera, also bisected by the ESE-WNW low gravity lineament, inside the caldera seen on surface. The rims of this inferred inner caldera and the bisecting ESE-WNW low gravity lineament are shown on Figure 18.

The outer caldera has been dated as being 110,000 years old. Even though the last glacial stage is normally considered to have started at about that time, geological studies show that the Krafla area was not glaciated until sometime before 80,000 years ago (Kristján Sæmundsson, pers. comm., Nov. 2010). In the 20,000 to 30,000 years between its formation and until glaciation, the outer caldera has been mostly filled with lava flows, up to the lowest parts of its rims in the fissure swarm. The inner caldera was probably formed after the area was covered with ice. It was probably formed as a consequence of eruptions of silicic magma forming Jörundur, Hlíðarfjall and the riolite south of Gæsafjöll, about 80,000 years ago. The caldera was later filled with hyaloclastite of considerably lower density than the subaerial lavas filling the outer caldera. No trace of the inner caldera is visible on surface because Holocene lavas now cover the area.

The Bouguer gravity map of the Krafla volcanic complex shows yet another interesting feature. There is a sharp gravity gradient on a line in the fissure swarm to the north, out of the calderas (grey dashed line on Figure 18). The rift low gravity lineament hosts less dense rocks east of this line than to the west. This indicates that after the glaciation, the spreading and subsidence has mainly been in the eastern part, which was active in the Krafla fires.

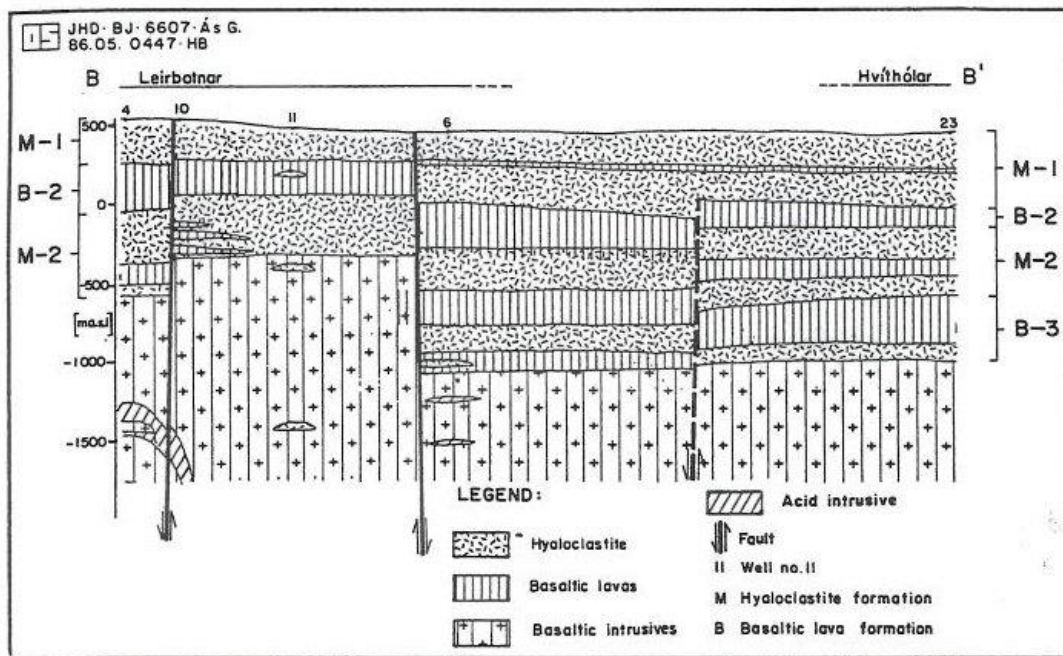


**Figure 19.** Lithological section based on wells, from north (left) to south (right) within the Krafla caldera (from Ármannsson et al., 1987). For location of the section se Figure 17.

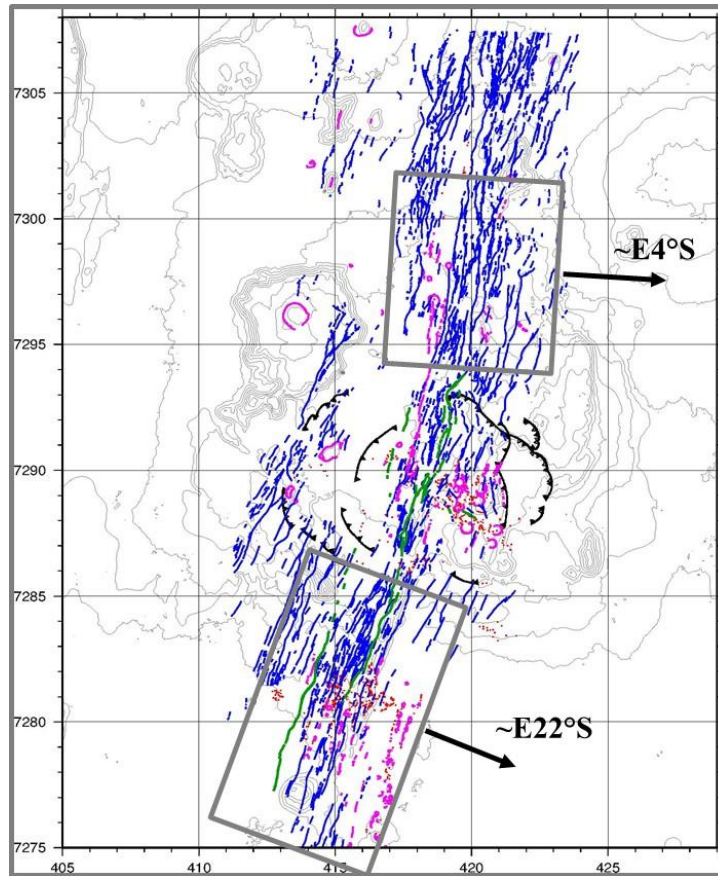


**Figure 20.** *Faults and fissures in the Krafla fissure swarm (blue) and eruptive fissures and craters (purple). Calderas are shown as black hatched lines. The figure shows different orientation of the fissure swarm and spreading directions south and north of the caldera(s) (coordinates are UTM-WGS84 in km).*

## 6.2 Resistivity

The geothermal system in Krafla is complicated, both in lateral extent and in thermo-hydraulic conditions. The lateral complexity is well displayed by looking at geothermal alteration at relatively shallow depth through resistivity. Figure 21 shows resistivity at 200 m above sea level (about 200 m depth below surface) according to TEM-soundings. The red hatched areas show where high-resistivity caused by high-temperature alteration minerals (formed at temperatures at or above 230–240°C) is found underlying a low-resistivity clay cap formed at lower temperatures (100–230°C). The figure shows that high temperature alteration is mainly found within the inner caldera and north of the inferred low gravity lineament, showing clear linear trend coinciding with the northern margin of the low gravity lineament. High-temperature alteration is seen inside the SW rim of the inner caldera and extending towards south in the presently active fissure swarm. High-temperature alteration is also seen arcing the east rim of the outer caldera. Both of these anomalies have been drilled into and geothermal alteration was found but the present temperature is far below that responsible for the alteration. No indication of high-

temperature alteration is seen at this depth in the western part of the large caldera, west of the inner caldera. It is clear from Figure 21 that the inner caldera and the ENE-WNW low gravity lineament are structures that are of great importance in the geothermal systems.

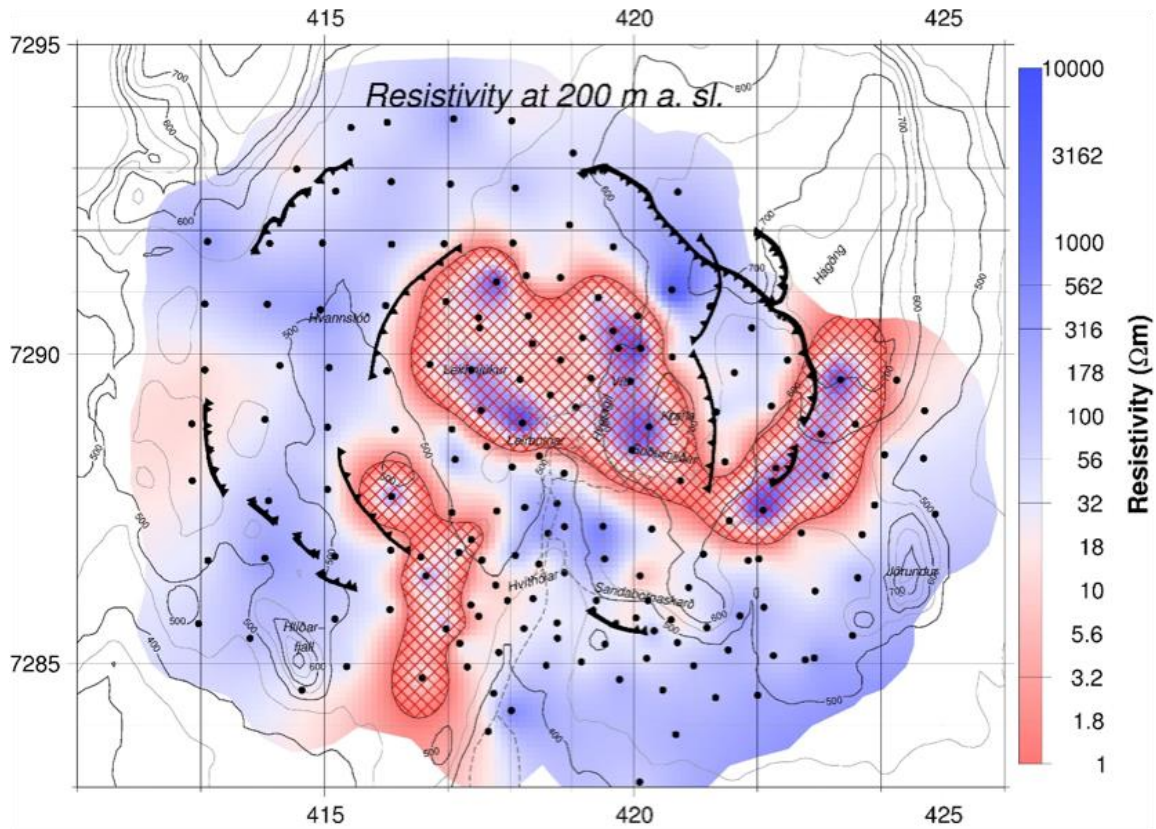


**Figure 21.** Resistivity at 200 m a.s.l. based on TEM soundings. Areas where higher resistivity is observed below low resistivity are shown as red crossed. The inner and outer calderas are shown as black hatched lines (Árnason and Magnússon, 2001).

1D (layered earth) interpretation of the Magneto-Telluric soundings gave consistent results, showing a conductor in the uppermost few hundred meters, reflecting clay alteration of the rocks, underlain by more resistive rocks with high-temperature alteration. The 1D inversion also showed deep conductors. The depth to the deep conductors varies greatly as shown on Figure 22. They are at the depth of about 8–12 km at the margins of the survey area but dome up within the inner caldera with two “chimneys” reaching up to a depth of about 2.5 km, one under and to the north of Leirhnjúkur and another under Víti and Mount Krafla. A third narrow “chimney” is seen under Leirhnjúkshraun. The two main “chimneys” roughly coincided with the magma chambers defined by S-wave shadows during the Krafla fires. The deeper resistivity structure seems also to be influenced by the low gravity lineament.

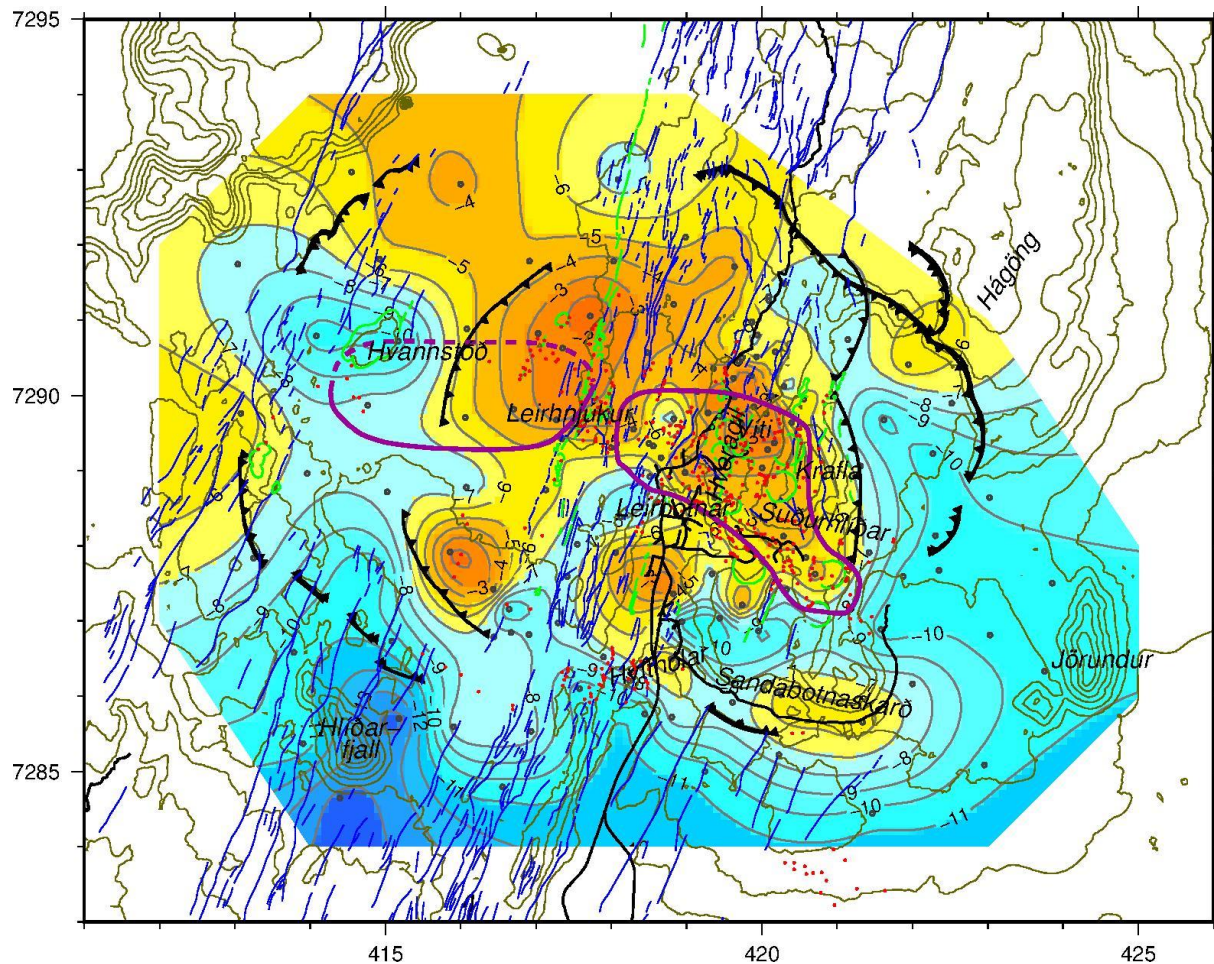


**Figure 22.** Elevation (km above sea level) of the upper boundary of deep conductors in the Krafla volcanic complex as seen by 1D inversion. Black hatched lines show caldera rims and S-wave shadows as mapped by Einarsson (1978). Faults and fissures and eruptive fissures/craters are shown by blue and green lines respectively and geothermal surface manifestation by red dots.

ÍSOR has done 3D inversion of the MT-soundings in Krafla. This was done within an externally funded international research project. The 3D model largely agrees with the resistivity model from 1D inversion in the uppermost 1.5 km, but sharpens the resistivity picture considerably, as was to be expected. At greater depth the 3D inversion also sharpens the picture and shows the volume above and within the S-wave shadows as high resistivity body are bordered by low resistivity (Figure 23). This was not resolved by the 1D inversion. The resistivity model from the 3D inversion has been compared to the distribution of hypo-centers recorded by the permanent seismic network. This comparison seems to indicate an interesting feature, i.e. that the seismicity seems to cluster at boundaries between low- and high-resistivity bodies (Figure 23). The seismic clusters also correlate with injection wells, but at least two clusters, south and north of Leirhnjúkur, can hardly be attributed to injection. It is an important question whether, or how much of the seismicity has tensile cracking focal mechanism, reflecting heat mining from hot rocks. This calls for a study of the focal mechanisms of the micro-earthquakes in the geothermal system.

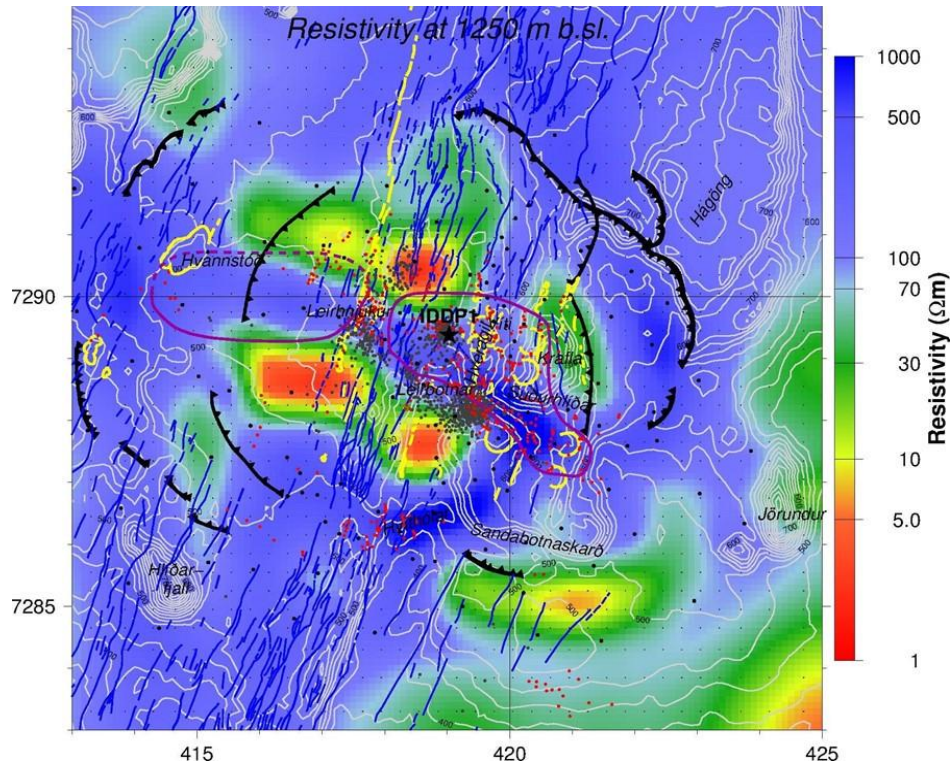


**Figure 23.** Resistivity at 1.25 km b.s.l. (about 1.7 km below surface) in the Krafla volcanic complex according to 3D inversion of MT. Caldera rims are shown by black hatched lines and S-wave shadows as mapped by Einarsson (1978) (purple). Micro-earthquake epi-centers are shown as grey dots and faults and fissures are shown by blue lines.

## 7 Chemical composition of reservoir liquid

### 7.1 Data set

Raw chemical data for wells at Krafla was provided by Landsvirkjun. The majority of the samples are from annual production monitoring, but some samples are from flow tests and may not be representative of the deep liquids. The raw data has been filtered and only analyses of samples collected after the year 2000 were selected for this report. This excludes wells that have not been sampled in this millennium, including K-26, K-25, K-22 and most of the single-digit wells. It should be noted that the chemical analyses for individual wells are not continuous throughout the time interval from 2000 to 2014. For the purpose of deep liquid calculation only samples with a complete two-phase (i.e. steam and liquid) analysis are taken into account. Liquid-phase samples with a large charge balance error (>10%) are disregarded. Some of the liquid-phase samples from high-enthalpy wells are obviously mixed with condensed steam (recognized by a lower pH, lower concentrations of solutes and higher concentrations of dissolved gases) and are therefore disregarded. For wells K-31 and K-39 only steam samples are available. Stable isotope

data was provided only for a few wells, but was supplemented by older data from the ÍSOR geochemical database.

**Table 2.** Average temperatures and enthalpies for individual wells in the Krafla geothermal system based from raw data provided by Landsvirkjun from the period 2000–2014).

Well	Subarea	T <sub>Qz</sub> (°C)	T <sub>Na/K</sub> (°C)	T <sub>H2S</sub> (°C)	T <sub>average</sub> (°C)*	T (°C)**	Enthalpy (kJ/kg)***
K-5	Leirbotnar upper	212	180	226	200	200	947
K-6	Leirbotnar upper	244	219	226	245	245	1118
K-9	Leirbotnar upper	229	199	225	215	215	1032
K-11	Leirbotnar lower	249	233	257	240	240	2021
K-12	Leirbotnar lower	272	268	263	275	270	2118
K-13A	Leirbotnar upper	255	200	259	230	230	1496
K-14	Suðurhlíðar	258	241	274	245	255	2718
K-15	Leirbotnar lower	251	221	244	265	250	1387
K-16A	Suðurhlíðar	253	258	275	275	275	2660
K-17	Suðurhlíðar	289	255	266	275	275	2415
K-19	Suðurhlíðar	249	262	280	245	245	2567
K-20	Suðurhlíðar	300	253	282	280	280	2607
K-21	Hvíthólar	260	230	238	245	245	1172
K-24	Leirbotnar upper	219	170	226	200	200	942
K-27	Leirbotnar lower	247	218	237	250	250	1085
K-28	Leirbotnar upper	233	199	229	210	210	1158
K-29	Leirbotnar lower	260	235	253	-	260	1499
K-30	Suðurhlíðar	256	274	277	290	280	2709
K-32	Vítismór	251	227	268	-	260	1414
K-33	Vesturhlíðar	297	252	290	-	290	2623
K-34	Vesturhlíðar	270	254	284	-	270	2626
K-35	Leirhnjúkur	287	282	243	-	285	2176
K-36	Vesturhlíðar	259	244	286	-	255	2555
K-37	Suðurhlíðar	282	238	279	-	260	2516
K-38	Vesturhlíðar	258	250	279	-	260	1928
K-40	Vesturhlíðar	227	262	226	-	260	2658
KS-01	Sandabotnar	268	266	245	-	265	1450

\* average temperature (solutes and H<sub>2</sub>S temperatures) and assumed aquifer temperatures after Guðmundsson and Arnórsson (2005)

\*\* selected temperature for deep-liquid calculation

\*\*\* average enthalpy from raw data (2000–2014)

## 7.2 Subarea division

The Krafla geothermal field has been grouped into several subareas. Ármannsson et al., (1987) divided the Krafla fluids into seven groups upper (shallower) Leirbotnar, north and south lower (deeper) Leirbotnar, Hveragil, Suðurhlíðar, upper and lower Hvíthólar) according to different chemical characteristics, geography and depth of the wells. The basic premises for the division were gas concentrations (CO<sub>2</sub>, CO<sub>2</sub>/H<sub>2</sub>S) and chloride concentrations and ratios (Cl, Na/Cl, F/Cl). Many wells were considered to draw mixtures from two or more groups. Guðmundsson and Arnórsson (2002) used sulphate and silica concentrations as a further criterion. This was revised

by Mortensen et al. (2009a) who eliminated the subarea Hveragil and added Vítismór. Ármannsson et al. (2015) included three additional geographical settings (Sandabotnar, Leirhnjúkur and Vesturhlíðar) and classified the different subareas by the following chemical criteria:  $\delta D$ , Cl,  $SO_4$ , quartz and Na/K geothermometers and the relation to enthalpies and feed temperatures.

For this work, the division by Ármannsson et al. (2015) will be adopted and wells classified accordingly. The subareas considered are: Leirbotnar (upper and lower), Leirhnjúkur, Vítismór, Suðurhlíðar, Vesturhlíðar, Hvíthólar, and Sandabotnar (Figure 4 and Figure 5). It should be noted that such classification will always be ambiguous, as many wells probably draw from different feeds. For the newer directional wells it seems that the location of aquifers and their depth is very important for well classification into subareas.

### 7.3 Reference temperature

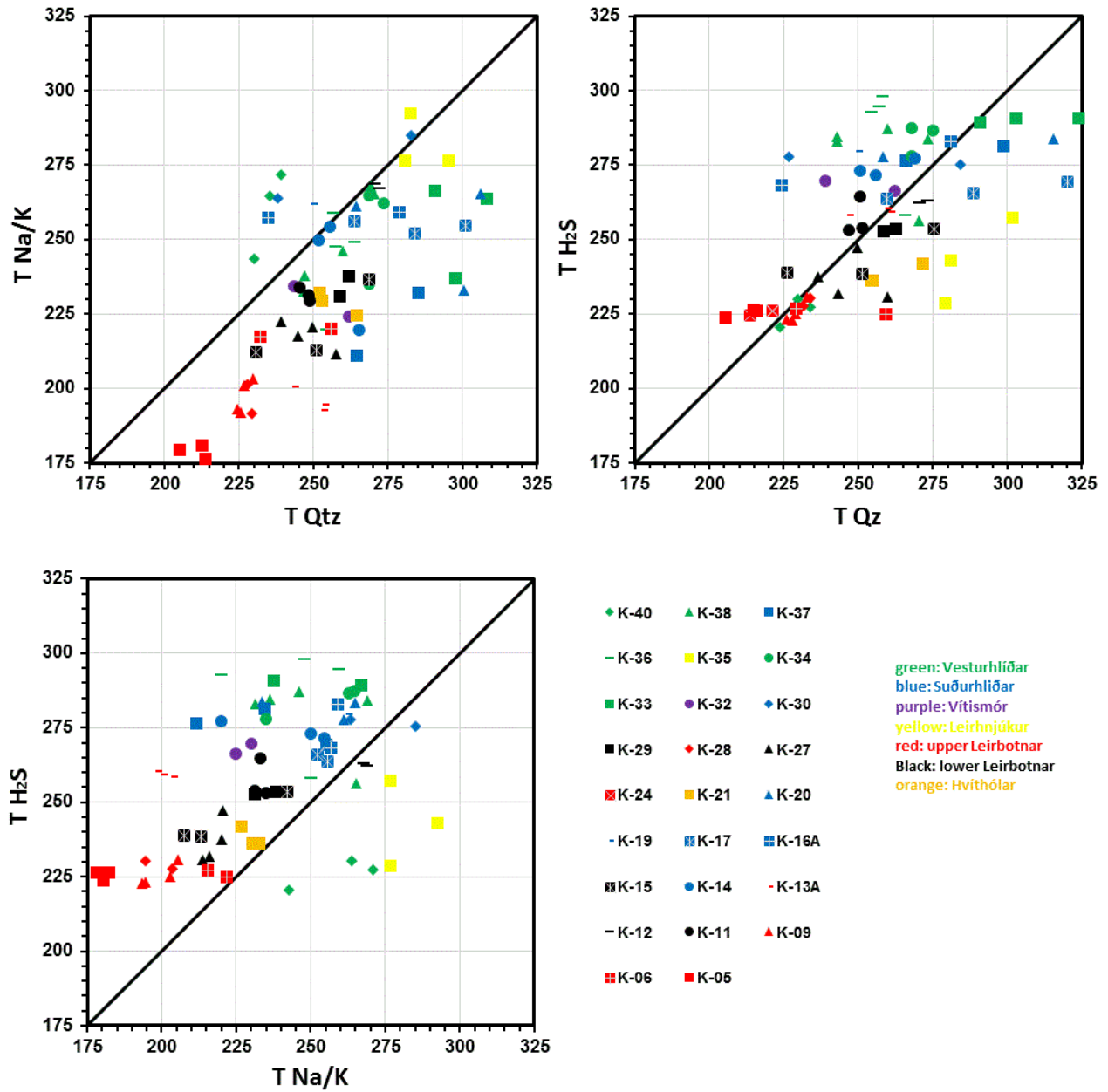
For a deep fluid composition calculation a reference temperature needs to be selected. Therefore different geothermometer temperatures were calculated and compared besides referring to temperature log profiles. A summary of various geothermometer temperatures is given in Table 2 and Figure 24. Geothermometer temperatures show a large variation for Krafla wells as already noted by Guðmundsson and Arnórsson (2002, 2005), and Ármannsson et al. (2015). In general, all calculated geothermometer temperatures (quartz, Na/K,  $H_2S$ ) are lower than the maximum aquifer temperatures derived from temperature logs, which may indicate an inflow or circulation of colder fluids and/or the existence of multiple aquifers within a single well – which is often the case. Temperatures calculated using the Na/K geothermometer (Arnórsson et al., 1983) are generally significantly lower (Figure 24) than temperatures calculated using the quartz geothermometer (Fournier and Potter, 1982). Nevertheless, calculated temperatures for various subareas within the Krafla geothermal system are in general consistent (Figure 24). An exception is found for Vesturhlíðar, where K-34 and K-33 show  $H_2S$  temperatures of 285–290°C in contrast to K-40, which yields a significantly lower  $H_2S$  temperature of 226°C. Temperatures calculated based on  $H_2S$  geothermometry (Arnórsson et al., 1998) show a narrow temperature interval for high enthalpy wells in specific subareas (lower Leirbotnar, Vesturhlíðar, Suðurhlíðar) (Figure 24), indicating phase segregation at depth.

Reference temperatures for wells K-5 to K-28 are adapted with slight modifications from Guðmundsson and Arnórsson (2002, 2005). For wells K-29 to K-40 reference temperatures are selected using calculated geothermometer temperatures and temperature logs.

### 7.4 Deep liquid composition

Results of the analyses of two-phase samples are presented as the chemical composition of the deep liquid, as calculated by the chemical speciation program WATCH, version 2.4 (Bjarnason, 2010), with slightly modified carbonate data, and using the reference temperatures listed in Table 2. For wells with excess enthalpy, i.e. enthalpy significantly higher than enthalpy of steam-saturated water at the selected reference temperature (Table 2; Figure A 1 to Figure A 6) the deep liquid composition is calculated by assuming phase segregation at  $T_{ref}-30^\circ C$  based on the method described by Arnórsson et al. (2007).

The calculated chemical composition of the deep liquid in the two-phase wells in the Krafla geothermal field is shown in Table 3 as average composition. The concentration of each component is given as milligrams of solute per kilogram of solution.



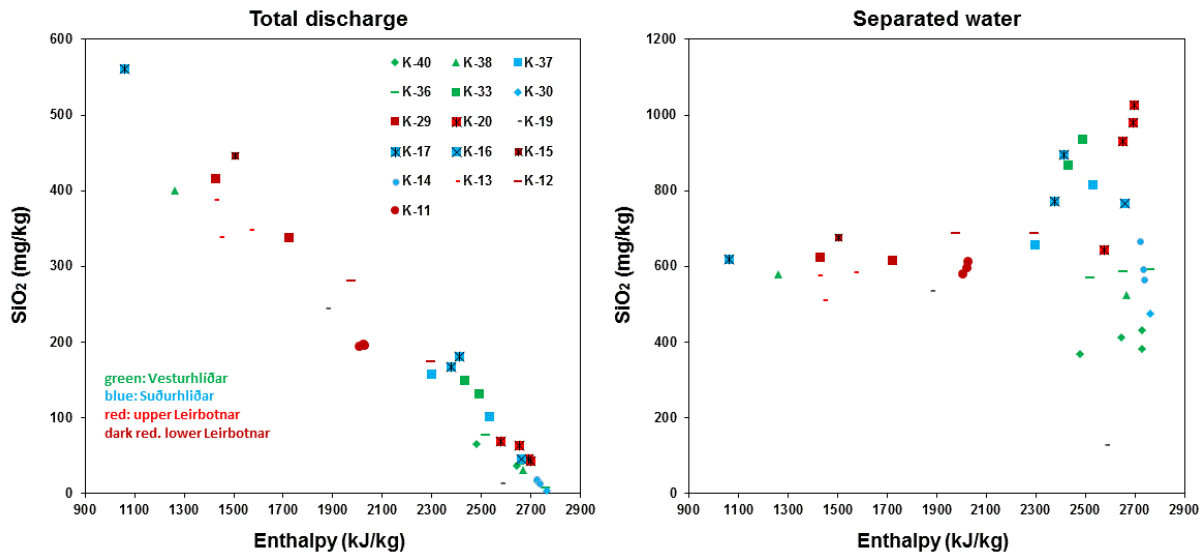
**Figure 24.** Correlation of calculated temperatures by using different geothermometers: quartz (Fournier and Potter, 1982), Na/K (Arnórsson et al., 1983), and H<sub>2</sub>S (Arnórsson et al., 1998).

Figure 26 to Figure 34 show the temporal evolution of the deep liquid composition of individual wells in the Krafla geothermal area for the reporting interval 2000–2014.

In general, the variation within individual wells in the period studied is rather limited, in contrast with the variation between different wells and subareas. It should be pointed out that no two wells have very similar chemical characteristics, which illustrates the complex geological and hydrological system of the Krafla geothermal field.

All deep liquid compositions yield low CO<sub>2</sub>/H<sub>2</sub>S ratios (<15) (Table 3) implying that no magmatic fluids contribute to the Krafla geothermal system, in contrast to fluids encountered in the wake of the Krafla Fires in the 1970s and 1980s (e.g. Ármannsson et al., 1989; Mortensen et al., 2009a).

In high enthalpy wells (Table 2, Figure A 1 to Figure A 6) phase segregation (i.e. two-phase flow conditions) is assumed within specific subarea reservoirs (Suðurhlíðar, Vesturhlíðar, lower Leirbotnar, Vítismór). The silica content of total discharge and separated water from excess enthalpy wells are plotted against measured enthalpy in Figure 25. The total discharge concentration steadily decreases as the discharge enthalpy approaches saturated dry steam. The observed correlation suggests that phase segregation in the producing aquifers is, largely the cause of excess discharge enthalpy, at least for wells with discharge enthalpy > 2000 kJ/kg. High boron concentrations (Table 3, Figure 28) are indicative for phase segregation (Arnórsson and Andrésdóttir, 1995).



**Figure 25.** Silica content of discharge from the excess enthalpy wells against discharge enthalpy.

Chloride is mainly derived from atmospheric precipitation but may be added from magmatic sources, which can be expected in the deepest hottest wells. However, this trend is not observed throughout the Krafla geothermal system (Figure 32). The fluids from wells K-16A, K-20, K-21, and K-34 show some increase in chloride concentration with time (Figure 32). In contrast, the chloride concentration and that of other solute components in K-37 and K-38 fluids (Figure 32) appears to decrease with time. An increase of chlorine concentration may be caused by distillation of the liquid fraction during boiling in the reservoir or wells (the latter is likely for the high enthalpy wells K-16A, K-20 and K-34), but declining chloride concentration may be attributed to inflow of colder waters into the reservoir as a result of production. However, it seems that in the

most recent samples from K-37 and K-38, the liquid phase has been mixed with steam condensate, and therefore the observed changes in deep liquid Cl concentration, are probably not real.

Sulphate is the dominant anion in cooler and especially low enthalpy wells, in particular in lower Leirbotnar (Table 3, Figure 34). Guðmundsson and Arnórsson (2002) suggest that sulphate concentrations are controlled by anhydrite solubility in all except the hottest wells, and that this effect is caused by the retrograde solubility of anhydrite, i.e. that anhydrite is being dissolved from rock as a result of cooling of the reservoir. Increasing sulphate concentrations in wells producing from the lower Leirbotnar reservoir (e.g. K-15) indicate that cooling, or influx of cooler fluids is now affecting the deeper part as well.

Carbonate concentrations are remarkably high in the fluids from Suðurhlíðar, Vesturhlíðar, and Vítismór and is in most cases the dominant anion (

Figure 30). This is consistent with high CO<sub>2</sub> concentration in fumarole steams in these subareas (Kristinsson et al., 2014) and could be a remnant of the volcanic activity. The CO<sub>2</sub> concentration declines significantly in wells K-16A and K-36, whereas the CO<sub>2</sub> concentration increases in wells K-17, K-30 and K-34 (

Figure 30). The change may possibly be explained as contamination of liquid with steam condensate as well as changes in the wellhead pressure for K-36. It should also be noted that for excess enthalpy wells, the gas concentrations calculated using the method of Arnórsson et al., (2007) depend on the measured enthalpy and selected phase segregation temperature, which may cause some scatter.

The deep liquid in the Krafla production wells generally has a pH of 6.3 to 7.5 (Figure 26), but separated water at atmospheric pressure is typically quite basic, with a pH of 8 to 10. The wells with lowest pH are excess enthalpy wells in Vesturhlíðar, samples from which may be slightly mixed with steam condensate. During and after the Krafla Fires, some wells, particularly those producing from the lower Leirbotnar reservoir (K-12, K-15, K-29) discharged acidic fluids with pH < 6 and in the extreme case of well K-4 which blew up, the liquid pH was as low as 1.8 (Gíslason and Arnórsson, 1976). Low discharge pH has also been observed in some samples from K-38.

In summary, individual subareas show a distinct pattern in B, Ca, Cl, CO<sub>2</sub>, F, H<sub>2</sub>, H<sub>2</sub>S, Na, and SO<sub>4</sub> concentrations (Figure 28 to Figure 34). However, there are several inconsistencies suggesting fluid contribution from different aquifers and different subareas in marginal or deviated wells.

## 7.5 Subarea characteristics

In the following section the basic chemical characterization of deep liquid composition of each subarea is summarized and information given about relative concentration differences between fluids from subareas (Figure 25 to Figure 34; Table 3 and Table 4, Figure A 1 to Figure A 6).

### 7.5.1 Leirbotnar

The Leirbotnar subarea (K-1, K-3A, K-5, K-6, K-7, K-9, K-11, K-12, K-13A, K-15, K-24, K-26, K-27, K-28, and K-29) can be further distinguished into upper (shallower) and lower (deeper) reservoirs, with different temperatures and characteristics. Upper Leirbotnar wells are in general low enthalpy wells with an average feed temperature of about 200°C, whereas in the lower reservoir

higher temperatures and enthalpy are encountered. The chemical composition of the deep liquid is characterized by a very narrow composition range, in contrast to other subareas, which show a larger variation. The deep fluids show low concentrations of B, Cl, CO<sub>2</sub>, and H<sub>2</sub>S. On the other hand, the lower Leirbotnar reservoir fluids have slightly higher concentrations of CO<sub>2</sub> and H<sub>2</sub>S. Na and Ca concentrations are high in the upper Leirbotnar reservoir fluids, whereas lower Leirbotnar fluids have slightly lower concentrations of both. High SO<sub>4</sub> concentrations are a distinctive feature of the Leirbotnar fluids. Only the K-32 (Vítismór) fluid has similar SO<sub>4</sub> concentrations. Deuterium values ( $\delta D$ ) are in the range -85 to -89‰ SMOW (see chapter 7.6).

### 7.5.2 Vítismór

The Vítismór subarea consists of following wells: K-2, K-4, K-8, K-10, K-25, K, 32, and IDDP-1. The reservoir is divided into upper and lower parts, like Leirbotnar, with higher enthalpy and temperatures in the deeper reservoir. Only well K-32 is considered here. It is directionally drilled from the well pad of K-15 (Leirbotnar, near Hveragil) to NE and then NW, thus going through upper Leirbotnar, into Suðurhlíðar and then towards Vítismór. The well-bottom is near K-2. The enthalpy evolution (Figure A 1 to Figure A 6) of the well is interesting. It started as a high enthalpy well, but with time the enthalpy declined significantly to low enthalpy (~1200 kJ/kg) conditions between 2000 and 2005. Deep liquid composition is characterized by high H<sub>2</sub>S concentrations and medium CO<sub>2</sub> concentrations. SO<sub>4</sub> concentrations are higher now than before 2005 and at a similar range as wells from upper Leirbotnar. Ca and Na are found in medium and high concentrations. In fact, it may be said that the liquid phase of the well appears to be typical for upper Leirbotnar, although slightly richer in CO<sub>2</sub>, but the steam phase looks as if it originates in Suðurhlíðar. Deuterium values ( $\delta D$ ) for the liquid phase are -85‰SMOW, again similar to Leirbotnar, but about -92‰SMOW for the steam phase, which is typical for Suðurhlíðar.

### 7.5.3 Leirhnjúkur

Well K-35 is the only well in subarea Leirhnjúkur. It is a high enthalpy well (average 2176 kJ/kg) characterized by high Cl and low SO<sub>4</sub> concentrations. CO<sub>2</sub> concentrations are higher than in the Leirbotnar and Hvíthólar subareas, but distinctively lower than in Suðurhlíðar. This reflects a similar trend seen in fumaroles in Krafla; the CO<sub>2</sub> and H<sub>2</sub>S concentrations in the Leirhnjúkur area are much lower than in fumaroles on the slopes of Mt. Krafla (Kristinsson et al., 2014). The sample from 2014 has  $\delta D = -91\text{‰SMOW}$ .

### 7.5.4 Suðurhlíðar

The Suðurhlíðar subarea comprises the following wells: K-14, K-16A, K-17, K-19, K-20, K-30, K-31, K-37, and K-39, which are all high enthalpy wells (Figure A 1 to Figure A 6). As a result, many samples bear marks of mixing with condensate. The deep liquid composition (calculated taking the excess enthalpy into account) is characterized by low Na, SO<sub>4</sub>, and Ca concentrations. On the other hand, CO<sub>2</sub> and H<sub>2</sub>S concentrations are high in all wells and Cl and B concentrations in some wells. The F concentration in well K-14 is unusually high (Figure 33) and has been so persistently since the well was drilled. Wells K-17 and K-19 also have high F concentrations and high F/Cl ratios (Table 3). It is possible that some of the Cl and F are magma-derived, as both HCl and HF were found in the discharge of nearby well IDDP-1 (Ármansson et al., 2014). Deuterium isotope values range from -91 to -95‰ (SMOW).

**Table 3.** Average deep liquid composition.

Subarea	Well	SiO <sub>2</sub>	Na	K	Mg	Ca	F	Cl	SO <sub>4</sub>	B	Fe	Al	CO <sub>2</sub>	H <sub>2</sub> S	H <sub>2</sub>	N <sub>2</sub>	O <sub>2</sub>	CH <sub>4</sub>	pH	CO <sub>2</sub> /H <sub>2</sub> S	Cl/SO <sub>4</sub>	Na/Cl	F/Cl *1000
Hvíthólar	K-21	516	158	21	0.001	1.20	0.86	130	54	0.6	0.004	1.18	356	79	1.15	6.25	0.16	2.47	7.0	4.5	2.4	1.2	7
Leirbotnar lower	K-29*	514	163	25	0.024	2.08	1.03	28	156	0.7	0.013	1.47	653	113	1.89	2.56	0.28	0.25	7.1	5.8	0.2	5.9	37
Leirbotnar lower	K-27	461	185	25	0.001	2.69	0.80	34	219	0.5	0.004	1.16	388	85	1.25	5.78	0.19	0.90	7.1	4.6	0.2	5.5	24
Leirbotnar lower	K-15	493	226	32	0.026	2.32	1.02	27	269	0.4	0.002	0.86	218	103	0.83	1.35	0.26	0.30	7.5	2.1	0.1	8.5	38
Leirbotnar lower	K-12*	554	105	22	0.022	1.41	1.35	30	93	1.2	0.010	1.19	1076	119	2.55	1.55	0.31	0.36	6.8	9.0	0.3	3.5	45
Leirbotnar lower	K-11*	442	158	23	0.005	1.56	1.29	29	126	0.9	0.012	0.76	422	100	1.13	2.16	0.23	0.19	7.1	4.2	0.2	5.3	44
Leirbotnar upper	K-28	396	204	22	0.004	4.69	0.64	32	244	0.5	0.010	0.71	362	54	0.31	2.81	0.16	0.46	6.9	6.7	0.1	6.4	20
Leirbotnar upper	K-24	342	187	15	0.001	3.02	0.66	39	218	0.5	0.001	0.72	138	46	0.05	4.94	0.28	0.67	7.2	3.0	0.2	4.8	17
Leirbotnar upper	K-13A*	492	207	23	0.001	3.23	1.02	35	258	0.9	0.002	1.04	272	114	2.76	0.99	0.12	0.15	7.0	2.4	0.1	5.8	29
Leirbotnar upper	K-9	384	194	21	0.025	4.91	0.77	32	229	0.5	0.024	0.92	209	51	0.13	3.30	0.16	0.30	7.2	4.1	0.1	6.0	24
Leirbotnar upper	K-6	455	154	20	0.001	0.92	0.59	13	118	0.2	0.002	0.62	318	64	0.87	16.90	0.24	1.45	7.4	4.9	0.1	11.8	45
Leirbotnar upper	K-5	315	175	15	0.001	3.68	0.89	38	214	0.5	0.001	0.84	110	45	0.18	4.32	0.23	0.51	7.2	2.5	0.2	4.6	23
Leirhnjúkur	K-35*	748	123	24	0.023	0.31	1.63	132	6	2.9	0.041	0.51	511	106	2.22	2.63	0.01	1.48	7.1	4.8	21.3	0.9	12
Suðurhlíðar	K-37*	573	127	16	0.002	0.55	0.82	33	27	2.6	0.004	0.71	799	181	6.66	0.99	0.14	0.27	7.0	4.4	1.2	3.8	25
Suðurhlíðar	K-30*	415	76	17	0.001	0.76	1.17	43	22	3.0	0.003	0.75	1213	195	5.21	0.82	0.07	0.30	6.6	6.2	2.0	1.8	27
Suðurhlíðar	K-20*	597	190	31	0.001	0.94	1.29	157	9	2.4	0.002	0.30	1472	202	5.53	1.35	0.14	0.43	7.0	7.3	17.5	1.2	8
Suðurhlíðar	K-19*	280	121	18	0.001	0.17	4.37	20	6	12.9	0.008	0.60	971	193	4.09	1.13	0.08	0.19	6.7	5.0	3.6	6.0	217
Suðurhlíðar	K-17*	643	111	18	0.000	0.30	1.99	15	5	1.3	0.003	1.03	507	161	3.78	2.31	0.15	0.64	7.4	3.2	2.8	7.6	136
Suðurhlíðar	K-16A*	451	109	18	0.001	0.44	0.98	80	6	1.5	0.003	0.68	1571	189	9.18	1.92	0.15	1.09	6.7	8.3	14.4	1.4	12
Suðurhlíðar	K-14*	354	101	15	0.001	0.12	3.20	11	2	7.0	0.008	0.11	805	160	5.13	0.91	0.07	0.20	6.9	5.0	5.2	9.2	292
Vesturhlíðar	K-40*	365	49	9	0.005	0.68	1.02	13	12	2.0	0.015	1.14	1474	105	2.09	2.29	0.28	0.52	6.4	14.0	1.1	3.7	78
Vesturhlíðar	K-38*	406	138	20	0.001	1.90	0.90	66	65	0.2	0.002	0.45	1647	236	4.00	16.98	1.03	0.31	6.6	7.0	1.0	2.1	14
Vesturhlíðar	K-36*	404	77	11	0.002	0.74	0.51	38	17	1.6	0.006	0.82	1212	262	5.18	2.29	0.14	0.18	6.4	4.6	2.2	2.0	14
Vesturhlíðar	K-34*	532	141	24	0.005	1.64	1.42	144	49	4.4	0.083	0.62	688	182	3.47	1.79	0.07	0.12	6.7	3.8	2.9	1.0	10
Vesturhlíðar	K-33*	630	124	20	0.001	0.53	1.58	81	10	2.1	0.002	0.49	343	253	4.62	1.41	0.13	0.13	7.2	1.4	8.3	1.5	19
Vítismór	K-32	473	217	33	0.001	2.85	0.93	32	240	0.5	0.001	1.15	424	234	3.70	1.73	0.08	0.34	7.0	1.8	0.1	6.8	29

\* deep liquid calculation calculated by assuming phase segregation at  $T_{ref} - 30^{\circ}\text{C}$  (method as described in Arnórsson et al., 2007). For reference temperature ( $T_{ref}$ ) see Table 2.

### 7.5.5 Vesturhlíðar

Wells K-33, K-34, K-36, K-38, and K-40 are located in the Vesturhlíðar subarea. The wells are high in enthalpy ( $> 2400$  kJ/kg). Judging by the conductivity of the liquid phase, well K-40 appears to be relatively dry, but the other wells give a proper liquid phase, albeit quite dilute and with a fairly low pH (6–7), which is reflected in the calculated deep liquid. This may be due to some mixing with condensed steam. B and CO<sub>2</sub> concentrations are high in the deep liquid. Cl concentrations are varied, but SO<sub>4</sub> concentrations are low. H<sub>2</sub>S occurs in medium concentrations and Ca and Na appear in medium to low concentrations. Whereas the chemical characteristics of the Vesturhlíðar wells are similar to Suðurhlíðar, the deuterium isotope values are similar to those of the Leirbotnar fluids, ranging from -84 to -89‰SMOW.

### 7.5.6 Hvíthólar

The Hvíthólar subarea (K-21, K-22, and K-23) comprises currently low enthalpy wells (~1200 kJ/kg) (Figure A 1 to Figure A 6). In this work only K-21 was considered as no samples have been collected from K-22 (which has a slightly lower enthalpy and draws fluid from cooler parts of the reservoir) since 1998, K-23 is non-productive. Cl concentrations are high and CO<sub>2</sub> concentrations are low in K-21. SO<sub>4</sub> values range between medium and low concentrations. Ca in general shows medium values. Deuterium values are similar to Suðurhlíðar; -91 to -93‰SMOW.

### 7.5.7 Sandabotnar

Only one well has been drilled in Sandabotnar, well KS-1, for which no chemical data were available. However, there exists a flow test report for the well (Giroud et al., 2008), which was drilled in 2007, where analyses of three samples are reported. After flowing for one month, the well had an enthalpy of 1450 kJ/kg and solute geothermometers agreed on a temperature of about 265–270 °C. The deep liquid has a TDS of about 950 mg/kg, and solute concentrations similar to upper Leirbotnar, except that SO<sub>4</sub> is very low. CO<sub>2</sub> and H<sub>2</sub>S are also higher than what is typical in Leirbotnar. However, what is most intriguing about well KS-1 is that the fluid is very depleted in heavy isotopes, with a  $\delta D$  of -115‰ (SMOW).

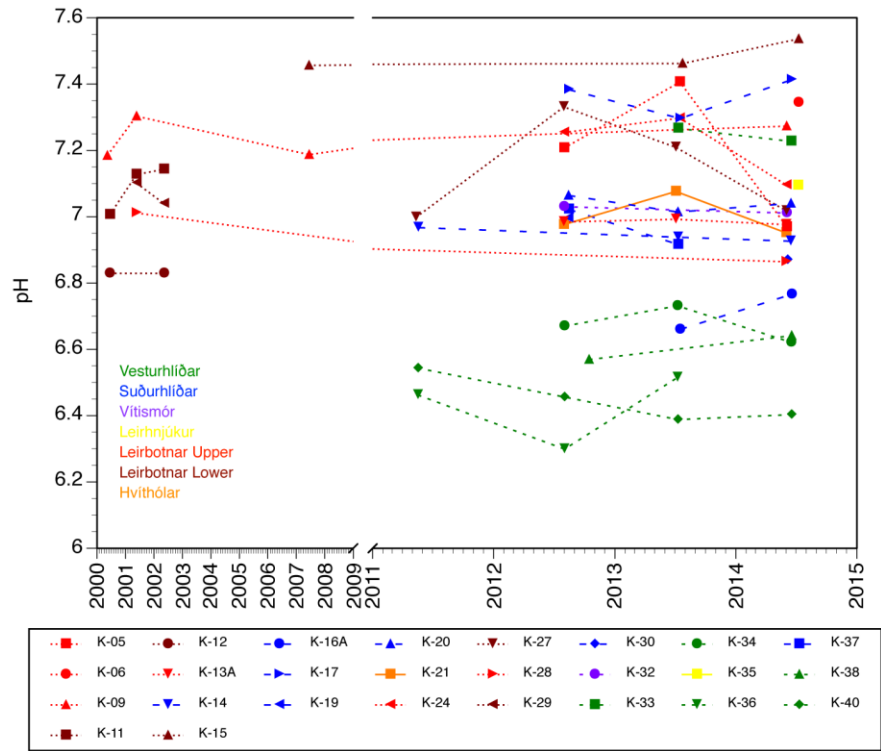


Figure 26. Evolution of pH in the deep liquid.

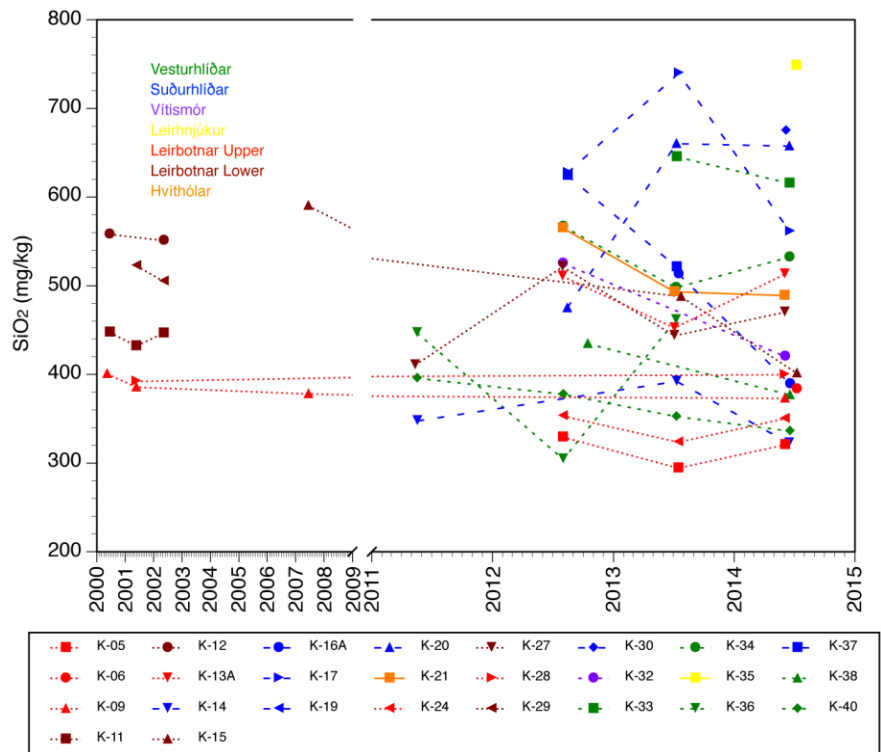


Figure 27. Concentration of silica in the deep liquid.

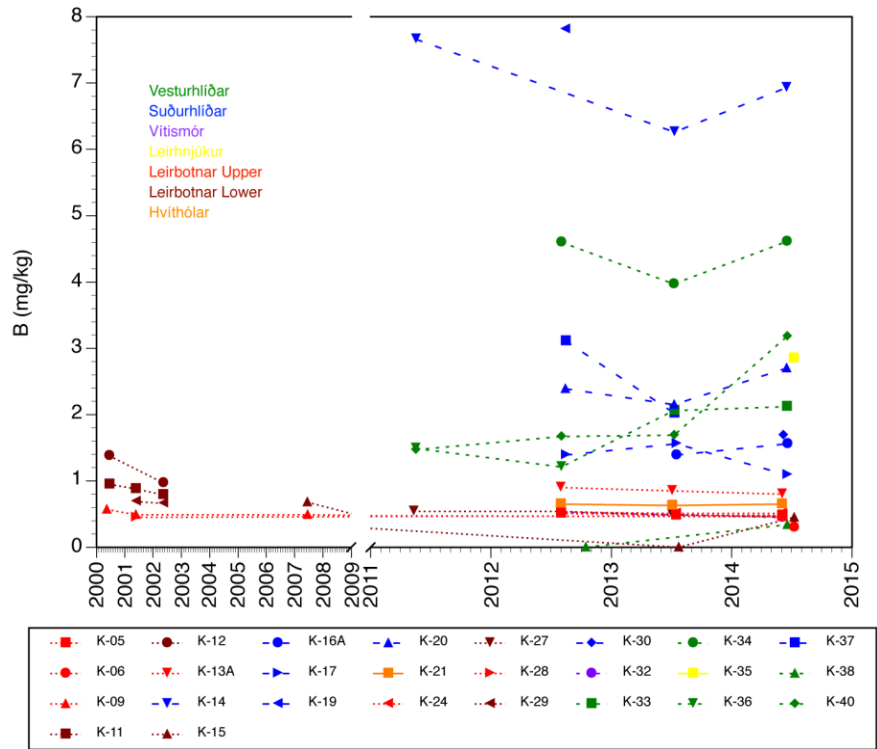


Figure 28. Concentration of boron in the deep liquid.

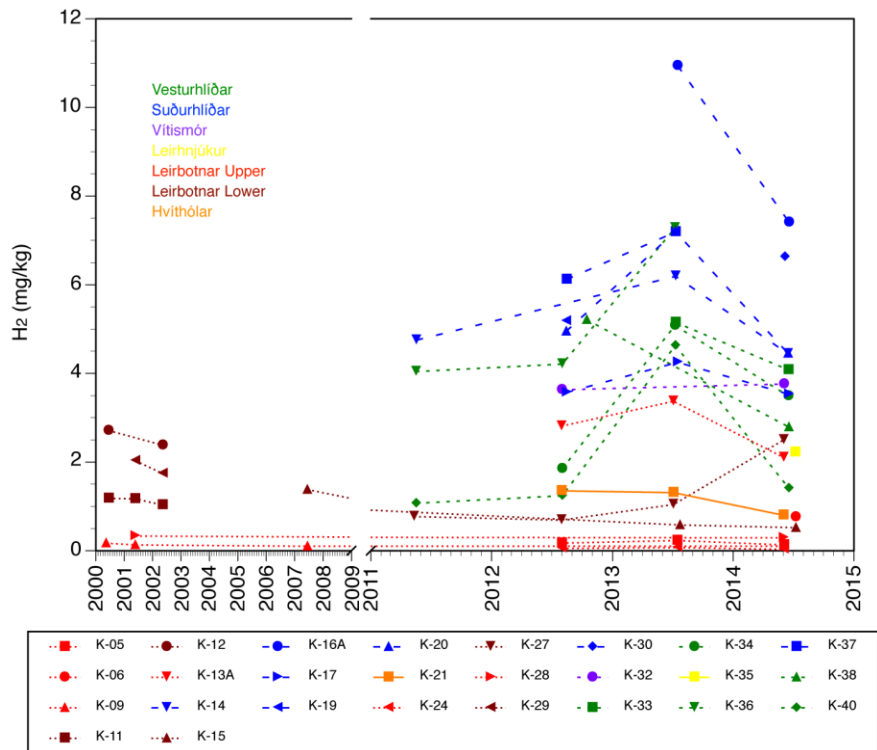


Figure 29. Concentration of hydrogen in the deep liquid.

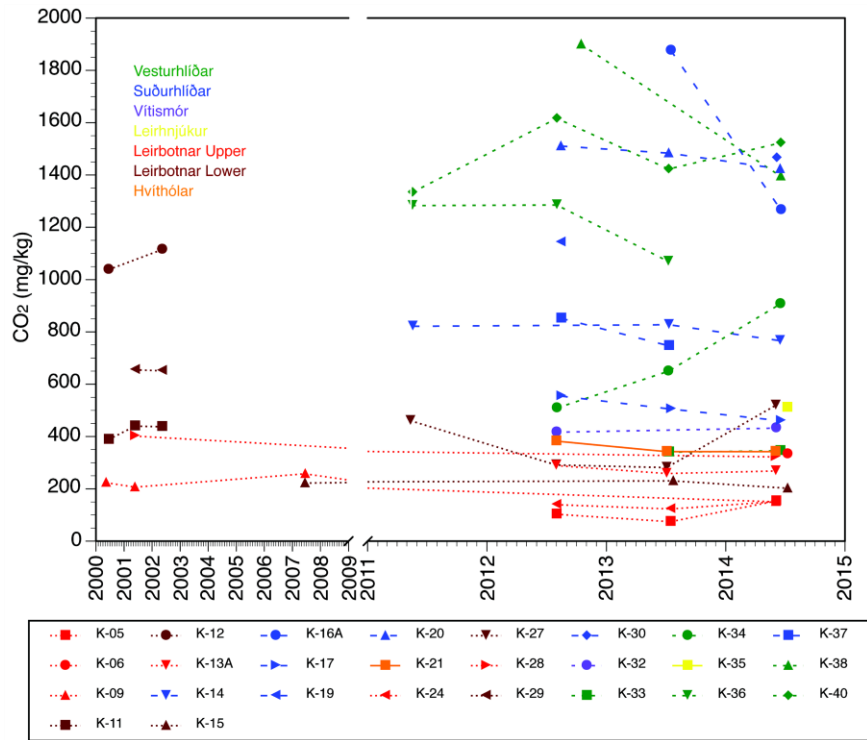


Figure 30. Concentration of carbon dioxide in the deep liquid.

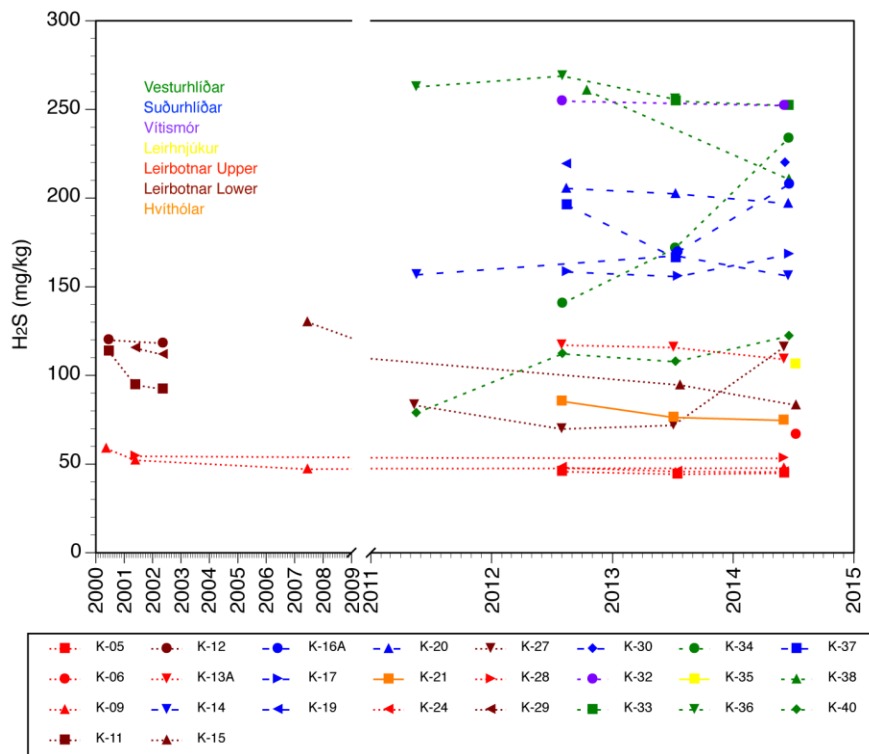


Figure 31. Concentration of hydrogen sulfide in the deep liquid.

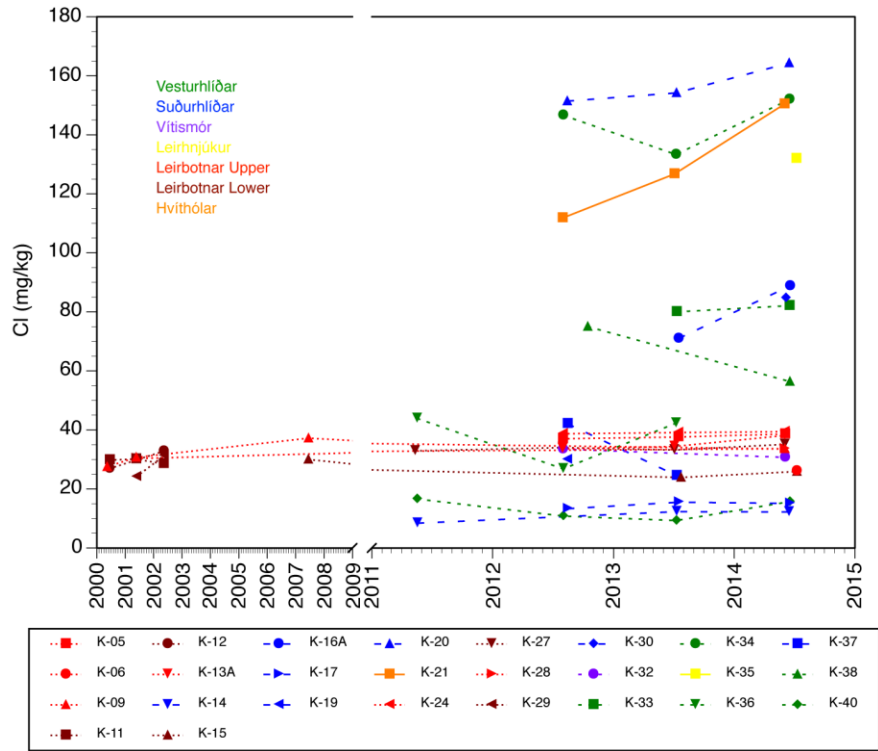


Figure 32. Concentration of chloride in the deep liquid.

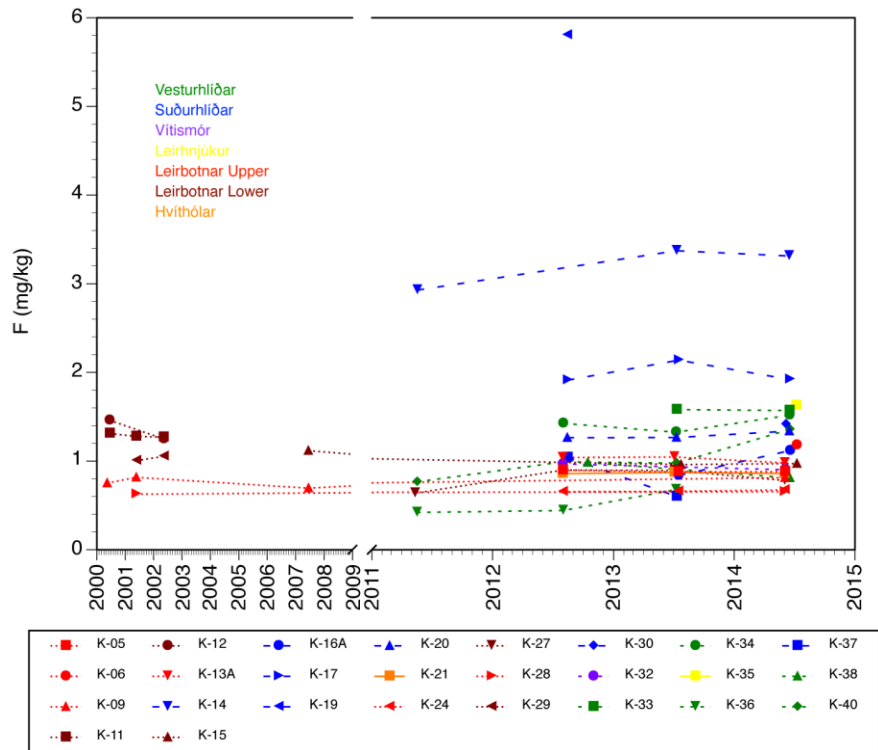


Figure 33. Concentration of fluoride in the deep liquid.

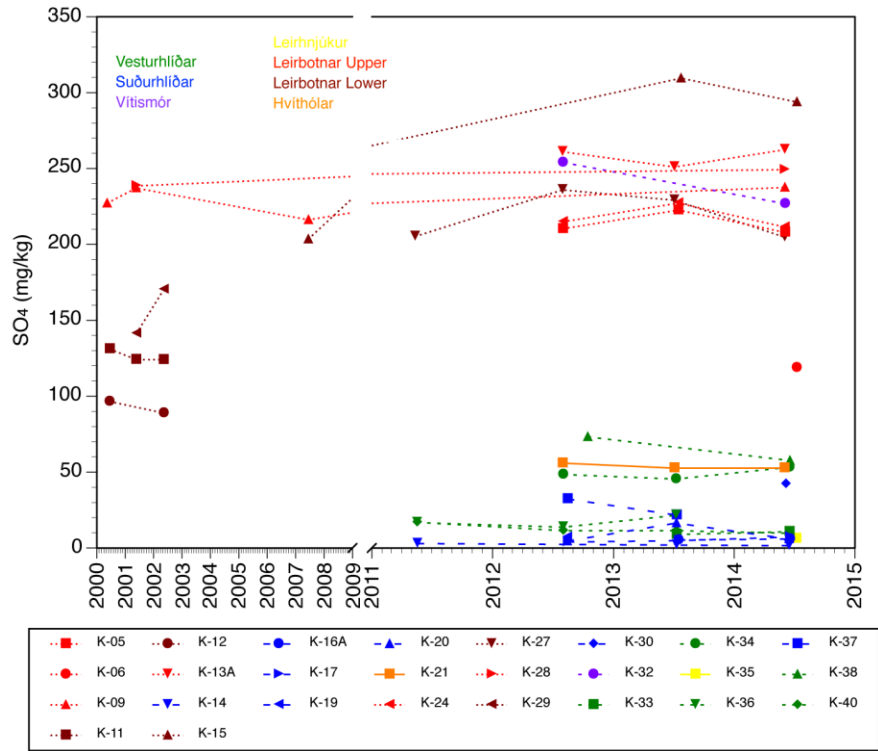


Figure 34. Concentration of sulphate in the deep liquid.

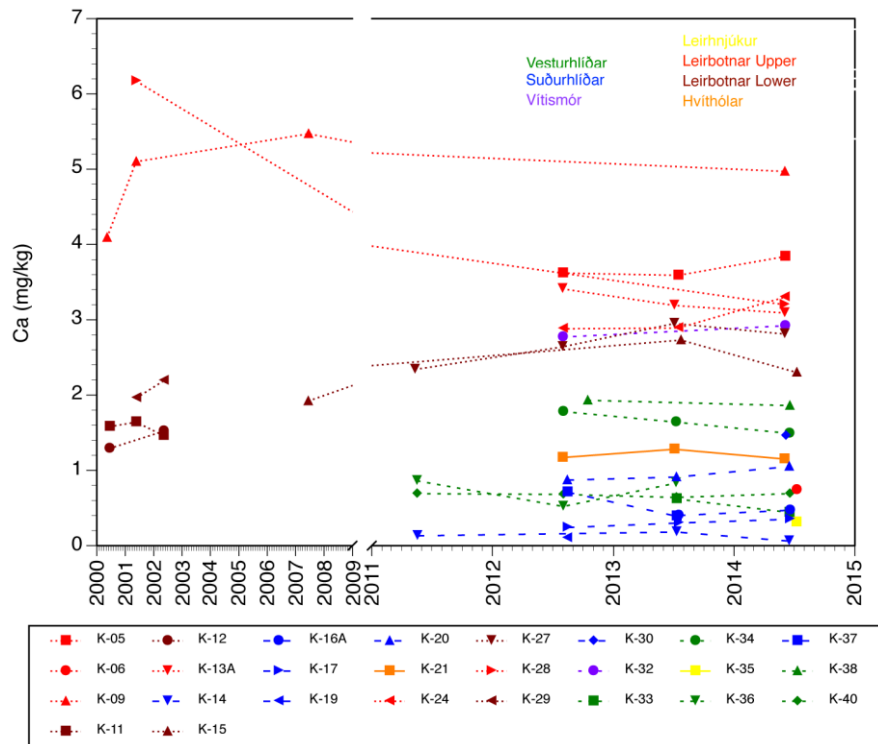


Figure 35. Concentration of calcium in the deep liquid.

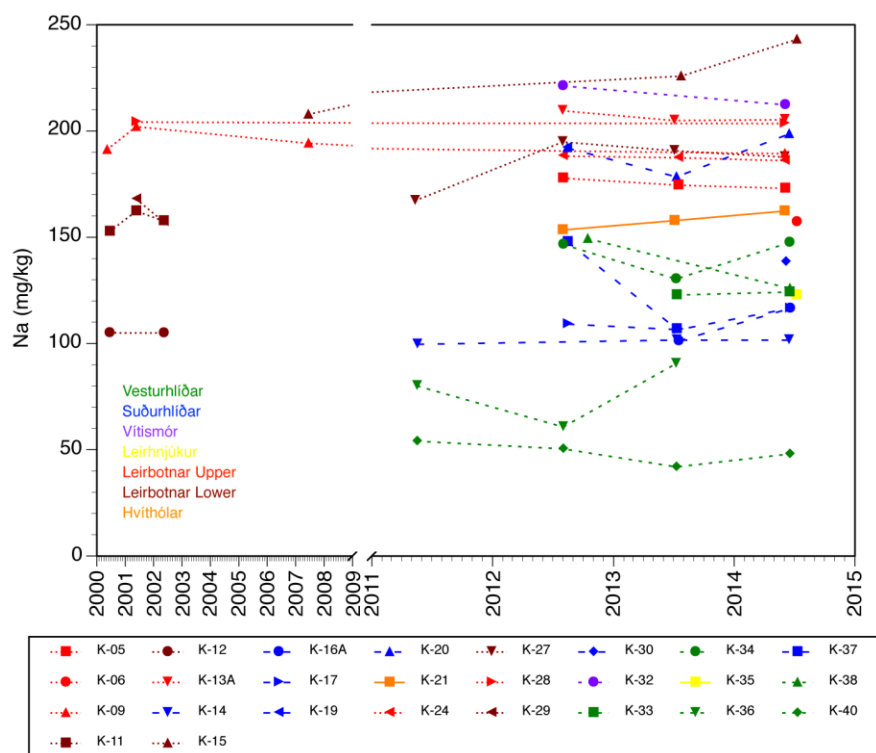


Figure 36. Concentration of sodium in the deep liquid.

Table 4. Krafla wells. General trends and average values for subareas

Area	Wells		Enthalpy* (kJ/kg)	Feed temperature* (°C)	T <sub>O<sub>2</sub></sub> * (°C)	T <sub>Na/K</sub> * (°C)	Cl vs SO <sub>4</sub> concentration	δD ‰
Hvíthólar	K-21, K-22, K-23	Upper part	1580	260	270	240	Cl > SO <sub>4</sub>	-91 - -93
		Lower part	1030	200	210	200	Cl <sub>2</sub> > SO <sub>4</sub>	-91 - -93
Sandabotnar	KS-1		1450	300	260	280	Cl > SO <sub>4</sub>	-115
Suðurhlíðar	K-14, K-16, K-16A, K-17, K-18, K-19, K- 20, K-30, K-31, K- 37, K-39		2600	290	250	270	Cl > SO <sub>4</sub>	-91 - -95
Leirbotnar	K-1, K-3, K-3A, K-5, K-6, K-7, K-9, K-11, K-12, K-13, K-13A, K-15, K-24, K-26, K- 27, K-28, K-29	Upper part	980	205	230	190	SO <sub>4</sub> > Cl	-85 - -89
		Lower part	1200	320	250	220	SO <sub>4</sub> > Cl	-85 - -89
Leirhnjúkur	K-35		2260	320	350	310	Cl > SO <sub>4</sub>	-79 - -88
Vítismór	K-2, K-4, K-8, K-10, K-25, K-32, IDDP-1	Upper part	1060	210	-	-	SO <sub>4</sub> > Cl	-80 - -90
		Lower part	1420	300	250	230	SO <sub>4</sub> > Cl	-80 - -90
Vesturhlíðar	K-33, K-34, K-36, K- 38, K-40		2700	320	290	280	Cl > SO <sub>4</sub>	-84 - -89

\* average

## 7.6 Origin of recharge to the Námafjall Krafla area

It is suggested that fluid flow in the Leirbotnar, Leirhnjúkur, Vítismór and Vesturhlíðar areas is locally derived as the deuterium isotope shifts are close to values of local precipitation. Darling and Ármannsson (1989) suggested that the Suðurhlíðar and Hvíthólar fluids originated from nearby high ground Hágöng. However, the hydrology of the area implies that Hágöng is unlikely to be able to supply such a large flow and that deep flow from the south, i.e. the same stream that is predicted to feed the Námafjall system is responsible (Ármannsson et al., 2015; Figure 37). As previously mentioned, the Sandabotnar well is quite different and its isotopic composition suggests a deep inflow from far south and possibly old fluids. It seems possible that the Hveragil fissure and related features (Figure 4) may act as a barrier between the local and southerly flows although some mixing is likely to occur.

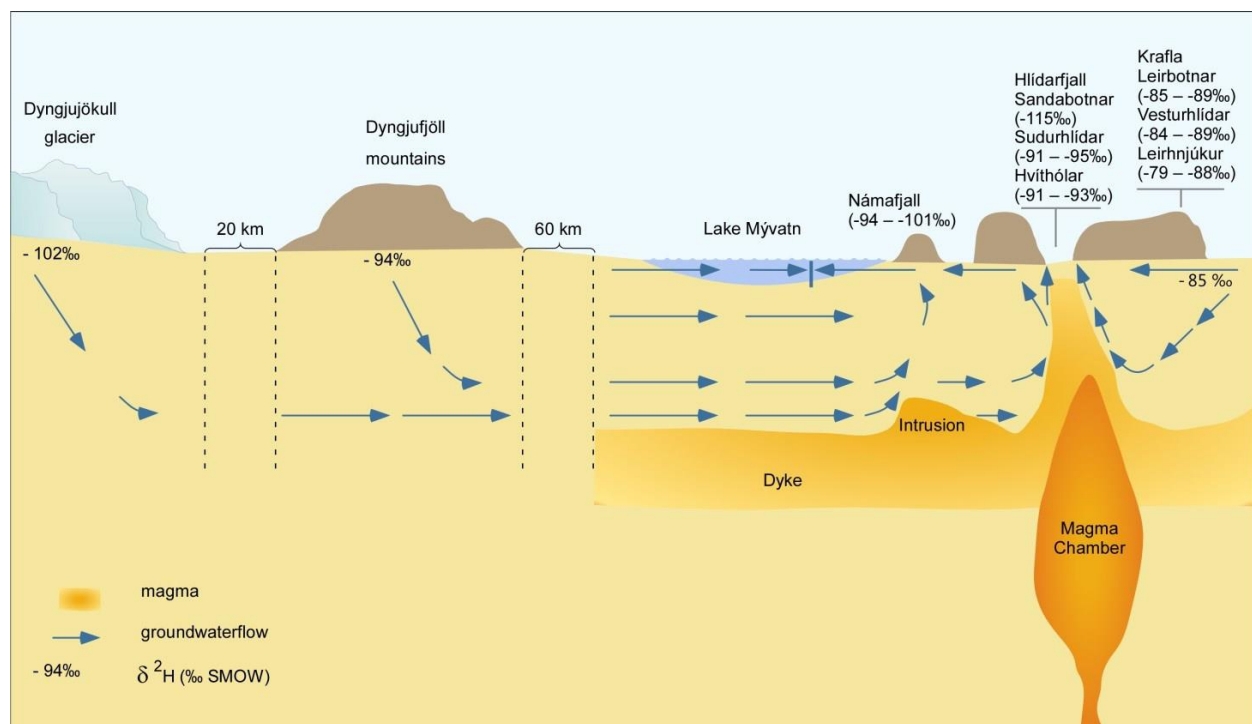


**Figure 37.** Proposed groundwater flow to the Námafjall and Krafla geothermal systems (after Hjartarson et al., 2004).

It should be mentioned that phase segregation (see chapter 7.4) in wells of the Krafla geothermal system exhibiting excess enthalpy distorts the isotope composition of fluids discharged at the wellhead, such that they do not represent aquifer fluids. In a recent study by Pope et al. (2015) a new hydrogeological model is presented, which is based on epidote stable isotope analysis, re-evaluation of stable isotope data (unpublished data from Guðmundsson and Arnórsson, 2002) considering phase segregation and estimation of the original vapor fraction of aquifers in the Krafla geothermal system. The model, which considers wells from Leirbotnar and Suðurhlíðar expands upon previous interpretations by Böðvarsson et al. (1984), Giroud (2008), and Arnórsson (2012). They state that the local groundwater that sourced from the highland to the north (Hágöng)

are the primary fluid source for the Krafla geothermal system. Groundwater enters the hydrothermal system via N-S trending fissure swarms west of the geothermal system flowing into discrete zones of high permeability that are separated by low-permeable lithologies. Below ~1900 m groundwater is heated to boiling by a conductive layer of superheated steam overlying the magma heat source. Vapor is risings rapidly along discrete steeply dipping structure in the Leirbotnar portion of the hydrothermal system and mixes with cooler groundwater of upper (shallower) aquifers. Increased permeability at Hveragil drives convective circulation and, increasing temperatures of the primary aquifer cause boiling. Fluids are vapor-rich, due to depressurization in the high-permeability zone, and CO<sub>2</sub>-rich due to increased input of magmatic volatiles. The hydrological gradient cause southward migration of groundwater. The mixing of primary aquifer fluids with vapor and magmatic-rich lower aquifer fluids results in progressively lower  $\delta D_{\text{FLUID}}$  values observed in Suðurhlíðar, Hvíthólar, and Námafjall.

Pope et al. (2015) conclude that although the subareas Leirbotnar and Suðurhlíðar have widely different physical and chemical characteristics, the variability in stable isotope composition of the geothermal fluids in those subareas does not require different meteoric water sources. In fact, it is the result of localized boiling, phase separation with variable mobilization of the vapor and liquid-fractions of the fluids, and intermittent mixing with magmatic gases.

## 7.7 Parameters controlling fluid flow

Fluid flow is controlled by porosity and permeability and those parameters vary depending on rock type and alteration state. For example, the porosity of fresh hyaloclastite is on average 25–35%. In contrast, the porosity of basaltic lavas is 5–15% with a large porosity heterogeneity within a single lava flow (Sigurðsson and Stefánsson, 1994). During hydrothermal alteration open pore space (e.g. vesicles) are filled with secondary minerals. The reduction in pore space by alteration and secondary mineral formation (Weisenberger and Selbekk, 2009) results in permeability decrease within the altered rock.

The Krafla geothermal system is characterized by intense alteration and fresh rocks occur only rarely at shallow depths within Vítismór, Leirbotnar, and Suðurhlíðar. Due to the high alteration degree and secondary mineral precipitation, porosity in the Krafla geothermal system is low and results in low permeability. Permeability is therefore mostly related to faults and fissures, as well as in structural positions associated with intrusions. Wells have been located and designed to penetrate through fissures, faults, and intrusions. Such structural features are usually steeply dipping and directional drilling has been used more frequently to direct the wells with more certainty towards a pre given target zone.

Fissures in Krafla volcanic system strike dominantly in NNE-SSW direction. High permeability is associated with the fault zone related to the explosive craters by Hveragil, the Víti fault system, the eruption fissures of the Hólar fires, and the Dalur fires, and the fissures south of Leirhnjúkur, towards the eruption fissure of the Mývatn fires

In addition to the major strike direction (NNE-SSW), E-W faults occur in Suðurhlíðar, which were active during the Krafla fires. These faults are intersected by wells K-16A, K-20 and K-37 and feed

zone are associated with the fault planes. Furthermore, a fault in Leirbotnar with N-S to NNW-SSE strike has also been linked to high permeability.

Permeability by the southern rim of the caldera is related to the prevailing NNE-SSW strike of eruption fissures and faults as well as to the caldera fracture. Minor permeability was noted in well KV-1 in Vestursvæðið even though it is located at the western side of the NNE-SSW fissure swarm. The area appears to have cooled down and low permeability is presumed to be caused by the precipitation of alteration minerals in vesicles and fractures. It is also possible that the vertical well does not intersect the fracture zone.

Increased permeability in wells can also be associated with felsic intrusions. In the Leirbotnar and Vítismór areas wells penetrate through thin felsic intrusions at various depths. There is, furthermore, a thick and widespread granophyre intrusion at around 1500 m b.s.l. beneath Vítismór where powerful feed zones have been associated with acid fluids. Major feed zones in the wells in Suðurhlíðar are associated with a 200–400 m thick felsic intrusion complex at 200–600 m b.s.l. (Mortensen et al., 2009a).

## **8 Reservoir conditions and production analysis**

### **8.1 Temperature conditions**

The interpreted formation temperature in wells drilled in Krafla and the available temperature well logs were examined in order to estimate the need for reinterpretation, especially with respect to signs of the superheated state believed to exist below 2 km b.s.l. The conclusion is that the interpreted temperature profiles are in accordance with the available data and a reinterpretation would not add significantly to the current conceptual model. As for the existence of a superheated state deep in the system, the scarcity of measurements makes it difficult to provide a comprehensive picture. Of the wells that were found to intersect superheated feed zones, only well K-39 has enough temperature and pressure logs to warrant an investigation.

The temperature model for the Krafla system, as based on formation temperature profiles, is discussed thoroughly by Mortensen et al. (2009a). Figure 38 to Figure 40 show a glimpse into the model, as it is incorporated into the Petrel model of the Krafla system.

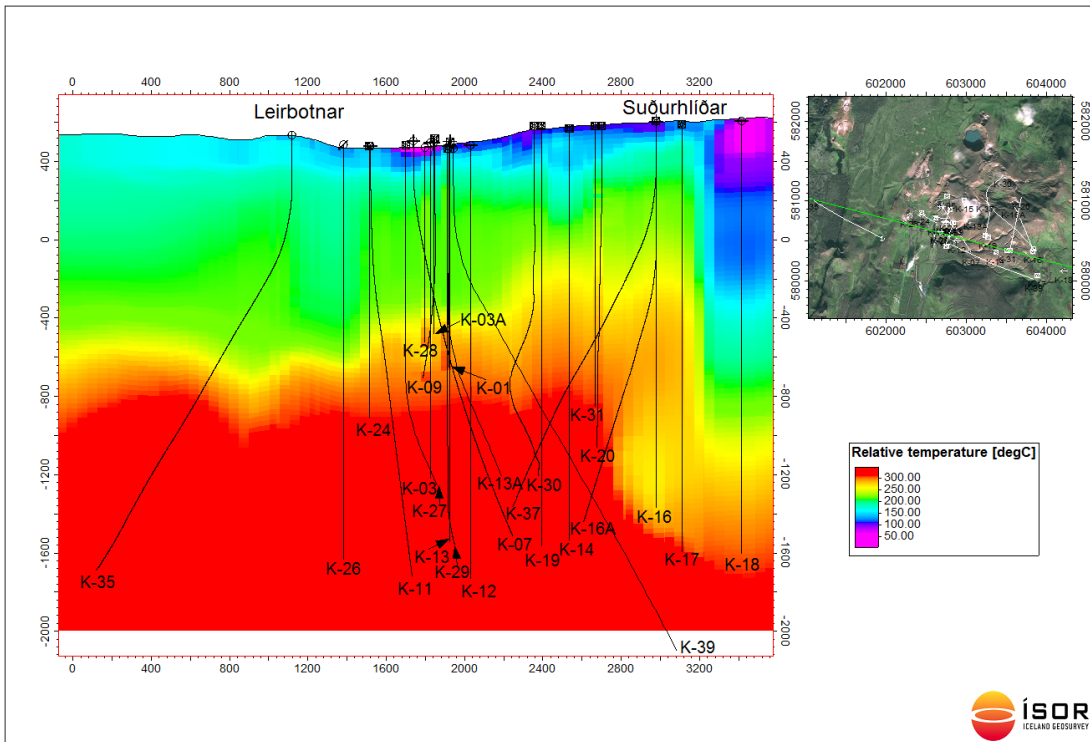


Figure 38. A WNW-ESE cross-section through the temperature model for the Krafla system.

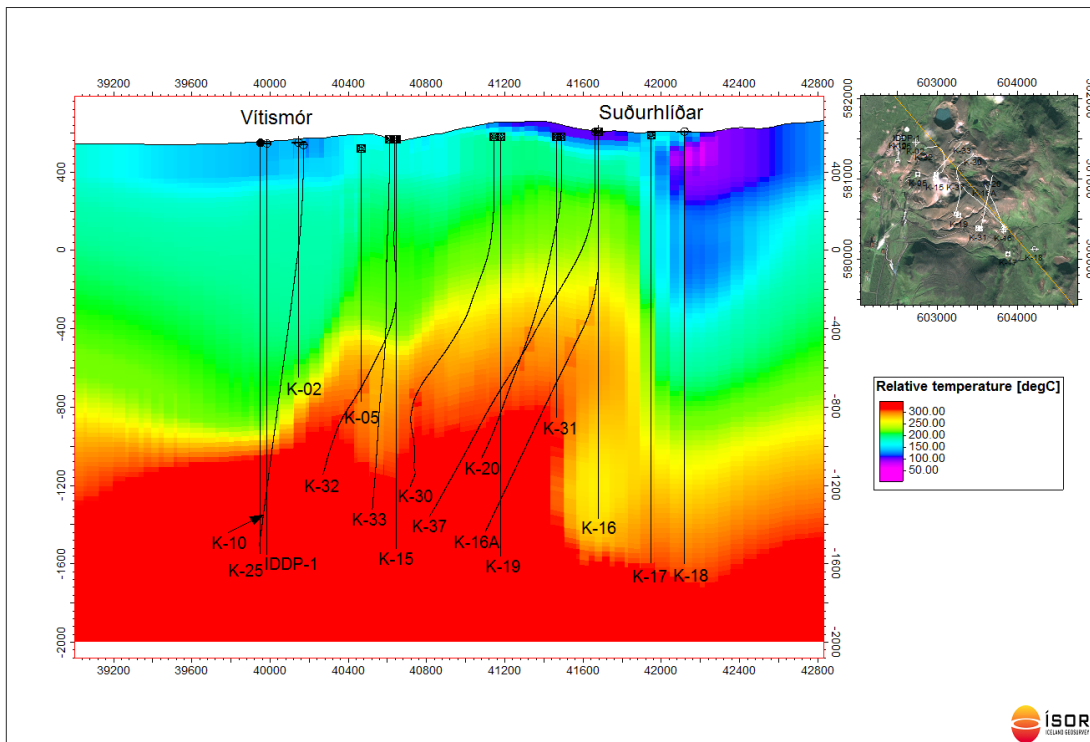
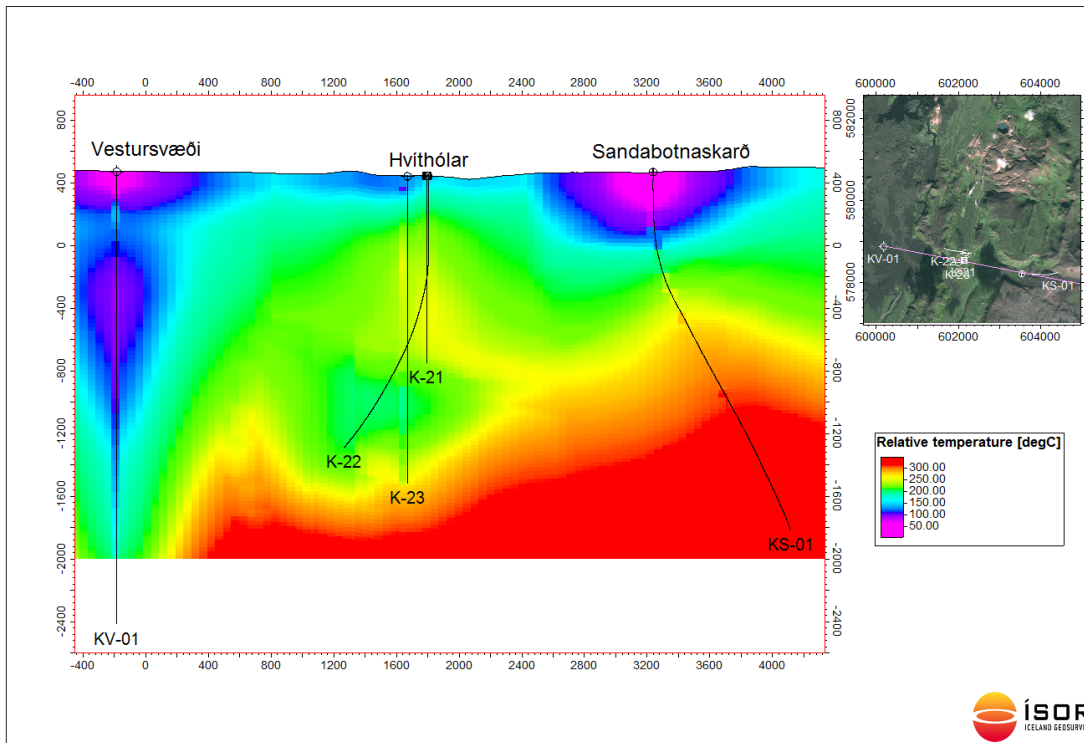


Figure 39. A NW-SE cross-section through the temperature model for the Krafla system.



**Figure 40.** A WNW-ESE cross-section through the temperature model for the Krafla system (in Hvíthólar region).

The lower Leirbotnar reservoir in Krafla is considered to be able to sustain significant production but due to intense scaling problems, feed zones exhibit a rapid decline in output during discharge. Therefore, the probable energy contained within the reservoir has been estimated by employing the volumetric assessment method (Gylfadóttir and Gunnarsdóttir, 2014). To address the uncertainty inherent in input parameter estimates, the Monte Carlo method was used in conjunction with the volumetric assessment.

## 8.2 Hypothetical modelling of Krafla temperature conditions

Model calculations for geothermal systems initiated by magmatic intrusion(s) (Hayba and Ingebritsen, 1997) show that the typical lifetime of such systems is of the order of 10,000 years. If permeability is in the range of 0.5–5 mD (1 mD =  $10^{-15}$  m<sup>2</sup>, the role of permeability will be further discussed below) a two phase convective geothermal system forms in about 1000 years. Near the end of the lifetime of the system (of the order of 10,000 years, if the heat source is not renewed), the heat source has lost most of its heat, and cold downwards convected water can no longer gain enough heat and the system cools down at depth. Two-phase conditions (boiling) may still prevail (for some hundreds to thousand years) at a shallower depth in a slowly upwards migrating “bubble” and leading to temperature inversion with depth. It is considered likely that the geothermal system in Hvíthólar (and in the Krýsuvík area and maybe some others) are such systems, near the end of their lifetime. At the end of the glaciation, the rapid pressure drop in the

crust has probably initiated extensive intrusions and the geothermal systems that were formed are still present today, but fading out.

Permeability plays a very crucial role in the existence and development of volcanic geothermal systems. Model calculations show that in order for magmatic intrusions in the crust to produce a two-phase geothermal system, the permeability has to be in a very narrow range of 0.5–5 mD (Hayba and Ingebritsen, 1997). If the permeability is lower, the intrusion cools in a long time by heat conduction, but if the permeability is higher the intrusion cools rapidly by vigorous one-phase (water) convection.

Figure 41 shows results of modelling a geothermal system generated by a magmatic intrusion using the HYDROTHERM programme (Kipp et al., 2008). This is a two-dimensional model with an 800 m wide “dike” intrusion extending up to 2.45 km below surface. The intrusion is placed in a host rock of permeability 1 mD extending up to 1 km depth (grey line on Figure 41). The permeability in the uppermost 1 km is much higher (50 mD in this case). Figure 41 shows a conventional two phase convecting geothermal system is formed in the low permeability below 1 km. In the high-permeability region above a vigorous one-phase (water) reservoir convection is observed. The temperature profile above the centre of the intrusion shows two-phase conditions close to the surface and then almost isothermal conditions, at about 200 °C, down to a little above the lower permeability rocks where it rises, approximately linearly to the boiling-point curve in the lower permeability. This is very similar to what is observed in the western part of the main geothermal system, west of Hveragil. It seems clear from this modelling that the reason for the “two systems” in this part of the system is due to a large difference in permeability. The “deep system” has permeability around 1 mD (or between 0.5 and 5 mD) while the upper system has ten times (or more) higher permeability. The temperature profiles further away, where there is less support of heat from below, bear some resemblance to the temperature profile in well KV-1 in Leirhnjúkshraun.

It should be noted here that the model in Figure 41 is a hypothetical 2D section along the active fissure swarm and fluid flow is only along the swarm. In reality the permeability is probably very anisotropic, being very high in the direction of the swarm but much lower perpendicular to it.

# up50mD 3000 yr

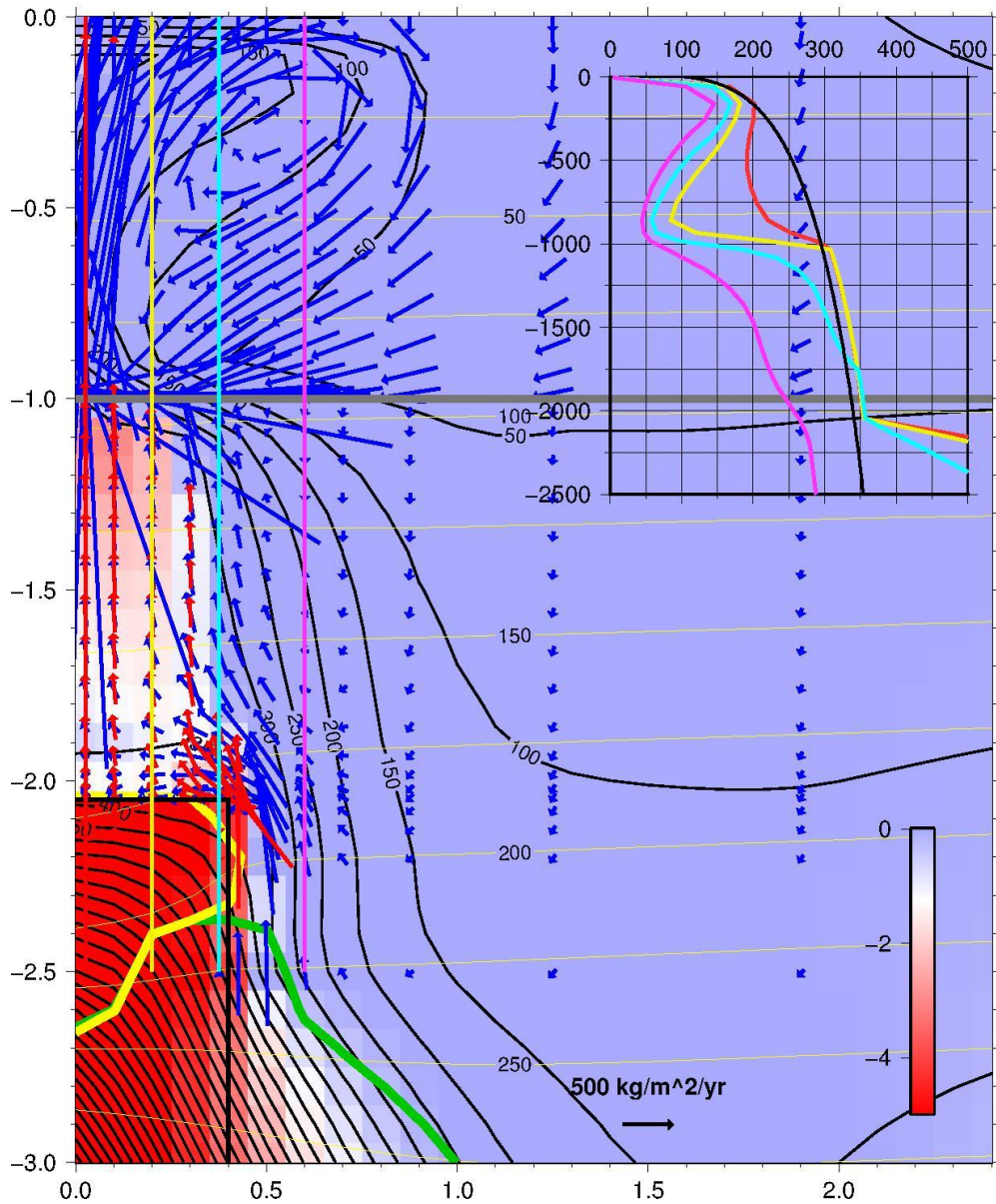


**Figure 41.** Thermo-hydraulic state of a geothermal system 3000 years after emplacement of an 800 m wide “dike” intrusion extending up to 2.45 km below surface. The intrusion is placed in a host rock of permeability 1 mD, extending up to 1 km depth (thick grey line). The permeability in the uppermost 1 km is much higher (50 mD in this case). Temperature ( $^{\circ}\text{C}$ ) is shown by black contours and pressure (bars) by yellow contours. Phase conditions (water/steam) are shown by colors (light blue is pure water and dark red is pure steam, the actual scale 10 times logarithm of water saturation). Mass flow is shown by arrows (scale at the bottom of the figure), blue for water phase and red for steam phase. The graph in the upper right hand corner shows temperature profiles from hypothetical wells at different distances from the center of the intrusion. Thick yellow line marks region of superheated steam and green line region with supercritical conditions.

### 8.3 Enthalpy and production

The total mass production history of Krafla is shown in Figure 42 as annual values along with the yearly weighted mean enthalpy. This data is provided by Landsvirkjun, from the company's production monitoring database. The total annual reinjection is depicted as an addition to the production columns, in light gray.

In the years 1996–1999 production was approximately doubled and 9 new wells drilled. The mean enthalpy has decreased slowly since then, most markedly in the well in lower Leirbotnar system and the Hvíthólar area (Figure 43 and Figure 44). Production decreased in the following years but increased again as 8 new wells were drilled in the years 2006–2009. Production and reinjection has been stable for the past 5 years. Inflow of colder water is thought to contribute to the cooling of the lower Leirbotnar area (Mortsensen et al., 2009a).

Figure 43 shows the enthalpy and production in Hvíthólar where one well is in production, K-21. With declining enthalpy, this well has transformed from a steam dominated well to a liquid dominated one over the course of the past 26 years. Its mass output however is the second greatest for all wells in the Krafla geothermal field. Enthalpy is declining in the lower Leirbotnar system alongside an approximately stable production in the past 7 years (Figure 44). Figure 45 shows that enthalpy in the upper Leirbotnar system has remained stable over the past 10 years with varying production levels sustained by 2–3 wells.

Enthalpy is increasing in Suðurhlíðar (Figure 46) while production is on the decline. This is thought to be due to reduced pressure and increased boiling in the geothermal reservoir (Mortsensen et al., 2009a). The wells in Vesturhlíðar area are stable high-enthalpy wells (Figure A 2). The area shows stable enthalpy and production since 2010 when the last well was opened for production (Figure 47).

In Vítismór the main production well is K-32 where the enthalpy has decreased steadily since shortly after drilling alongside increased water output. The data in Figure 48 show the drilling and closing of K-8 then K-25, followed by the opening of K-32 in 1998 and then IDDP-1 in 2010 (seen as a jump in enthalpy). Note that Figure 42 to Figure 48 show the mass production and enthalpy of subareas as defined in Table 1.

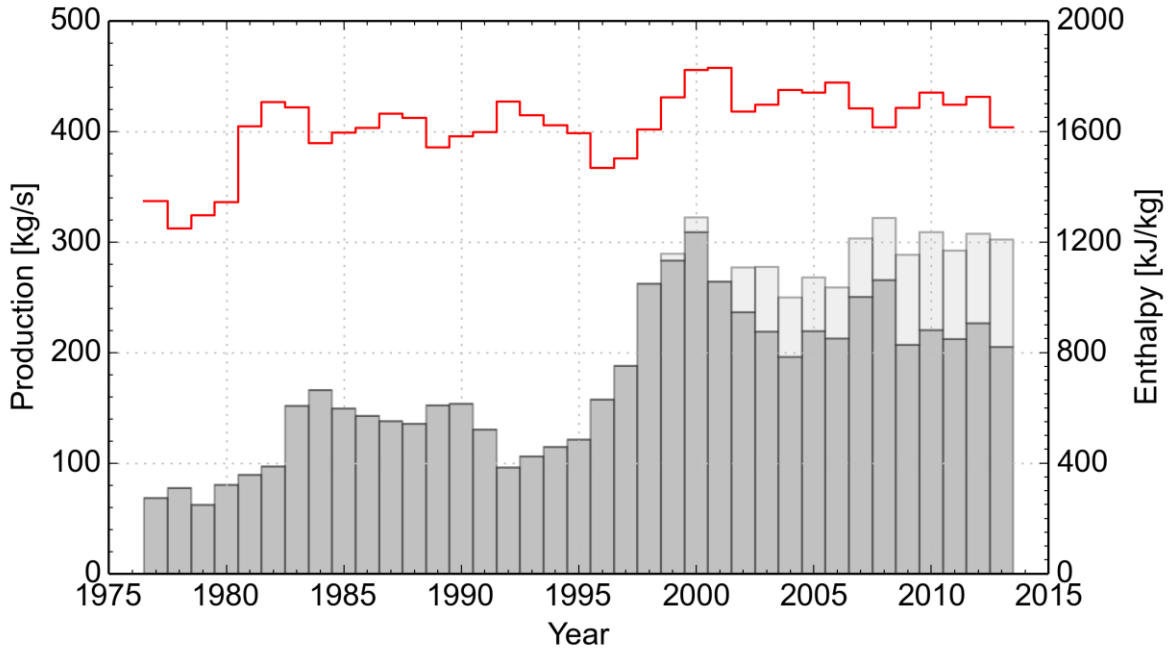


**Figure 42.** Average total mass production per year (columns) and weighted yearly mean enthalpy (red line) for all Krafla production wells. The darker shaded bars represent production while the lighter shaded bars represent reinjection.

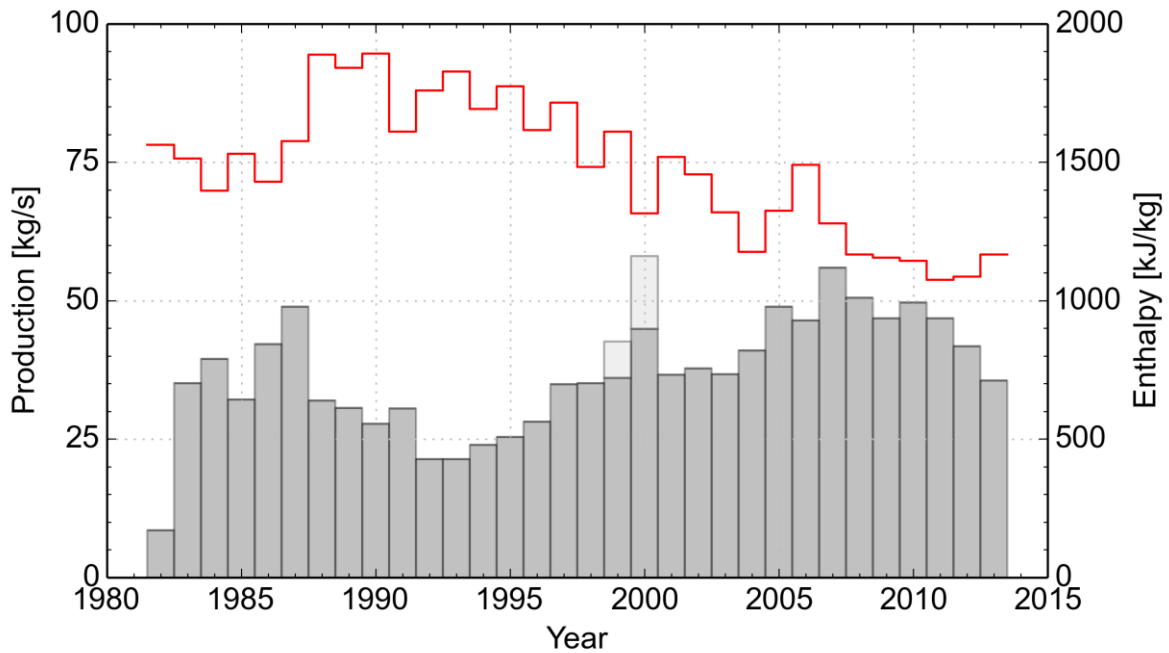


**Figure 43.** Hvíthólar (well K-21) average mass production per year (bars) and weighted yearly mean enthalpy (red line). The darker shaded bars represent production while the lighter shaded bars represent reinjection.

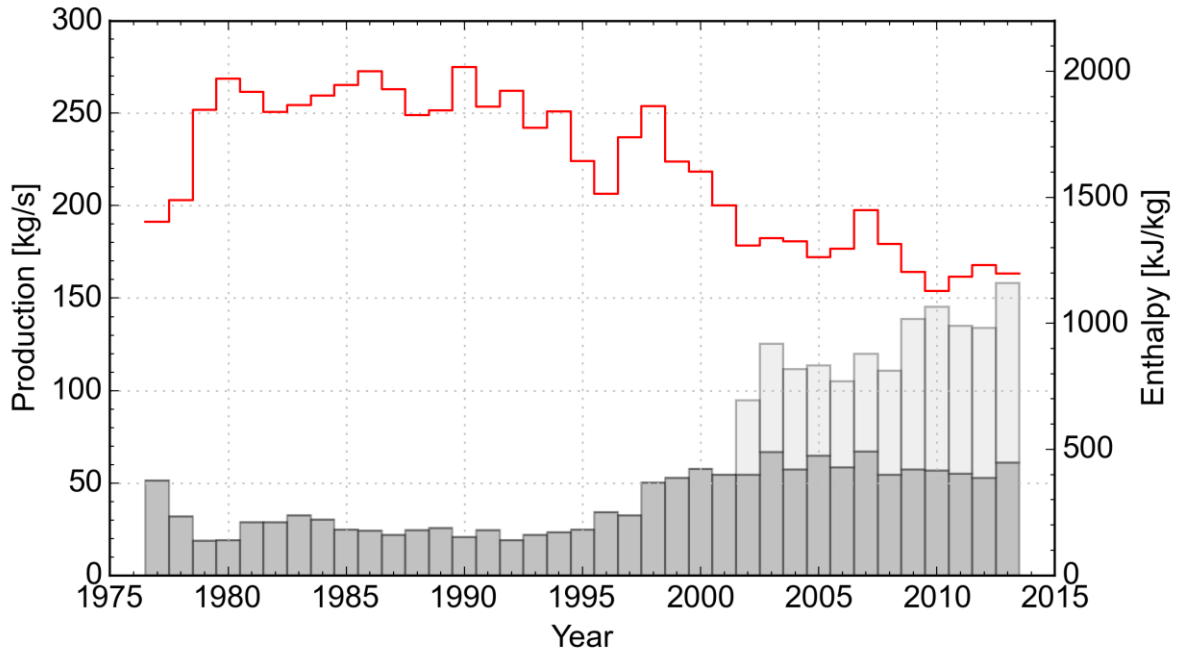


**Figure 44.** *Leirbotnar lower system (9 wells out of which 3 are currently producing wells) average mass production per year (columns) and weighted yearly mean enthalpy (red line).*

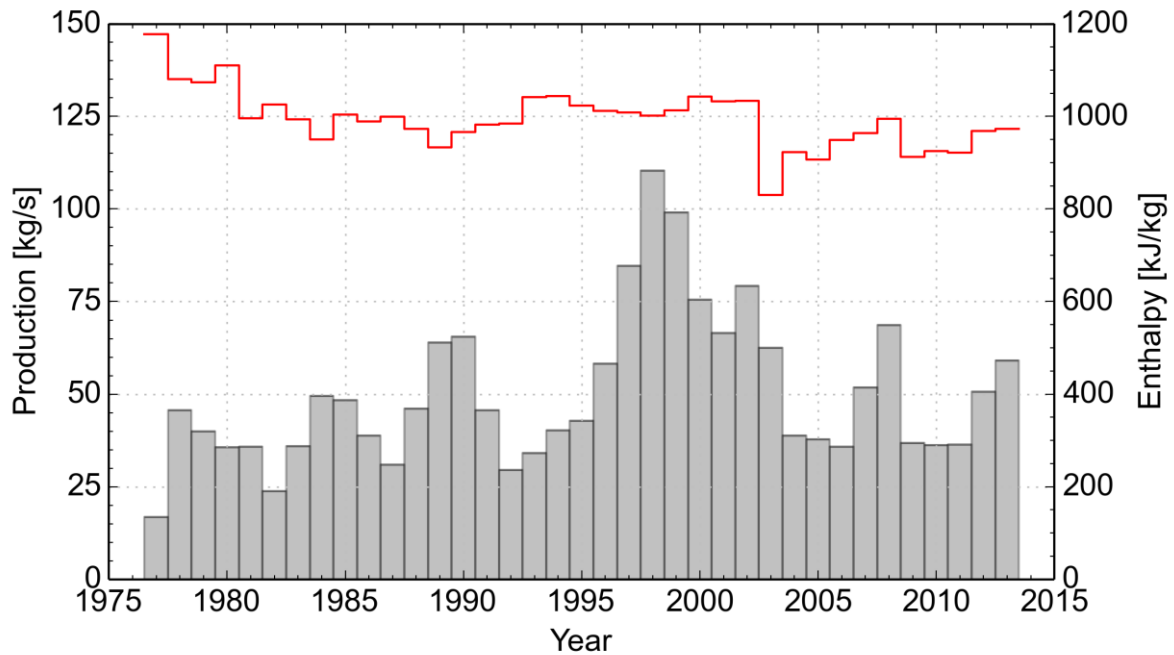


**Figure 45.** *Leirbotnar upper system (5 production wells, 2 currently producing wells) average mass production per year (bars) and weighted yearly mean enthalpy (red line).*

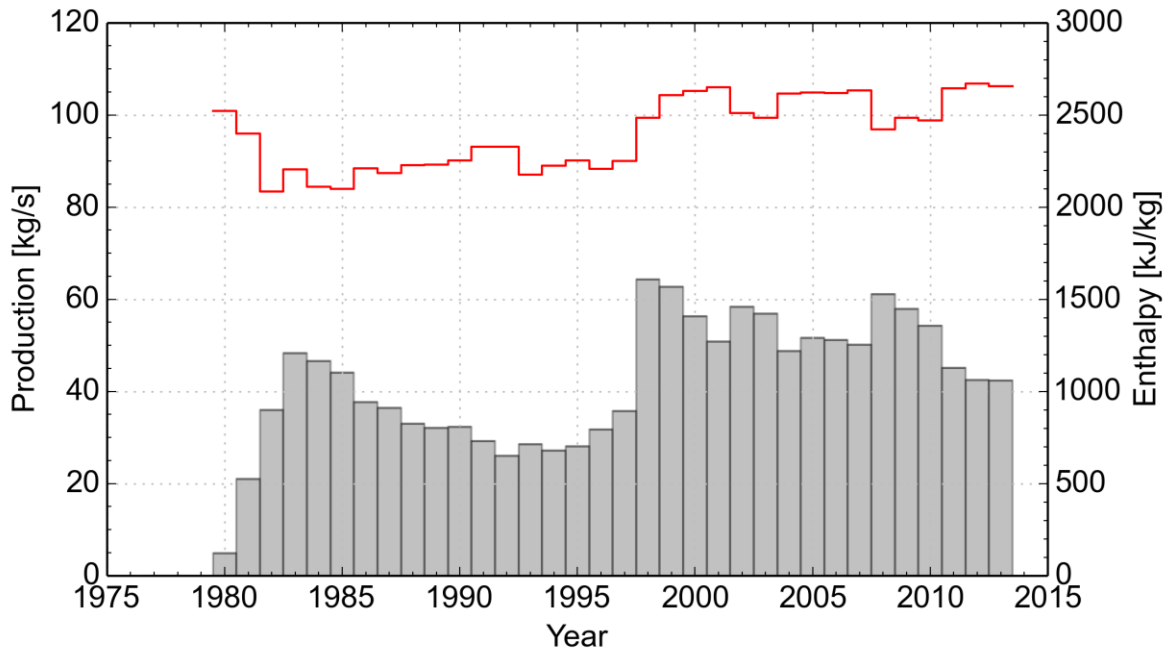


**Figure 46.** *Suðurhlíðar* (9 production wells, all currently producing) average mass production per year (columns) and weighted yearly mean enthalpy (red line).

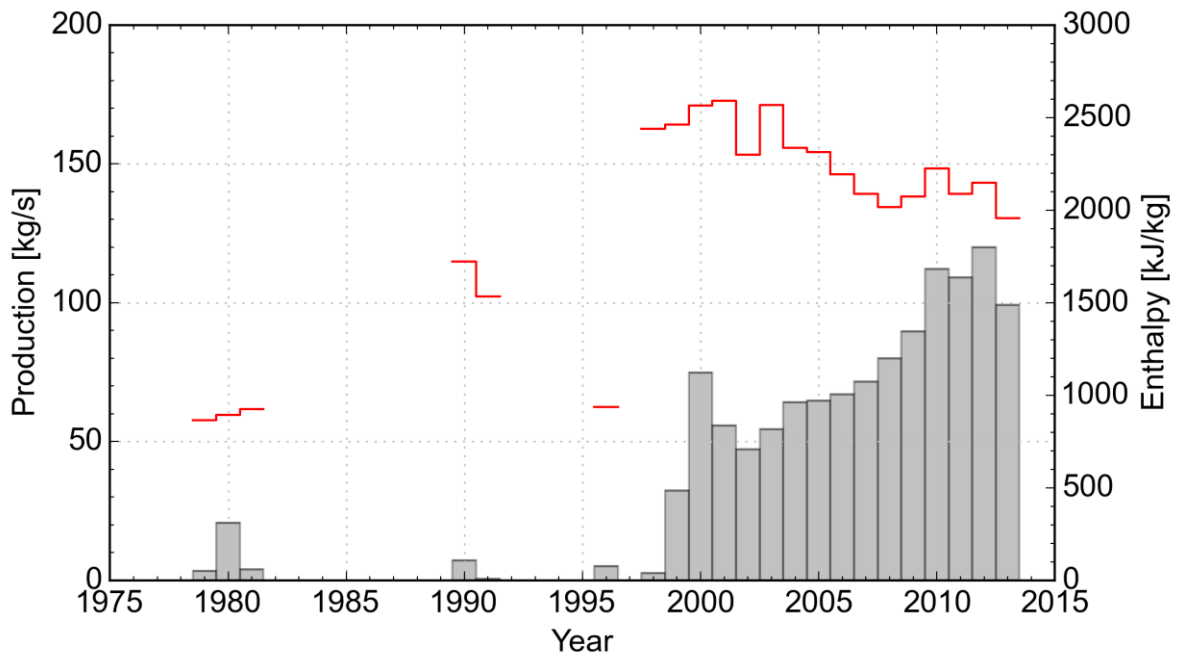


**Figure 47.** *Vesturhlíðar* (5 production wells, all currently producing) average mass production per year (columns) and weighted yearly mean enthalpy (red line).

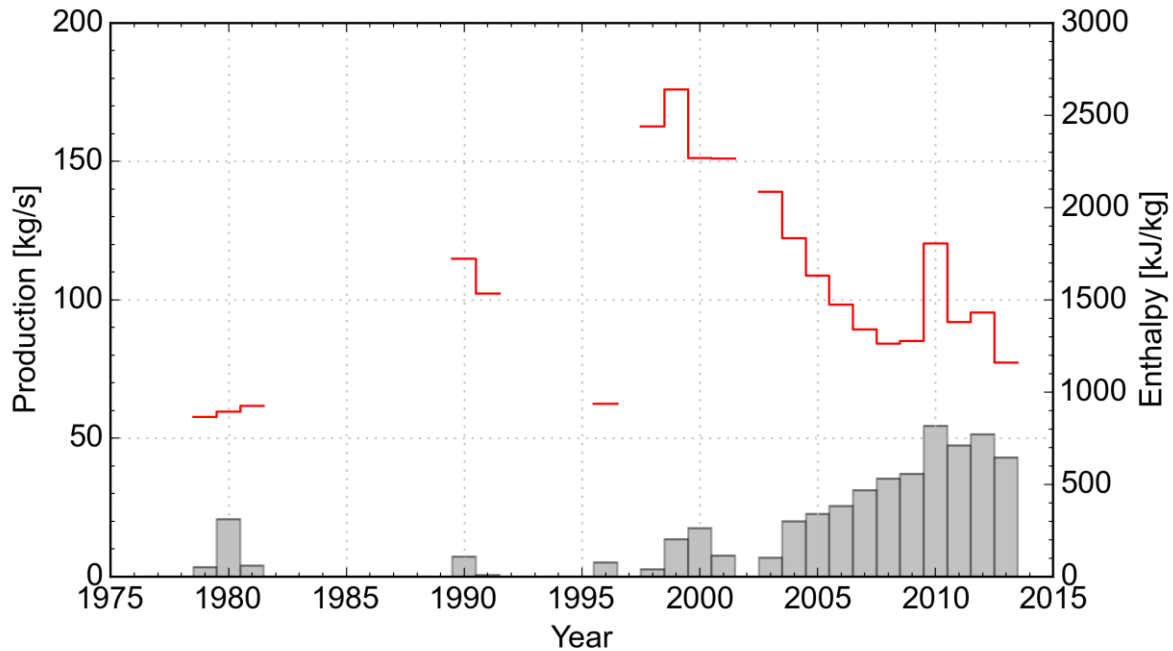


**Figure 48.** *Vítismór (4 production wells, 1 currently producing well) average mass production per year (columns) and weighted yearly mean enthalpy (red line).*

## 8.4 Simple lumped parameter modelling

This modeling technique can be used to characterize the main features of a geothermal production field. The model uses reservoir pressure and production data to estimate the behavior of the system around it. In addition, the models can be used to predict the system's response to continued production. The technique was first presented by Axelsson (1989) and has since been successfully applied in numerous geothermal fields (Axelsson and Gunnlaugsson, 2000; O'Sullivan et al., 2001).

The lumped parameter model simulates the geothermal reservoir as a series of tanks that are connected by flow conductors. These conductors simulate the flow between the tanks. The process of simulating the reservoir starts by assuming the simplest model, a one-tank model, proceeding to attempt to fit the data to increasingly complex models, two and then three tank models. The first tank represents the central part of the reservoir, where production takes place while the additional two tanks that may be added to the model, if the data permits, represent the outer parts of the reservoir and the recharge part of the reservoir. The model produces parameters to quantify the flow between the tanks. This is a simulation of the permeability between different parts of the reservoir, permeability being a key feature of geothermal production systems.

The models are either open or closed systems an important feature when forecasting the systems response to continued production. In an open system, the pressure drawdown generally takes place more slowly in contrast to a closed system.

Several different sized models may fit the data. The model chosen to represent the reservoir must have the following qualities: It must give as good a statistical fit to the data as possible, it must be reasonably simple or complex based on the conceptual model of the reservoir and it must give descriptive parameters of reasonable orders of magnitude. Once a model is chosen to represent the reservoir the descriptive parameters of this model may be used to calculate key parameters of the reservoir. These include the volume of the tanks proposed by the model and the permeability between them.

Pressure data from a monitoring well, K-6, is used to simulate the Leirbotnar area while data from K-21 is used to simulate the Hvíthólar area. K-21 is the only well currently in production in Hvíthólar and the only well for which pressure logs exist. The results of the modeling process are presented in Table 5.

#### 8.4.1 Leirbotnar

The Leirbotnar system is divided into two systems, a lower and an upper system. In this section we focus on the upper system. Well K-6 has served as a monitoring well in Leirbotnar and is generally logged down to a depth of 1200 m. The pressure data used for the lumped parameter modeling are measured at a depth of 800 m.

The model that consistently fits the pressure and production data from K-6 in Leirbotnar best is a two-tank model, as seen in Figure 49. The results of the open and closed models are very similar in K-6 (Table 5). For the open two-tank model the parameter that determines the permeability from outside of the reservoir into the outer part of the reservoir (the second tank) is so small that the open model is effectively closed. Therefore, the available pressure monitoring data seem to indicate that the upper Leirbotnar system is closed, in contrast to the enthalpy data discussed above. It must be kept in mind, however, that the pressure data is quite inaccurate, as represented by the scatter in the data and that the pressure in well K-6 may have been influenced by the lower Leirbotnar system or the southern Vítismór area.

The output parameter  $\kappa$  for the different tanks of the lumped parameter models is used to calculate the volume of the corresponding parts of the reservoir. For well K-6 the volume of the central part of the reservoir is estimated at 2.8 km<sup>3</sup> while the second tank representing the outer part of the reservoir is estimated at approximately 50 km<sup>3</sup>.

The thickness of the reservoir was estimated to be 1000 m, an average porosity of 10% was assumed for the reservoir volume and the storativity of the volume was calculated based on these parameters to be  $1.02 \cdot 10^{-5} \text{ s}^2 \text{ m}^{-2}$ . The kinematic viscosity of water, based on an estimated average water temperature in the reservoir of 200°C, is  $1.55 \cdot 10^{-7} \text{ Pa} \cdot \text{s}$ . This leads to an estimate of permeability determined by the model parameter  $\sigma$ , the kinematic viscosity and the dimensions of the reservoir. In the Leirbotnar system, the permeability between the outer and central parts of the reservoir is estimated to be 17 mDarcy.

As discussed in Mortensen et al. (2009a) the pressure in the upper Leirbotnar system follows fluctuations in production from the area. The pressure dropped by about 17 bar in two years following the doubling of the power plants capacity. This pressure drop, along with a high level

of scatter, compromises the accuracy of the model-fit to the data. Nonetheless, the model manages to capture the general trend in the data.

**Table 5.** Results of the lumped parameter modeling of pressure and production data from Leirbotnar and Hvíthólar.

Model	Leirbotnar K-6		Hvíthólar K-21	
	Two tank closed	Two tank open	Two tank closed	Two tank open
Initial pressure (bar-g)	77	77	67	67
R <sup>2</sup>	73.09	73.06	75.96	85.93
STD	2.52	2.56	4.48	3.49
$\kappa_1$	2.85E+04	2.87E+04	2.32E+04	3.81E-01
$\kappa_2$	5.38E+05	5.24E+05	5.37E+11	6.77E+04
$\sigma_1$	6.08E-04	6.18E-04	1.36E-04	3.61E-04
$\sigma_2$		1.20E-09		2.03E-04
Volume of tank 1 (km <sup>3</sup> )	2.8	2.8	2.3	0.00004
Volume of tank 2 (km <sup>3</sup> )	52.8	51.3	$\infty$	6.6
Permeability between tanks 1 and 2 (mDarcy)	16.7	17.0	3.3	48.1
Permeability between tank 2 and the outside of the reservoir (mDarcy)		$\sim 0$		4.9

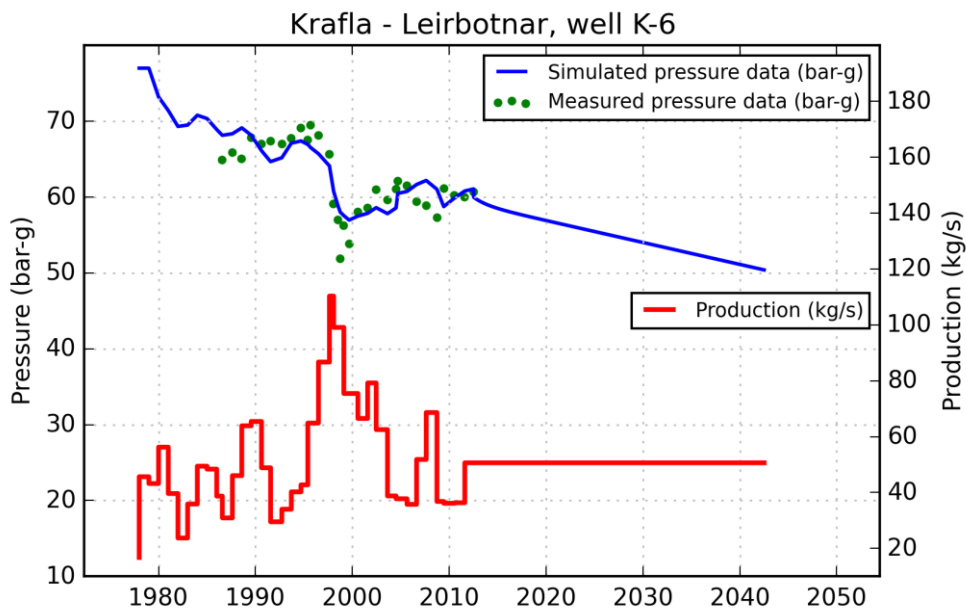


**Figure 49.** Pressure and production data for Leirbotnar; the fit to the pressure data for well K-6 is obtained using lumped parameter modeling, including a 30 year forecast.

### 8.4.2 Hvíthólar K-21

The Hvíthólar subsystem is on the southern rim of the Krafla caldera (Figure 4). Pressure logs and production data from well K-21 is used to model this part of the system. Reinjection that took place in the area in the years 1999 and 2000 is accounted for in the modelling process by using the net production. The pressure data used for the modeling process are measured at 900 m depth in the well, which is below the boiling level in the well and therefore more representative of the pressure in the system. Boiling point is reached around 750 meters depth. The well is disconnected and closed over the summer months and generally the pressure logging is done when the well has been closed and off-line for 2–5 months.

The best-fit model to the data is a two tank open model (Figure 50). The model simulates the fluctuations in the pressure data due to increased production. Three periods of pressure recovery during times of decreased production are simulated; however the most recent one is only partially reflected by the model. The high level of scatter in the data compromises the accuracy of the model but the model does manage to capture the general trend in the data

The output parameters reflect the fact that Hvíthólar is a small reservoir. The volume of the central and outer parts of the reservoir is estimated to be 0.00004 km<sup>3</sup> and 7 km<sup>3</sup>, respectively, with a very high permeability between them (40 Darcy). This high permeability results from the small value of the output parameter  $\kappa_1$ . The permeability from the outside of the reservoir into the recharge part of the reservoir is estimated at 5 mDarcy.

Decreased enthalpy measured in the area in the past few years, increased total flow, pressure recovery simultaneous to high production levels in the years 2002–2005; all these factors point towards an influx of cold water into the system supporting the open model hypothesis.

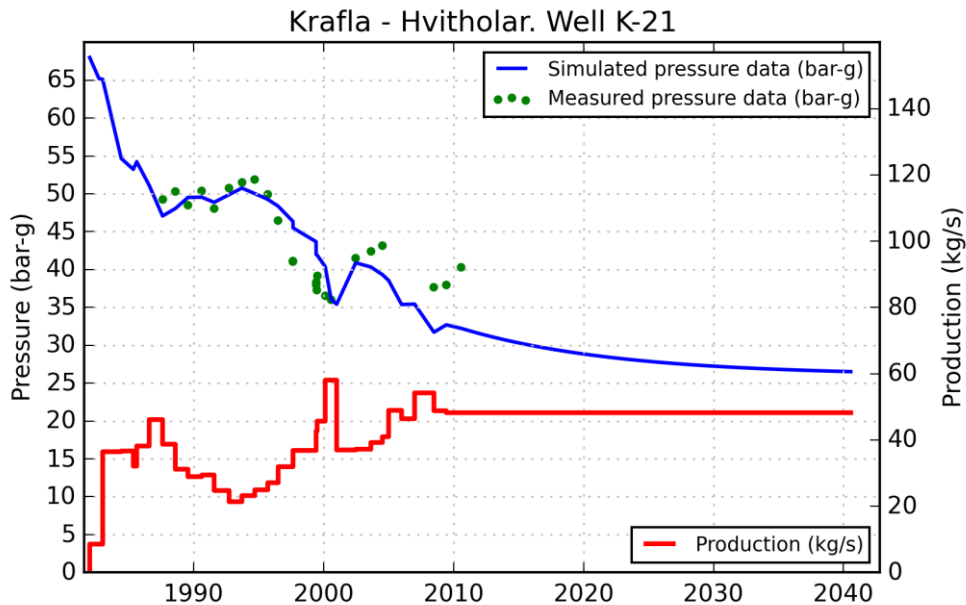


**Figure 50.** Pressure and production data for Hvíthólar, the fit to the pressure data from well K-21 is obtained using lumped parameter modeling, including a 30-year forecast.

## 8.5 Analysis of production well output

The Krafla geothermal production field is divided into several subfields based on chemical data, temperature and pressure data, geological conditions and production data. The exact classification of wells into subareas is still being reviewed and updated. There are seven subareas adopted at the present: Suðurhlíðar, Vesturhlíðar, Leirbotnar upper and lower systems, Vítismór, Hvíthólar, and Sandbotnar. Production and reinjection affect the state of the reservoirs from which the wells draw steam and water, but different subareas react differently to production. This is e.g. seen in variations that occur, in both steam and water output from the wells. These variations reflect reservoir conditions, which may also be studied on basis of data from other disciplines, in particular chemical monitoring data.

The aim of the present sub-chapter is to recount developments in both steam and total output from production wells in different parts of the Krafla system. The total output refers to total mass output, water and steam combined. In most wells the output decays with time, either the steam or total output, and below is a further analysis of this decay, see also Figure A 7 to Figure A 26.

### 8.5.1 Estimating well output decay

An estimate of the total output decay is obtained by fitting an exponential function to the measured total output time series of geothermal wells. The following exponential is used to obtain the decay coefficient:

$$q(t) = q_0 e^{-\alpha(t-t_i)}$$

Where  $q(t)$  is the output at time  $t$ ,  $q_0$  is the initial output and  $\alpha$  is the decay coefficient giving the estimated decay in well output per year. Both decay in total output and steam output were estimated in the same way, using this equation.

The initial time of the data series was adjusted with respect to an estimate of the time when steady decay of the production began; this was not always at the beginning of production. Only wells with good time series were used for the modelling. These include 18 wells currently in production (80% of production wells) and two wells that have now been closed for production (well K-9 closed since 2009, well K-15 closed since 2013). In the same way separate exponential equations were fitted to the steam and total output data to obtain steam and total output decay coefficients. The coefficients give decay in percent per year.

The total output and the steam output will be covered separately below, since steam and mass output data give insight into different underlying processes.

Figure A 7 to Figure A 26 contain plots detailing steam output, total output and enthalpy histories for the wells analyzed in this section. The figures furthermore show the fitted curves used to estimate the decay in output.

### 8.5.2 Total output decay

Figure 52 shows how the total output decay varies between the different subareas and as a function of the depth of the feed zones. While some boreholes have well defined main feed zones (even just one) others have numerous feed zones over a specific depth range. These are seen as a series of points in the y-direction of Figure 52. The feed zones are not classified as steam and liquid



feed zones indicated in the figure are the same as those in Figure 52 and do not reflect the origin of steam specifically. The plot is intended to give an idea of the general decay behavior of the different subareas as well as the depth at which the wells produce from. While most other regions show similar behavior of a decay between 0 and 5% exceptions are found in several wells in Vesturhlíðar and Suðurhlíðar.

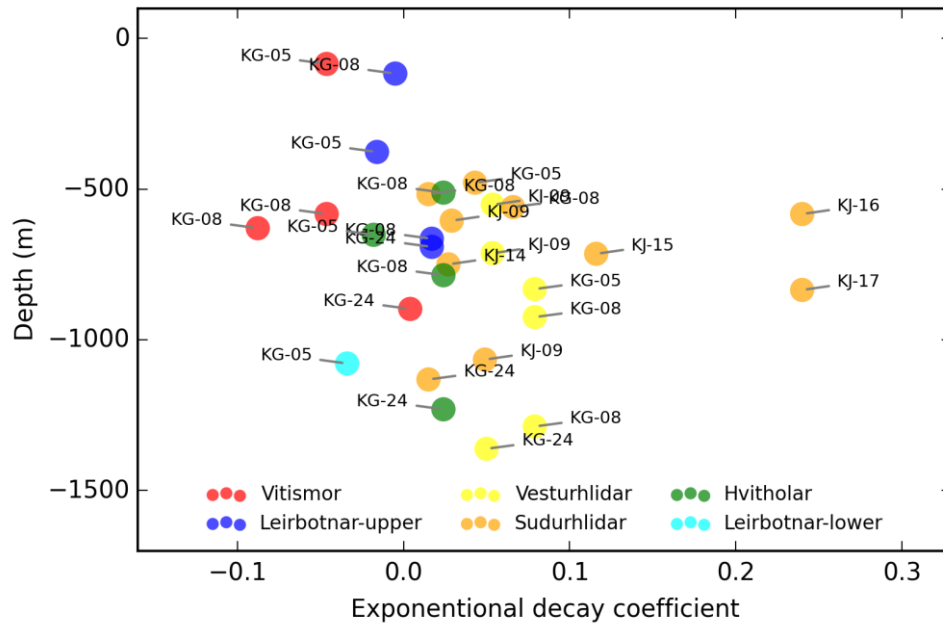


**Figure 52.** Total output decay plotted against feed zone depth in the wells analyzed in this section. The points in the plot have been color coded according to the sub-fields of Krafla to give an idea of how decay and feed zone depth vary between areas. Negative decay implies an increase in output.

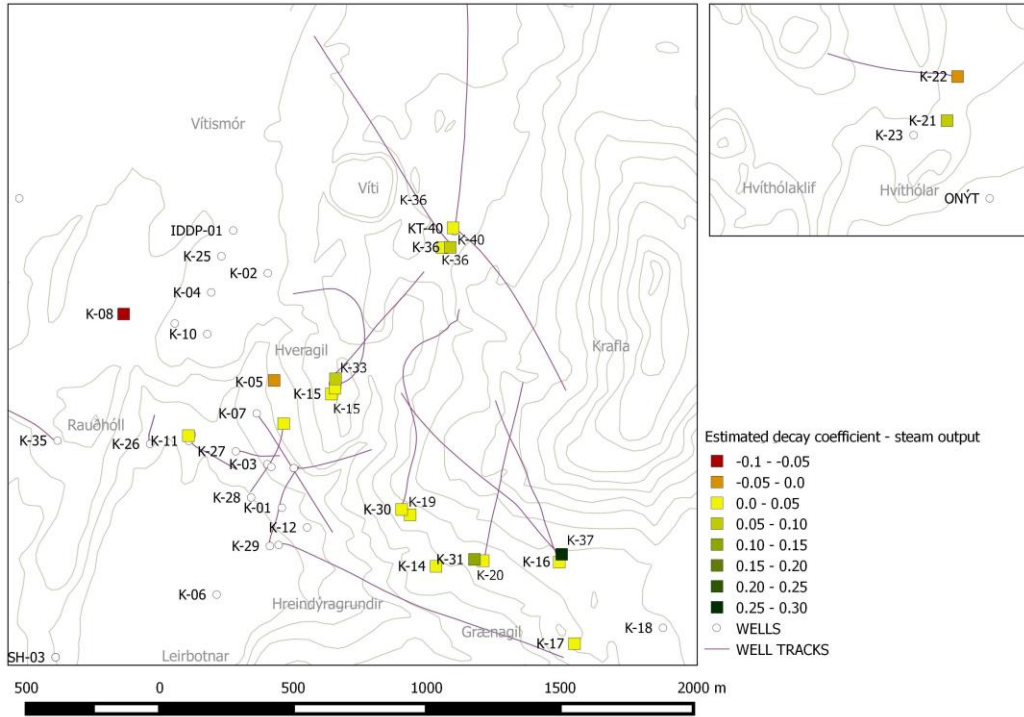


**Figure 53.** The estimated steam output decay in % per year for 20 wells in the Krafla caldera. Red indicates increased steam output, the orange colored data points indicate that no decay took place in the well, while yellow and green refer to decreased steam output from wells.

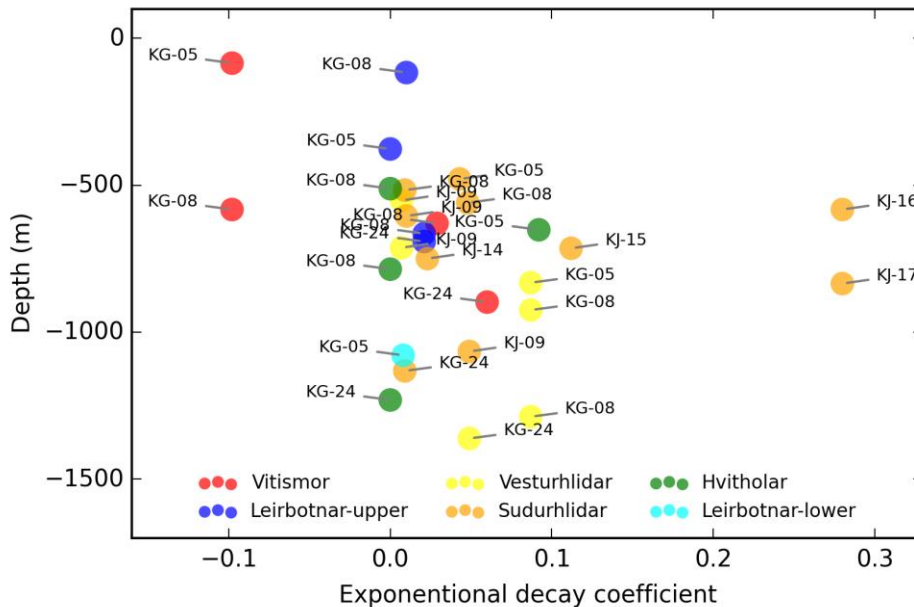


**Figure 54.** Steam output decay plotted against feed zone depth in the wells analyzed in this section. The feed zone depths are not steam feed zones and do not reflect the origin of steam specifically. The points in the plot have been color coded according to the sub-fields of Krafla to give an idea of how decay and feed zone depth vary between areas.



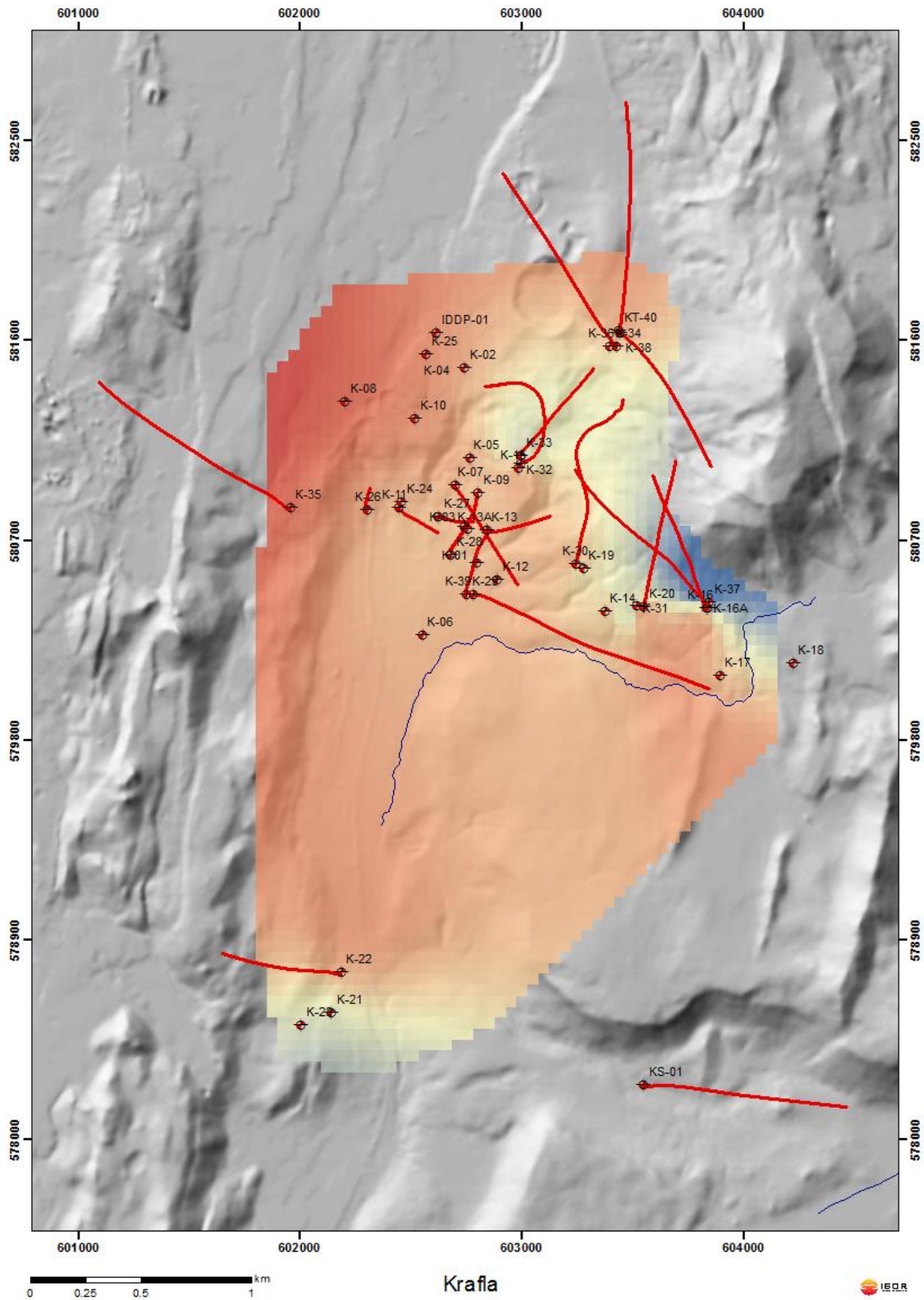


**Figure 56.** Steam decay of selected wells mapped onto the surface of the Krafla geothermal field. Cold colors indicate decay while hot colors indicate increased output.

## 8.6 Simulation of geothermal wells

Vatnaskil has developed a well-bore module within the iTOUGH2 modelling environment (Finsterle, 2007) for simulating geothermal wells producing at constant wellhead pressure. The module was recently used to model production in the Þeistareykir wellfield and a report describing this work was published (Berthet et al., 2014).

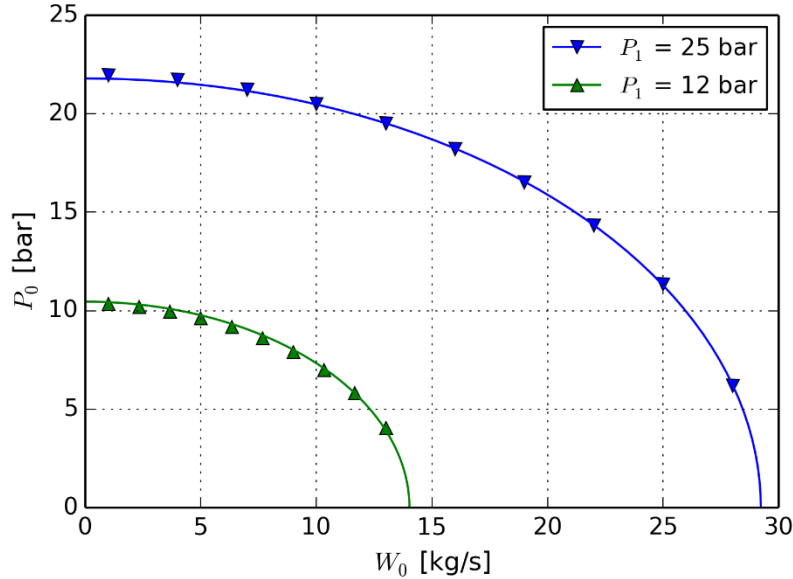


**Figure 57.** The well-head pressures calculated by WellSim are fitted at constant enthalpy to find  $a_0$  and  $b_0$  for a given enthalpy.

The aim of the work presented in this section is to use the well-bore module to model production in the Krafla wellfield. Vatnaskil has analyzed the available production data from the Krafla wellfield and has determined that the data is of sufficient quality for parameterizing the well-bore module. The three thermodynamic parameters required for the module, wellhead pressure, flow rate and enthalpy (or saturation) have been recorded regularly since production from the field began. Vatnaskil has recently received the additional data required to model the production wells, including well tracks, feed-zone locations and well design parameters (casing and liner lengths, types, diameters, etc.), and the first stage of the well-bore model parameterization is now nearly complete.

In the well-bore model, the pressure loss observed in the wells while the fluid is flowing up to the surface is modelled using the equations (Berthet et al., 2014):

$$\left(\frac{W_0}{a_0}\right) + \left(\frac{P_0}{b_0}\right) = P_1^2$$

$$a_0 = \alpha_0 h_0 + \beta_0$$

$$b_0^2 = \gamma_0 h_0 + \delta_0$$

where  $W_0$ ,  $P_0$ ,  $P_1$  and  $h_0$  are the flow rate, wellhead pressure, feed-zone pressure and enthalpy respectively, and  $\alpha_0$ ,  $\beta_0$ ,  $\gamma_0$  and  $\delta_0$  are fitting parameters introduced by the model. The fitting parameters are specific to each well and depend on the feed-zone location, casing, liner types and inner diameters. For wells that have two feed-zones, the same set of equations are used to describe the pressure loss between the two feed-zones. In this case, a second set of parameters ( $\alpha_1$ ,  $\beta_1$ ,  $\gamma_1$  and  $\delta_1$ ) are defined for the section of the well between the two feed-zones.

The  $\alpha_0$ ,  $\beta_0$ ,  $\gamma_0$  and  $\delta_0$  parameters are found for each production well by fitting the equations to results calculated by WellSim (Gradient Geodata, 2015). In WellSim, well-head pressures are calculated for ranges of flow rates, feed-zone pressures and enthalpies. Then, a first series of regression analyses are performed to obtain sets of  $a_0$  and  $b_0$  parameters, each valid at one specific enthalpy (an example of the procedure is shown in Figure 57 for well K-37). Finally, a last regression analysis is performed on  $a_0$  and  $b_0^2$  versus the enthalpy to determine the  $\alpha_0$ ,  $\beta_0$ ,  $\gamma_0$  and  $\delta_0$  parameters (Figure 58).

**Table 6.** Preliminary sets of  $\alpha_0$ ,  $\beta_0$ ,  $\gamma_0$ ,  $\delta_0$ ,  $\alpha_1$ ,  $\beta_1$ ,  $\gamma_1$  and  $\delta_1$  for the producing wells in Krafla.

Well /	$\alpha$ (J kg <sup>-1</sup> ) <sup>-1</sup> kg s <sup>-1</sup> Pa <sup>-1</sup>	$\beta$ kg s <sup>-1</sup> Pa <sup>-1</sup>	$\gamma$ (J kg <sup>-1</sup> ) <sup>-1</sup>	$\delta$	measured depth (m)
K-5	1.93E-11	5.03E-06	6.35E-07	-5.39E-01	900
K-13A	-5.74E-12	2.67E-05	4.67E-07	-4.94E-01	1695
K-14	-1.36E-11	4.92E-05	4.30E-07	-3.15E-01	1050
K-15	-5.59E-12	2.72E-05	4.81E-07	-4.94E-01	1400
	-5.59E-12	2.72E-05	4.81E-07	-4.94E-01	1730
K-16A	-7.81E-12	3.40E-05	4.64E-07	-4.35E-01	1204
K-17	-1.39E-11	5.34E-05	4.49E-07	-3.48E-01	1110
K-19	-1.25E-11	4.94E-05	3.92E-07	-1.78E-01	830
	-1.25E-11	4.94E-05	3.92E-07	-1.78E-01	1920
K-20	-1.08E-11	4.27E-05	3.95E-07	-1.94E-01	940
	-1.08E-11	4.27E-05	3.95E-07	-1.94E-01	1645
K-21	-6.15E-12	2.60E-05	4.42E-07	-3.43E-01	1160
K-24	-1.45E-11	5.65E-05	5.44E-07	-3.75E-01	600
K-27	-2.16E-12	2.57E-05	5.96E-07	-5.85E-01	1220
	-2.16E-12	2.57E-05	5.96E-07	-5.85E-01	1573
K-29	-6.93E-12	2.85E-05	4.41E-07	-4.35E-01	1610
K-33	-1.57E-12	6.88E-06	4.28E-07	-3.74E-01	1464
	-1.57E-12	6.88E-06	4.28E-07	-3.74E-01	1970
K-34	-5.34E-12	2.36E-05	4.78E-07	-5.65E-01	1790
K-36	-4.49E-12	2.34E-05	4.97E-07	-5.13E-01	1570
	-4.49E-12	2.34E-05	4.97E-07	-5.13E-01	2346
K-37	-7.88E-12	3.23E-05	4.38E-07	-3.78E-01	1293

The wells currently producing in Krafla are K-5, K-13A, K-14, K-15, K-16A, K-17, K-18, K-19, K-20, K-21, K-24, K-27, K-29, K-30, K-31, K-32, K-33, K-34, K-35, K-36 and K-37. A WellSim database has been created that contains the characteristics of all these wells, and output data have been produced for different values of down-hole pressures, flow rates and enthalpies. Preliminary sets of  $\alpha_0$ ,  $\beta_0$ ,  $\gamma_0$ ,  $\delta_0$  (plus  $\alpha_1$ ,  $\beta_1$ ,  $\gamma_1$ ,  $\delta_1$ , if two feed-zones) have been produced for most wells (Table 6). As, the work on the iTOUGH2 reservoir model has not yet begun, the parameters have not been tested yet with real production data and the productivity indices of the feed-zones have not been calculated. This work will be performed as soon as the reservoir model is ready. Routine checks will be performed for high enthalpy wells to attest the accuracy of the model. This should not bring any difficulty since the method has already been tested for such wells (Berthet et al., 2014). A greater attention will be given to low enthalpy wells (for instance K-24 which produces a fluid at 1000 kJ/kg) to assess the validity of the model. Modifications may be brought into the model in order to describe the low enthalpy wells more accurately.

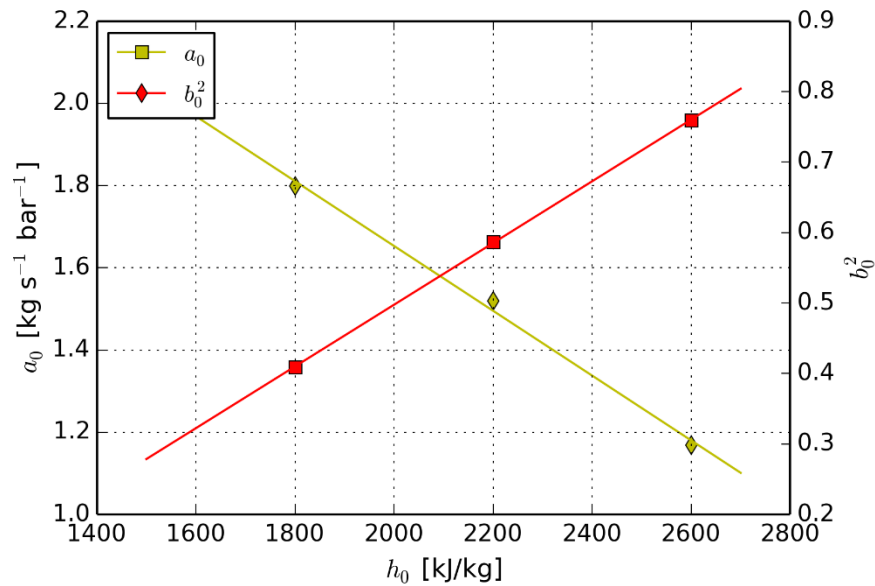


**Figure 58.** Regression analysis of  $a_0$  and  $b_0^2$  versus enthalpy used to determine  $\alpha_0$ ,  $\beta_0$ ,  $\gamma_0$  and  $\delta_0$  for well K-31.

## 9 Tracer test results

Four tracer tests have been conducted in Krafla to evaluate flow-paths within the geothermal system and study the potential cooling of production wells due to reinjection.

The first test involved wells K-21 and K-22 in Hvíthólar in 1999–2000, where 200 kg of KI were injected into the latter and the recovery monitored for 7 months in the former. About 30% of the tracer was recovered relatively rapidly, which was interpreted to indicate a considerable danger of cooling of the production borehole K-21. The distance between the wells was only 200 m. Therefore, the reinjection borehole was abandoned as such (Axelsson, 2013).

The second test was conducted during 2005–2007 to study the effect of injection into well K-26. About 450 kg of KI were injected into the well and the recovery monitored in 9 production wells. The tracer recovery was negligible (< 1%) during this test, however, most likely because the tracer was left behind in a stagnant water phase when the reinjected water evaporated in the reservoir (Ármannsson et al., 2009).

The third Krafla tracer test was conducted during the summer of 2009 under the supervision of BRGM (the French Geological Survey). It involved the injection of three naphthalene sulphonate tracers into wells K-26 and IDDP-1 and recovery monitoring in 18 production wells. During this test, which actually lasted only 3 months, total tracer recovery was only around 0.5%, even though rapid recovery was observed in some of the wells (Gadalia et al., 2010).

The fourth tracer test was carried out during 2013–2014. This was the most comprehensive tracer test conducted so far in Krafla with 8 different tracers injected into 3 wells and their recovery monitored in 20 production wells. The tracers were both phase-specific and phase-partitioning; three liquid-phase naphthalene sulphonate tracers, three perfluorocarbon vapor phase tracers and two phase-partitioning alcohol tracers (Júlíusson et al., 2015).

Only the liquid-phase tracer injected into well IDDP-1 was recovered in a detectable amount. That was through well K-36, which is east-northeast of IDDP-1 and directionally drilled to the NW. The main feed-zones of well K-36 are, however, located about 800 m NNE of IDDP-1. The tracer recovery was, however, minute.

The gas-phase tracer injected into well K-39 was recovered through well K-19, which is a vertical well located about 350 m north of the main feed-zones of the injection well. In this case, the recovery was small, or a little over 2%. Some minor recovery was also observed through well K-14, which is also vertical and only about 200 m NE of the feed-zones of well K-39. It should be noted that both of the phase-specific tracers were detected in feed-zones located north or northeast of the injection feed-zones.

The alcohol tracers (phase-partitioning) were detected in most of the wells in the field, in an irregular manner. Therefore it is believed that either the sampling or sample analysis may have been incorrect in some way (Júlíusson et al., 2015).

## **10 Summarized results**

### **10.1 Major new findings since 2009**

The main new findings associated with the revision of the conceptual model of the Krafla geothermal system are the following:

- Only two new wells have been completed and drilled in Krafla since the latest version of the conceptual model was 2009. Therefore, not much new borehole geology data has become available. A detailed stratigraphical model is available in Petrel, which has been upgraded and developed further since that time. The same applies to the Petrel alteration model.

- The lateral distribution of seismic activity in Krafla trends WNW–ESE, with the same trend as fissures in Suðurhlíðar, a local gravity ridge in the middle of the caldera and high gradients in the resistivity. The activity can also be divided into distinct clusters, some associated with production and reinjection. There are e.g. clear indications of induced seismicity around well IDDP-1 while activity around Leihnjúkur is most likely natural. Other clusters may include mixtures of natural and induced activity. The brittle-ductile boundary is about 1400 m shallower in the center of the Krafla system relative to the adjacent crust, reflecting high temperature at shallow depths (heat-sources). The  $V_p/V_s$  ratio is lower within the geothermal system than average, which can likely be attributed to high silica content (rhyolitic rocks) and existence of steam-zones.
- Only limited additional geophysical surveying has been conducted in the Krafla area since the latest conceptual model report was published in 2009, yet comprehensive reinterpretation of the data, in conjunction with geological information, has been carried out. This includes e.g. interpretation of gravity data and 3-dimensional modelling of resistivity data. One of the most significant aspects of the interpretation is the possibility that the caldera may be intersected by a major ESE-WNW low gravity lineament. Further aspects of this new interpretation are discussed below.
- Complete two-phase (i.e. steam and liquid) analyses of samples collected since year 2000 were used to calculate the deep liquid composition of individual Krafla production wells. Thereby, significant discrepancies appear between different geothermometer temperatures as well as temperature logs, whereas no single well shows characteristics comparable to that of another well. This reflects the complex geological and hydrological conditions in the Krafla geothermal system. In high enthalpy wells within specific subarea reservoirs (Suðurhlíðar, Vesturhlíðar, lower Leirbotnar, Vítismór) phase segregation is assumed, which is largely the cause of excess discharge enthalpy, at least for wells with discharge enthalpy > 2000 kJ/kg. Based on the low  $\text{CO}_2/\text{H}_2\text{S}$  concentration no input of magmatic gasses are detected in deep liquids of well samples. Individual wells can be grouped into specific subareas (Table 4) based on their distinct chemical patterns (e.g. B, Ca, Cl,  $\text{CO}_2$ , F,  $\text{H}_2$ ,  $\text{H}_2\text{S}$ , Na,  $\text{SO}_4$ ,  $\delta\text{D}$ ). For that matter, we propose a revision of the well classification into specific subareas previously presented in Mortensen et al. (2009a) as following: K-32 is classified into subarea Vítismór, and wells K-36 and K-38 are classified into Vesturhlíðar (Table 1).
- The reservoir engineering analysis done focused on an analysis of changes in well output with time. This shows that it appears to be possible to separate the Krafla area in two, based on output changes. Firstly the eastern part of the field, Suðurhlíðar and Vesturhlíðar, where production wells experience the greatest decline in mass output accompanied by high, and even increasing enthalpy. This may indicate that the underlying part of the geothermal system is relatively closed, with limited natural recharge. In contrast wells producing from the lower Leirbotnar system experience no decay in mass output, but a considerable decline in enthalpy, which can likely be both attributed to natural recharge induced by the pressure drop in the system (open system) and the effect of reinjection into well K-26. Simple lumped parameter modelling based on pressure changes in the upper

Leirbotnar system due to production reflect a permeability of the order of 20–30 mDarcy. The temperature model for the Krafla geothermal system developed in 2009 did not require any significant modifications.

- An evaluation of wellbore modelling in conjunction with the upcoming numerical modelling has shown that it is possible to describe the behavior of a production well by simple mathematical equations, which can be linked with the modelling software. This applies to high- and medium-enthalpy wells, down to 1300 kJ/kg. Only four parameters (per feed-zone) are needed instead of the data tables required by the original well-head module in ITOUGH2. Through this method well-head pressure measurements can be used to calibrate the reservoir model, improving its confidence.
- Tracer test have been conducted on four occasions in Krafla. Comprehensive and definite results were only obtained in a small-scale test conducted in Hvíthólar, while the results of the other tests are relatively inconclusive, mainly because of no or insignificant tracer recovery.

## 10.2 Main aspects of the revised conceptual model of the Krafla system

Any conceptual model of the structure and characteristics of the Krafla volcanic and geothermal system has to take into account the geological history. A very comprehensive description of the geological structure and the volcanic history of the Krafla volcanic system has been given by Sæmundsson (1991). The following summarizes that history.

The Krafla volcanic system is believed to have been active for about 200,000 years. It consists of a central volcano and a NNE-SSW trending fissure swarm running through it. Generally speaking the central volcano is characterized by a gently sloping topographic high with a caldera in the middle. The caldera has been associated with an eruption producing semi-acidic welded tuff about 110,000 years ago.

The fissure swarm of Krafla takes up and accommodates most of the crustal spreading in the part of the northern volcanic zone around it. The fissure swarm and the volcano seem, however, to have a sort of bimodal behaviour. Until about 8000 years ago, the presently active part of the fissure swarm was active with considerable volcanic activity, mainly within the caldera (Mt. Krafla) and to the south. Sigurður Þórarinnsson called this the Ludent-period. After the Ludent-period the spreading shifted, for about 5000 years, to the western part of the caldera. Sæmundsson (1991) calls this the Hvannstóð-period. There seems to have been amazingly little extrusive volcanic activity during the Hvannstóð-period; the main event being a phreatic eruption from the explosion crater Hvannstóð about 5000 year ago. About 3000 years ago the spreading shifted back to the eastern part of the fissure swarm, with substantial extrusive volcanism, persisting to present time, with the Mývatn- and Krafla fires the most recent events.

The geological studies of Sæmundsson are mainly based on studies of rocks and structures visible on surface and tephrochronological dating of postglacial lavas. The interpretation of the Bouguer gravity map of Krafla, discussed above, suggests that the geological history sketched here is missing some important events and structures that are not visible on surface, namely a possible

buried inner caldera formed about 80,000 years ago and an extensional WNW-ESE low gravity lineament, mostly filled with hyaloclastite.

Exploration, drilling and utilization of the Krafla geothermal system has shown that the geothermal system in Krafla is very complicated both in structure and in thermo-hydraulic conditions. It may even be considered to constitute more than one system. This is e.g. demonstrated in shallow resistivity, as discussed earlier (see e.g. Figure 19). The associated analysis shows that high temperature alteration is mainly found within the inner caldera and north of the low gravity lineament, reflecting that the inner caldera and the WNW-ESE low-gravity lineament are structures that are of great importance in the geothermal systems.

Different parts of the geothermal system(s) in Krafla have very different thermo-hydraulic character. The anomalies (Figure 21) in the SW-part, and furthest to the east, have cooled down and the one to the east is actually extinct. What appears as one system in the northern part of the inner caldera is actually divided into two or maybe three very different reservoirs. East of Hveragil (Vesturhlíðar- and Suðurhlíðar) there is, generally speaking, a boiling (two-phase) systems from about 2 km to shallow depths, except in the easternmost well (K-18) which shows cooling in the upper parts although hot near the bottom. West of Hveragil the geothermal reservoirs is divided into two very different reservoirs, a deep two-phase (boiling) reservoir, below 1–1.5 km, and overlain by about 200°C almost isothermal convective liquid dominated reservoir, except at shallow depths where it may reach two-phase conditions (boiling). Alteration in the upper system shows, however, that sometime in the past a two-phase reservoir existed there. In Hvíthólar there is a small geothermal reservoir, probably isolated from the main system(s) to the north, showing temperature inversion with depth.

This complexity of the geothermal system(s) in Krafla has puzzled geoscientists for many years. Here an attempt will be made to shed some light on this complexity. The ESE-WNW low gravity lineament seen as a gravity low on the Bouguer map is believed to have started to form after the area was glaciated; it cuts through the inner caldera (Figure 18). The extensional component that produced it seems to favor intrusion of ESE-WNW trending dikes north of the low-density low-gravity lineament. These are the relatively shallow intrusives seen in the northern part of the section on Figure 19. In the Krafla fires, faults in the south slopes of Mt. Krafla and with the same direction as the low gravity lineament, but a few hundred meters north of it, were activated. The intrusions seem to be confined within the inner caldera and not extending into the western part of the bigger caldera because the resistivity surveys show very little sign of geothermal alteration in the western part of the outer caldera. It is therefore postulated that the main heat source of the geothermal system in the northern part of the inner caldera is a complex of ESE-WNW trending dikes from Mt. Krafla and to the west of Leirhnjúkur.

This dike complex seems to be delineated by the 3D inversion models of the magnetotelluric (MT) data. It appears as a high-resistivity zone bordered by low-resistivity, to both the south and north. The resistive central part of the dike complex probably reflects fully crystalized rocks, while the conductive margins might indicate smaller volumes of partial melt. Models from both 1D and 3D inversion of the MT data show a deep conductor close to the rim of the outer caldera under Sandabotnaskarð which could reflect another smaller heat source. Neither of the models show a

deep conductor associated with the geothermal system in Hvíthólar. The wells in Hvíthólar show boiling conditions at a relatively shallow depth but temperature inversion below that.

Based on the studies presented in Chapter 8.2, it is now suggested that the so-called “upper reservoir” developed in the following way. As mentioned earlier, the spreading shifted from the eastern part of the fissure swarm to the western part of the outer caldera about 8000 years ago, but very little intrusive activity seems to have followed as shown by the resistivity surveys with no sign of extensive geothermal alteration there. Dike injection continued, however, in the inner caldera and produced a powerful geothermal system. The shallow high-temperature alteration seen in the now much colder “upper system” is probably from that time. About 3000 years ago, the spreading moved back to the eastern part, with extensive faulting. This greatly increased the permeability in the shallow crust, but repeated intrusions in the dike complex maintained low enough permeability at depth so that a two-phase geothermal system persisted. The much higher permeability above resulted in the vigorously convecting, almost isothermal system observed today. East of Hveragil permeability was not so much affected and two-phase conditions prevail to shallow depths.

Further to the south, under Leirhnjúkshraun, resistivity shows high temperature geothermal alteration. This is the fingerprint of a high temperature geothermal system, maybe formed by intrusions at the end of the glaciation. This system was also affected when the spreading shifted 3000 years ago, but lacked renewed support from below and cooled extensively as seen in well KV-1. The presently active part of the fissure swarm does, however, not extend east to Hvíthólar so that low permeability is maintained there in general and remnants of a fading geothermal system, as discussed above, are still found there. Yet the extensive cooling to the west is close, as was seen in well K-22, which was deviated to the west. It is much colder at depth than vertically drilled wells in Hvíthólar.

As mentioned above, the resistivity model from the 3D inversion of MT shows the ESE-WNW trending dike complex in the inner caldera as a high resistivity structure bordered by low resistivity on each side. It is also mentioned that the high resistivity could reflect fully crystallized rocks, while the bordering low resistivity could reflect partially molten rocks. This can be taken to suggest that there is no magma chamber in the Krafla volcano in the classical sense. Instead, there are, in periods of unrest, dike injections at the margins of the dike complex. The low resistivity at the southern border could be still partially molten dike, which was injected during Mývatn fires, where eruptions and magma injection into the fissure swarm was mainly to the south. The low resistivity on the northern margin could be a dike injected during Krafla fires, where eruptions and magma injection was mainly to the north. This type of scenario would lead to the S-wave shadows observed by Einarsson (1978).

To summarize, it is suggested that, at present, the Krafla volcano hosts three separated geothermal reservoirs: a big reservoir within the inner caldera and north of the WNW-ESE low gravity lineament (Suðurhlíðar, Leirbotnar, Vítismór and Leirhnjúkur), a small old system at Hvíthólar in its final stage and fading out and a small deep reservoir at the caldera rim in Sandabotnar. In addition, there is an extinct system under Leirhnjúkshraun. Before the rifting moved back to the eastern part, the systems in the inner caldera and Hvíthólar were convecting fluids from the

general groundwater flow from the south. When the rifting started 3000 years ago, local groundwater started to interfere with the system in the inner caldera and west of Hveragil. It would appear that intermittently, during rifting episodes, liquid from the extremely permeable upper part escapes into the lower part and recharges it. The small reservoir in Sandabotnar close to well KS-1 is recharged by what appears to be a fluid from far south and probably quite old, probably the deep current shown in Figure 21.

Finally, a word about the rhyolite magma drilled into in K-39 and IDDP-1. Analyses of Zierenberg et al. (2013) show that in both cases the magma is a re-melt from weathered basalt. In fact, the distinct meteoric water oxygen signature of rhyolite in Iceland suggests that rhyolite forms directly by crustal melting of hydrothermally altered basalt rather than by differentiation in “conventional” magma chambers. Zierenberg et al. (2013) conclude that the magma encountered in IDDP-1 was melted at a greater depth than the one encountered in K-39 which could be melted locally. Rhyolite magma “pockets” like this are a sort of “secondary” heat sources which can probably be widespread over the primary basaltic heat sources in the dike complex.

### **10.3 Conclusions and recommendations**

This report has described the latest revision of the conceptual model of the Krafla geothermal system. The revision is based on earlier conceptual models, with the oldest being from 1977 and the most comprehensive one from 2009. It is furthermore based on some re-evaluation of earlier information and interpretation and incorporation of new data. The model revision presented here is done in preparation of the development of a new detailed numerical reservoir model of the Krafla geothermal system.

The numerical model will be based on the principal, relevant aspects of the conceptual model. These include, with more details provided above:

- The main geological structures, both formations as well as faults and fracture-zones, as incorporated in the Petrel model for the Krafla system. This mainly relies on borehole geological data, but is also backed by gravity data.
- An inventory of the main feed-zones of wells in Krafla (see recommendation below).
- Indications of heat sources, both depth and lateral extent, as they appear through the interpretation of resistivity and seismic activity data.
- Subdivision of the Krafla system into zones, or sub-reservoirs, especially the apparent east-west separation between Suðurhlíðar and Vesturhlíðar on one hand and other parts of the system on the other hand, as evidenced by output and chemical content data. The subdivision between upper and lower Leirbotnar is also significant. The nature of these zones in terms of boundary conditions and recharge is most relevant.
- The formation-temperature model for the Krafla system, as now incorporated in the Krafla Petrel model, is of utmost significance for the numerical model, temperature being the primary calibration variable for the natural state.
- The reservoir pressure distribution and pressure changes due to production from the reservoir

- In addition changes in output, i.e. in mass flow and enthalpy, as monitored through time, will be used to calibrate the numerical reservoir model
- Wellhead pressure monitoring data for Krafla production wells should be incorporated as an additional calibration parameter, along the lines reviewed above.

The conceptual model of the Krafla geothermal system needs to be constantly evolving and the present revision has been limited by its purpose as well as the time and funds available for the revision. Therefore, the following recommendations are put forward for the purpose of further revision of the Krafla conceptual model as well as to enhance the process of the numerical model development:

- The incorporation of geo-scientific data into Petrel should be continued to enable 3-dimensional visualization and cross-correlation.
- The feed-zone inventory for Krafla wells needs to be upgraded with the purpose of confirming the principal productive feed-zones for each well (probably only 1–3 per well). The present list (included in Petrel) is too extensive as it includes most feed-zones detected during drilling and through borehole geology.
- Greatly increased understanding of dominant feed-zones in production and reinjection wells, and their contribution during utilization, can be achieved through televiewer- and spinner-logging (PTS-logging) in discharging wells.
- Seismic monitoring in the area should continue. Further analysis of the extensive seismic data available will add significantly to the understanding of the Krafla geothermal system, e.g. derivation of focal mechanisms and relative event locating.
- Further resistivity soundings (TEM and MT) to fill in gaps in data coverage and to enable more accurate 3-D modelling.
- The comprehensive monitoring of chemical content of reservoir fluid should continue, but added emphasis should be placed on stable isotopes, as analyses of these has been limited up to now and new speculation about the origin of fluids were rises recently (see Pope et al., 2015).
- Results of the EU-supported IMAGE-project related to Krafla, which aims at improving exploration methods for deep geothermal resources, should be incorporated into the Krafla conceptual model, once they become available.
- As the wellbore model, discussed above, was originally developed for high enthalpy wells, tests will also be performed to assess the accuracy of the method for wells producing fluid at low enthalpy (~1000 kJ/kg).
- It is recommended to use a revised version of TOUGH2/iTOUGH2 (Magnúsdóttir and Finsterle, 2015), which can model much more extreme temperature and pressure conditions than previous versions of the software, when this revision becomes available.

## 11 References

- Ágústsson, K. and Flóvenz, Ó.G. (2005). The thickness of the seismogenic crust in Iceland and its implications for geothermal systems in Iceland. *World Geothermal Congress 2005*.
- Ágústsson, K., Flóvenz, Ó.G., Guðmundsson, Á. and Árnadóttir, S (2012). Induced seismicity in the Krafla high temperature field. *GRCTransactions*, 36, 975–980.
- Ármannsson, H. Axelsson, G. and Ólafsson M. (2009). *Niðurdæling í KG-26 -Ferilprófun með KI 2005–2007*. ÍSOR-2009/050. LV-2009/092.
- Ármannsson, H., Benjamínsson, J. and Jeffrey, A.W.A. (1989). Gas changes in the Krafla geothermal system, Iceland. *Chemical Geology*, 76, 175–196.
- Ármannsson, H., Fridriksson, T., Gudfinnsson, G.H., Ólafsson, M., Óskarsson, F. and Thorbjörnsson, D. (2014). IDDP – The chemistry of the IDDP-01 well fluids in relation to the geochemistry of the Krafla geothermal system. *Geothermics* 49, 66–75.
- Ármannsson, H., Fridriksson, Th., Benjamínsson, J. and Hauksson, T. (2015). History of chemical composition of geothermal fluids in Krafla, northeast Iceland, with special emphasis on the liquid phase. *World Geothermal Congress 2015*.
- Ármannsson, H., Gíslason, G. and Hauksson, T. (1981). *Magmatic gases in well fluids aid. The mapping of the flow pattern in a geothermal system*. Orkustofnun OS- 81022/JHD-13.
- Ármannsson, H., Guðmundsson, Á. and Steingrímsson, B.S. (1987). Exploration and development of the Krafla geothermal area. *Jökull*, 37, 13–30.
- Árnadóttir, S., Mortensen, A.K., Ingimarsdóttir, A., Tryggvason, H., Jónsson, R.B. and Gunnarsson, H.S. (2009a). *Krafla – IDDP-1. Drilling completion and geology report for drilling stage 2*. Iceland GeoSurvey, ÍSOR-2009/021. LV-2009/099.
- Árnadóttir, S., Mortensen, A.K., Egilson, Þ., Gautason, B., Ingimarsdóttir, A., Massiot, C., Jónsson, R.B., Sveinbjörnsson, S., Tryggvason, H.H. and Eiríksson, E.J. (2009b). *Krafla – Leirbotnar. Hóla KJ-39. 3. áfangi: Jarðlagagreining og mælingar*. In Icelandic. Iceland GeoSurvey, ÍSOR-2009/059, LV-2009/129.
- Árnadóttir, S., Ingimarsdóttir, A., Massiot, C., Hilmarsdóttir, Á., Pétursson, F., Jónsson, R.B., Sveinbjörnsson, S. senior, Sveinbjörnsson S. junior and Haraldsson, H. (2009c). *Krafla – Leirbotnar. Hóla KJ-39. 2. áfangi: Jarðlagagreining og mælingar*. In Icelandic. Iceland GeoSurvey, ÍSOR-2009/046. LV-2009/092.
- Árnason K. and Magnússon I.Þ. (2001). *Niðurstöður viðnámsmælinga í Kröflu*, OS-2001/062.
- Arnórsson, S. (2012). The nature and renewability of geothermal systems. *Náttúrufræðingurinn*, 82, 49-72. (In Icelandic with an Icelandic summary.)
- Arnórsson, S. and Andrésdóttir, A. (1995). Processes controlling the distribution of boron and chlorine in natural waters in Iceland. *Geochimica et Cosmochimica Acta*, 59 (20), 4125-4146.

- Arnórsson, S., Gunnlaugsson, E. and Svavarsson, H. (1983). The chemistry of geothermal waters in Iceland. III. Chemical geothermometry in geothermal investigations. *Geochimica et Cosmochimica Acta*, 47 (3), 567-577.
- Arnórsson, S., Fridriksson, Th. and Gunnarsson, I. (1998). Gas chemistry of the Krafla Geothermal Field, Iceland. In Arehart, G. and Hulston, J.R. (eds). *Water-Rock Interaction 1998*.
- Arnórsson, S., Stefánsson, A. and Bjarnason, J.Ö. (2007). Fluid-Fluid Interactions in Geothermal. *Reviews in Mineralogy and Geochemistry*, 65, 259-312.
- Axelsson, G. (1989) Simulation of pressure response data from geothermal reservoirs by lumped parameter models. *Proceedings 14<sup>th</sup> Workshop on Geothermal Reservoir Engineering, Stanford University, USA*, 257-263.
- Axelsson, G. (2013). Tracer tests in geothermal resource management. *EPJ Web of Conferences*, 50, online.
- Axelsson, G. and E. Gunnlaugsson (2000). Long-term Monitoring of High- and Low-enthalpy Fields under Exploitation. *International Geothermal Association, World Geothermal Congress 2000 Short Course, Kokonoe, Kyushu District, Japan, May 2000*, 226pp.
- Berthet, J.-C., Arnaldsson, A. and Snorri, P.K. (2014). Development of a well-bore model for use in conjunction with iTOUGH2. *Reykjavik, Vatnaskil, 2014. 14.10*.
- Bjarnason, J.Ö. (2010). Manual for the chemical speciation program WATCH v. 2.4. [http://www.geothermal.is/sites/geothermal.is/files/download/watch\\_readme.pdf](http://www.geothermal.is/sites/geothermal.is/files/download/watch_readme.pdf)
- Björnsson, A. and Eysteinnsson, H. (1998). *Breytingar á landhæð við Kröflu 1974–1995 Samantekt á landhæðarmælingum*. (Samvinnuverk Orkustofnunar, Norrænu eldfjallastöðvarinnar og Landsvirkjunar). Orkustofnun, OS-98002, 161 bls.
- Björnsson, S. (1969). *Áætlun um rannsókn háhitasvæða*. Orkustofnun.
- Björnsson, G., Böðvarsson, G.S., Tulinius, H., Sigurðsson, Ó. and Thordarson S. (1997). *Áhrif nýborana á suðurhlíðar Kröflu. Áfangaskýrsla um þrívítt reiknilíkan*. Orkustofnun OS-97027.
- Björnsson, G., Böðvarsson, G.S. and Sigurðsson Ó. (1998). *Status of the development of the numerical model of the Krafla geothermal system - May 1998*. OST GRG GrBGSB-ÓS-98/02.
- Blanck, H., Ágústsson, K. and Gunnarsson, K. (2014). *Seismic monitoring of Krafla for the period October 2013 to October 2014*. ÍSOR-2014/061.
- Blischke, A., Gautason, B. and Guðmundsson, Á. (2004). *Krafla - well KV-01: pre-drilling for a 18 5/8" surface casing down to 79.5 m depth*. In Icelandic. Iceland GeoSurvey, ÍSOR-2004/046.
- Brandsdóttir, B. and Menke, W. (2008). The seismic structure of Iceland. *Jökull*, 58, 17–34.
- Christensen, N.I. (1996). Poisson's ratio and crustal seismology. *Journal of Geophysical Research*, 101 (B2), 3139-3156.
- Böðvarsson, G.S., Pruess, K., Stefánsson, V. and Eliásson, E.T. (1982). Modeling studies of the natural state of the Krafla geothermal field, Iceland. *Proceedings Eight Workshop of Geothermal Reservoir Engineering*.

- Böðvarsson, G.S., Pruess, K., Stefánsson, V. and Elíasson E.T. (1984). The Krafla geothermal field, Iceland: 2. The natural state of the system. *Water Resources Research*, 20, 1545–1559.
- Chen W-P. and Molnar P. (1983). Focal depths of intracontinental and intraplate earthquakes and their implications for the thermal and mechanical properties of the lithosphere. *Journal of Geophysical Research*, 88, 4183–4214.
- Darling, W.G. and Ármannsson, H. (1989). Stable isotopic aspects of fluid flow in the Krafla, Námafjall and Þeistareykir geothermal systems of Northeast Iceland. *Chemical Geology*, 76, 175–196.
- Einarsson, P. (1978). S-wave shadows in the Krafla caldera in NE-Iceland, evidence for a magma chamber in the crust. *Bulletin of Volcanology*, 41, 1–9.
- Einarsson, P. (1991). Umbrotin við Kröflu 1975–1989. In: Garðarsson, A. and Einarsson Á (Eds.), *Náttúra Myávats. Hið íslenska náttúrufræðifélag*, Reykjavík, 96–139.
- Finsterle, S. (2007). iTOUGH2 User's Guide. *Berkeley, Lawrence Berkeley National Laboratory*, 2007. LBNL-40040.
- Foulger, G.R., Miller, A.D., Julian, B.R. and Evans, J.R. (1995). Three-dimensional up and vp/vs structure of the Hengill Triple Junction and Geothermal Area, Iceland, and the repeatability of tomographic inversion. *Geophysical Research Letters*, 22 (10), 1309-1312.
- Fournier, R.O. and Potter, R.W. (1982): An equation correlating the solubility of quartz in water from 25°C to 900°C at pressures up to 10000 bars. *Geochimica et Cosmochimica Acta*, 46 (10), 1969–1974.
- Franzson, H., Guðmundsson, Á., Friðleifsson, G.Ó., Hólmjárn, J., Sigurðsson, Ó., Jónsson, S.S. and Sigursteinsson, D. (1996). *Krafla, hola KJ-28 3. áfangi: borun vinnsluhluta holunnar frá 392 m í 1003 m*. In Icelandic. Orkustofnun OS-96079/JHD-46.
- Franzson, H., Sigurðsson, Ó., Jónsson, S.S., Hermannsson, G. and Sigursteinsson, D. (1998). *Krafla, hola KJ-32 : 1. áfangi: Borun fyrir öryggisfóðringu í 295 m dýpi*. In Icelandic. Orkustofnun, OS-98055.
- Friðleifsson, G.Ó. and Sigvaldason, H. (1981). *Krafla. Hola KJ-17. Borun frá 212 m í 695 m og steyping 9 5/8" fóðringar*. In Icelandic. Orkustofnun GÓG-HI-81/02.
- Friðleifsson, G.Ó. and Stefánsson, V. (1981). *Krafla - Hola KJ-18. Borun í 206 m og steyping 13 3/8 fóðringar*. In Icelandic. Orkustofnun GÓF-VS-81/03.
- Friðleifsson, G.Ó., Guðmundsson, G. and Stefánsson V. (1981a). *Krafla KJ-18. Borun frá 200 m í 674 m og steyping 9 5/8" fóðringar*. Orkustofnun GÓF-GjF-VS-81/04 12
- Friðleifsson, G.Ó., Sigvaldason, H. and Steingrímsson, B. (1981b). *Krafla. Hola KJ-17. Borun frá 65 m í 212 m og steyping 13 3/8" fóðringar*. In Icelandic. Orkustofnun GÓF-HS-ÁG-81/01.
- Gadalia, A., Braibant, G., Touzelet, S. and Sanjuan B. (2010). *Tracing tests using organic compounds in a very high temperature geothermal field, Krafla (Iceland)*. Final Report, Bureau de Recherches Géologiques et Minières (BRGM), Orléans, France.

- Gautason, B., Egilson, P., Blischke, A., Pétursson, F., Jónsson, R.B., Ingólfsson, I., Eiríksson, E.J. and Haraldsson, K. (2007a). *Krafla - Víti. Hóla KJ-36. 2. áfangi: Borun fyrir 9½" vinnslufóðringu í 1111 m dýpi*. In Icelandic. Iceland GeoSurvey, ÍSOR-2007/060, LV-2007/118.
- Gautason, B., Egilson, P., Richter, B., Thordarson, S., Jónsson, P. and Jónsson, P.H. (2007b). *Krafla – Hóla KS-01. 3. áfangi: Borun vinnsluhluta fyrir 7" leiðara frá 899 m í 2502 m dýpi*. In Icelandic. Iceland GeoSurvey, ÍSOR-2007/024, LV-2007/071.
- Gautason, B., Egilson, P., Gunnarsson, H.S. and Ingólfsson, P. (2008a). *Krafla – Suðurhlíðar. Hóla KJ-37. Forborun og 1. áfangi: Borun fyrir 13¾" öryggisfóðringu í 236 m dýpi*. In Icelandic. Iceland GeoSurvey, ÍSOR-2008/022, LV-2008/065.
- Gautason, B., Guðmundsson, Á., Ásmundsson, R.K., Thordarson, S., Sigurðsson, G. and Jónsson, P.H. (2006). *Krafla – Hóla KV-01. 2. áfangi: Borun fyrir 9½" vinnslufóðringu frá 290 m í 804 m dýpi*. In Icelandic. Iceland GeoSurvey, ÍSOR-2006/040, LV-2006/124.
- Gautason, B., Tryggvason, H.H., Jónsson, R.B., Guðmundsson, Á., Eiríksson, E.J. and Haraldsson, K. (2008b). *Krafla – Suðurhlíðar. Hóla KJ-37. 2. áfangi: Borun fyrir 9½" vinnslufóðringu í 768 m dýpi*. In Icelandic. Iceland GeoSurvey, ÍSOR-2008/040, LV-2008/084.
- Gautason, B., Tryggvason, H., Sveinbjörnsson, S., Hilmarsdóttir, Á., Jónsson, R.B. and Guðnason, Ó. (2008c). *Krafla - hóla KJ-38. Forborun og 1. áfangi: Borverk*. Iceland GeoSurvey, ÍSOR-2008/072, LV-2008/205.
- Gautason, B., Tryggvason, H., Sveinbjörnsson, S., Hilmarsdóttir, Á., Jónsson, R.B. and Guðnason, Ó. (2008d). *Krafla - hóla KJ-38. Forborun og 1. áfangi: Jarðlagagreining og mælingar*. Iceland GeoSurvey, ÍSOR-2008/073, LV-2008/206.
- Gautason, B., Tryggvason, H., Sveinbjörnsson, S., Hilmarsdóttir, Á., Jónsson, R.B. and Guðnason, Ó. (2009). *Krafla – Hóla KJ-38. Forborun og 1. áfangi: Jarðlagagreining og mælingar*. In Icelandic. Iceland Geosurvey, ÍSOR-2008/073, LV-2008/206.
- Giroud, N. (2008). A chemical study of arsenic, boron and gases in high-temperature geothermal fluids in Iceland. PhD thesis, University of Iceland, Reykjavik, Iceland, 110p.
- Giroud, N., Ármannsson, H. and Ólafsson, M. (2008). *Krafla well KS-01. Chemical composition of liquid and steam during a flow test in autumn 2007* (In Icelandic). Iceland GeoSurvey, short report ÍSOR-08055.
- Gíslason, G. and Arnórsson, S. (1976). *Framvinduskýrsla um breytingar á rennsli og efnainnihaldi í borholum 3*. Orkustofnun, OS-JHD-7640, 14 pp.
- Gíslason, G., Ármannsson, H. and Hauksson, T. (1978). *Krafla. Hitaástand og gastegundir í jarðhitakerfinu*. Orkustofnun OS-JHD-7846.
- Gradient Geodata (2015). *WellSim. Gradient Geodata*. [Online] Gradient Geo Data, 2015. [Cited: January 19, 2015.] <http://www.gradientgeodata.com/wellsim/>.
- Grant, M.A., Donaldson, I.G. and Bixley, P.F. (1982). *Geothermal reservoir engineering*. Academic Press, NY, 369 pp.

- Guðmundsson, Á. (1983). Jarðfræði Suðurlíða Kröflu. *Hrafnæping um stöðu Kröflu Jarðhita Orkuver*. 2.–3. mars 1983, Akureyri; 77–85.
- Guðmundsson, Á. (2001). An expansion of the Krafla Power Plant from 30 to 60 MWe. Geothermal Considerations. *Geothermal Research Council Transactions*, 25, 741–746.
- Guðmundsson, B.T. and Arnórsson, S. (2002). Geochemical monitoring of the Krafla and Námafjall geothermal areas, N-Iceland. *Geothermics*, 31 (2), 195–243.
- Guðmundsson, B.T. and Arnórsson, S. (2005). Secondary mineral-fluid equilibria in the Krafla and Námafjall geothermal systems, Iceland. *Applied Geochemistry*, 20 (9), 1607–1625.
- Guðmundsson, Á., Steingrímsson, B. and Halldórsson, G.K. (1981a). *Krafla hola KJ-17. Áfangaskýrsla um borun vinnsluhluta holunnar*. In Icelandic. Orkustofnun ÁG-BS-GKH-81/04.
- Guðmundsson, Á., Steingrímsson, B., Halldórsson, G.K., Guðmundsson, G. and Stefánsson, V. (1981b). *Krafla hola KJ-18*. In Icelandic. Orkustofnun ÁG-BS-GKH-GjG-VS-81/05.
- Guðmundsson, Á., Steingrímsson, B., Guðmundsson, G. and Friðleifsson, G.Ó. (1982a). *Krafla, hola KJ-20. Borun fyrir 9 5/8" fódningu og steyping fódurröra*. Temporary report. In Icelandic. Orkustofnun OS-82116/JHD-32.
- Guðmundsson, Á., Steingrímsson, B., Guðmundsson, G., Friðleifsson, G.Ó., Sigvaldason, H., Sigurðsson, Ó., Guðlaugsson, S.P. and Stefánsson, V. (1982b). *Krafla, hola KJ-20. Borun vinnsluhluta holunnar og borlok*. Temporary report. In Icelandic. Orkustofnun OS-82117/JHD-33.
- Guðmundsson, Á., Steingrímsson, B., Friðleifsson, G.Ó. and Tryggvason, H. (1982c). *Krafla, hola KJ-21. Borun vinnsluhluta holunnar frá 293 til 1200 m*. Temporary report. In Icelandic. Orkustofnun OS-82119/JHD-35.
- Guðmundsson, Á., Friðleifsson, G.Ó., Guðmundsson, G., Sigvaldason, H., Tryggvason, H. and Benediktsson, S. (1983a). *Krafla, hola KJ-22. Borun frá 50 m í 198 m og steyping 13 3/8" fódningar*. In Icelandic. Orkustofnun OS-83062/JHD-17.
- Guðmundsson, Á., Sigursteinsson, D., Guðmundsson, G., Friðleifsson, G.Ó. and Tryggvason, H. (1983b). *Krafla, hola KJ-22. Borun fyrir vinnslufódningu frá 198 m til 567 m*. In Icelandic. Orkustofnun OS-83070/JHD-20.
- Guðmundsson, Á., Steingrímsson, B., Sigursteinsson, D., Guðmundsson, G., Friðleifsson, G.Ó., Tryggvason, H. and Sigurðsson, Ó. (1983c). *Krafla, hola KJ-22. Borun vinnsluhluta holunnar, frá 567 m til 1877 m*. In Icelandic. Orkustofnun OS-83071/JHD-22.
- Guðmundsson, Á., Steingrímsson, B., Ármannsson, H., Sigvaldason, H., Benjamínsson, J. and Sigurðsson, Ó. (1983d). *Krafla, hola KJ-9. Aflsaga, efnabreytingar og endurborun*. Report No. OS-83075/JHD-13, Orkustofnun.
- Guðmundsson, Á., Sigursteinsson, D., Sigvaldason, H., Tryggvason, H. and Benediktsson, S. (1983e). *Krafla, hola KJ-23. Borun frá 70 m í 196 m og steyping 13 3/8" fódningar*. In Icelandic. Orkustofnun OS-83079/JHD-25.

- Guðmundsson, Á., Steingrímsson, B., Sigursteinsson, D., Guðmundsson, G., Tryggvason, H. and Benediktsson, S. (1983f). *Krafla, hola KJ-23. Borun frá 196 m í 539 m og steyping 9 5/8" fódðringar*. In Icelandic. Orkustofnun OS-83080/JHD-26.
- Guðmundsson, Á., Steingrímsson, B., Guðmundsson, G., Friðleifsson, G.Ó., Sigvaldason, H., Tryggvason, H. and Sigurðsson, Ó. (1983g). *Krafla, hola KJ-23. Borun vinnsluhluta holunnar*. In Icelandic. Orkustofnun OS-83082/JHD-27.
- Guðmundsson, Á., Benediktsson, S. and Sigursteinsson, D. (1988a). *Borun holu KG-24. 1. áfangi - borun fyrir 13 3/8" öryggisfódðringu*. In Icelandic. Orkustofnun, summary ÁsG-SBen-DS-88/07.
- Guðmundsson, Á., Benediktsson, S. and Sigursteinsson, D. (1988b). *Borun holu KG-24. 2. áfangi - borun fyrir 9 5/8" vinnslufódðringu*. In Icelandic. Orkustofnun, summary ÁsG-SBen-DS-88/08.
- Guðmundsson, Á., Sigursteinsson, D., Steingrímsson, B., Sigurðsson, Ó., Sigvaldason, H. og Hólmjárn, J. (1988c). *Borun holu KG-24. 3. áfangi - borun vinnsluhluta*. In Icelandic. Orkustofnun, summary, ÁsG-DS-BS-ÓMAR-HS-JH-88/09.
- Guðmundsson, Á., Steingrímsson, B., Sigvaldason, H., Sigurður Benediktsson, S. and Dagbjartur Sigursteinsson, D. (1990a). *Krafla. Borun holu KG-25. 2. áfangi*. In Icelandic. Orkustofnun, summary ÁsG-BS-HS-SBen-DS-90/06.
- Guðmundsson, Á., Hólmjárn, J., Stefánsson, V., Benediktsson, S. and Sigursteinsson, D. (1990b). *Krafla. Borun holu KG-25. 3. áfangi*. In Icelandic. Orkustofnun, summary, ÁsG-JH-VS-SBen-DS-90/07.
- Guðmundsson, Á., Benediktsson, S., Sigvaldason, H. and Sigursteinsson (1991a). *Krafla. Borun 1. áfanga holu KG-26*. In Icelandic. Orkustofnun, OS-91040/JHD-23.
- Guðmundsson, Á., Sigurðsson, Ó., Benediktsson, S., Hólmjárn, J. and Sigursteinsson, D. (1991b). *Krafla. Borun 2. áfanga holu KG-26*. In Icelandic. Orkustofnun OS-91041/JHD-24.
- Guðmundsson, Á., Franzson, H., Sigurðsson, Ó., Benediktsson, S., Hólmjárn, J. and Sigursteinsson, D. (1992). *Krafla. Borun 3. áfanga holu KG-26*. In Icelandic. Orkustofnun OS-92009/JHD-03.
- Guðmundsson, Á., Steingrímsson, B., Hermannsson, G., Hólmjárn, J., Sigursteinsson, D. and Benediktsson, S. (1996). *Krafla, borun holu KJ-27. 1. áfangi (70-395)*. In Icelandic. Orkustofnun OS-96058/JHD-36.
- Guðmundsson, Á., Steingrímsson, B., Sigursteinsson, D., Hermannsson, G., Sigvaldason, H., Sigurðsson, Ó., Jónsson, S.S., Benediktsson, S. and Thordarson, S. (1997a). *Krafla, hola KJ-27. 3. áfangi: Fódðrun með 9 5/8" vinnslufódðringu og borun vinnsluhluta*. In Icelandic. Orkustofnun OS-97072.
- Guðmundsson, Á., Steingrímsson, B., Sigursteinsson, D., Hermannsson, G., Sverrisdóttir, G., Sigvaldason, H., Sigurðsson, Ó. and Jónsson, S.S. (1997b). *Krafla, hola KJ-30. 1. áfangi: Borun fyrir öryggisfódðringu í 308 m dýpi*. In Icelandic. Orkustofnun OS-97044.

- Guðmundsson, Á., Sigursteinsson, D., Sigvaldason, H., Franzson, H., Sigurðsson, Ó., Birgisson, K., Jónsson, S.S. and Thordarson, S. (1997c). *Krafla, hola KJ-30 2. áfangi: Borun fyrir vinnslufóðringu frá 309-818 m dýpi*. In Icelandic. Orkustofnun OS-97045.
- Guðmundsson, Á., Sigursteinsson, D., Sigvaldason, H., Benediktsson, S., Jónsson, S.S. and Thordarson, S. (1997d). *Krafla, hola KJ-31 1. áfangi: Borun fyrir öryggisfóðringu í 309 m dýpi*. In Icelandic. Orkustofnun OS-97047.
- Guðmundsson, Á., Sigursteinsson, D., Björnsson, G., Hermannsson, G., Sigvaldason, H., Sigurðsson, Ó. and Benediktsson, S. (1997e). *Krafla, hola KJ-31. 2. áfangi: Borun fyrir vinnslufóðringu frá 309 m í 800 dýpi vinnsluhluta*. In Icelandic. Orkustofnun OS-97073.
- Guðmundsson, Á., Sigursteinsson, D., Sigvaldason, H., Benediktsson, S., Jónsson, S.S. and Thordarson, S. (1997f). *Krafla, hola KJ-31. 1. áfangi: Borun fyrir öryggisfóðringu í 309 m dýpi*. In Icelandic. Orkustofnun OS-97047.
- Guðmundsson, Á., Sigursteinsson, D., Björnsson, G., Hermannsson, G., Sigvaldason, H., Sigurðsson, Ó. and Benediktsson, S. (1997g). *Krafla, hola KJ-31. 2. áfangi: Borun fyrir vinnslufóðringu frá 309 m í 800 dýpi vinnsluhluta*. In Icelandic. Orkustofnun OS-97073.
- Guðmundsson, Á., Franzson, H., Sigvaldason, H., Birgisson, K., Thordarson, S. and Sigursteinsson, D. (1998a). *Krafla, hola KJ-32: 2. áfangi: Borun fyrir vinnslufóðringu í 1077 m dýpi*. In Icelandic. Orkustofnun, OS-98057.
- Guðmundsson, Á., Richter, B., Sigvaldason, H., Birgisson, K., Sigurðsson, Ó., Thordarson, S., Matthíasson, M. and Sigursteinsson, D. (1998b). *Krafla, hola KJ-32 3. áfangi: Borun vinnsluhluta 1077-1875 m dýpi*. In Icelandic. Orkustofnun, OS-98058.
- Guðmundsson, Á., Steingrímsson, B., Björnsson, G., Jónsson, S.S., Thordarson, S., Sigurðsson, Ó. and Sigursteinsson, D. (1998c). *Krafla, hola KJ-29. 3. áfangi: Borun fyrir vinnsluhluta 1004–2103 m dýpi 13935*. In Icelandic. Orkustofnun, Rannsóknasvið OS-98084.
- Guðmundsson, Á., Steingrímsson, B., Björnsson, G., Hermannsson, G., Sigurðsson, H., Sigvaldason, H., Franzson, H., Birgisson, K., Jónsson, S.S., Thordarson, S. and Guðlaugsson, S.P. (1999a) *Krafla, hola KJ-33. 3. áfangi: Borun fyrir vinnsluhluta í 2011 m dýpi*. In Icelandic. Orkustofnun, OS-99072.
- Guðmundsson, Á., Jónsson, S.S., Gautason, B., Sigurðsson, Ó., Hermannsson, H., Thordarson, S. and Sigurðsson, H. (1999b). *Krafla hola KJ-34. 1. áfangi: Borun fyrir öryggisfóðringu í 377 m dýpi*. In Icelandic. Orkustofnun, OS-99073.
- Guðmundsson, Á., Steingrímsson, B., Björnsson, G., Hermannsson, G., Sigurðsson, H., Franzson, H., Birgisson, K. and Thordarson, S. (1999c). *Krafla, hola KJ-34. 2. áfangi: Borun fyrir vinnslufóðringu í 1031 m dýpi*. In Icelandic. Orkustofnun, OS-99089.
- Guðmundsson, Á., Gautason, B., Richter, B., Hermannsson, G., Birgisson, K., Sigurðsson, Ó., Jónsson, S.S. and Thordarson, S. (1999d). *Krafla, hola KJ-34. 3. áfangi: Borun vinnsluhluta frá 1031 í 2002 m dýpi*. In Icelandic. Orkustofnun, OS-99101.

- Guðmundsson, Á., Egilson, Þ. and Haraldsson, K. (2007a). *Krafla - hola KS-01 : Forborun og 1. áfangi: borun fyrir 18 5/8" yfirborðsfóðringu í 99 m og 13 3/8" öryggisfóðringu í 279 m dýpi*. In Icelandic. Landsvirkjun, LV-2007/055; Iceland GeoSurvey, ÍSOR-2007/015.
- Guðmundsson, Á., Egilson, Þ., Gautason, B., Thordarson, S., Jónsson, P. and Haraldsson, K. (2007b). *Krafla - hola KS-01 : 2. áfangi: borun fyrir 9 5/8" vinnslufóðringu frá 279 m í 899 m dýpi*. In Icelandic. Landsvirkjun, LV-2007/070; Iceland GeoSurvey, ÍSOR-2007/022.
- Guðmundsson, Á., Blischke, A., Thordarson, S., Jónsson, R.B. and Haraldsson, K. (2007c). *Krafla - hola KJ-36 : 1. áfangi: borun fyrir 13 3/8" öryggisfóðringu frá 75 m í 301 m dýpi*. In Icelandic. Landsvirkjun, LV-2007/090; Iceland GeoSurvey, ÍSOR-2007/048.
- Guðmundsson, Á., Gautason, B., Nielsson, S., Egilson, Þ., Jónsson, R.B., Gunnarsson, H.S. and Ingólfsson, Þ.K. (2008a). *Krafla - Suðurhlíðar: hola KJ-37 : 3. áfangi : borun vinnsluhluta með 8 1/2" krónu í 2194 m dýpi*. In Icelandic. Iceland GeoSurvey, ÍSOR-2008/041, LV-2008/085.
- Guðmundsson, Á., Jónsson, S.S., Gautason, B., Thordarson, S., Egilson, Þ., Pétursson, F., Eiríksson, E.J., Jónsson, R.B., Ingólfsson, H. and Haraldsson, K. (2008b). *Krafla - Víti hola KJ-36 : 3. áfangi: borun vinnsluhluta í 2501 m dýpi*. In Icelandic. Landsvirkjun, LV-2008/087; Iceland GeoSurvey, ÍSOR-2008/042.
- Guðmundsson, G., Pálmason, G., Grönvold, K., Ragnars, K., Sæmundsson, K. and Arnórsson, S. (1971). *Námafjall-Krafla. Áfangaskýrsla um rannsókn jarðhitasvæðanna*. Orkustofnun.
- Guðmundsson, G., Hólmjárn, J., Benediktsson, S., and Sigursteinsson, D. (1990). *Krafla. Borun holu KG-25. 1. áfangi*. In Icelandic. Orkustofnun, summary, ÁsG-JH-SBen-DS-90/05.
- Gylfadóttir, S.S. and Gunnarsdóttir, S.H. (2014). *Volumetric Assessment of the Lower Leirbotnar Geothermal Reservoir in Krafla, NE-Iceland*. Iceland GeoSurvey, report, ÍSOR-2014/046, LV-2014/089.
- Hjartarson, A., Guðmundsson, Á., Sigurðsson, H., Franzson, H., Birgisson, K., Jónsson, S.S. and Thordarson, S. (1999). *Krafla, hola KJ-33. 2. áfangi: Borun fyrir vinnslufóðringu í 1120 m dýpi*. In Icelandic. Orkustofnun, OS-99061.
- Hjartarson, A., Sigurðsson, Ó., Guðmundsson, Á., Ármannsson, H. and Karlsdóttir, R. (2004). *A numerical model of the Námafjall geothermal system and predictions on its response to a 30–90 MWe power production in Bjarnarflag* (in Icelandic). Iceland GeoSurvey, ÍSOR-2004/009.
- Hayba, D.O. and Ingebritsen, S.E. (1997). Multiphase groundwater flow near cooling plutons. *Journal of Geophysical Research*, 102 (B6), 12235-12252.
- Ingimarsdóttir, A., Mortensen, A.K., Gautason, B., Pétursson, F., Guðmundsson, H., Tryggvason, H.H., Jónsson, R.B., Sveinbjörnsson, S. and Haraldsson, K. (2009a). *Krafla - Víti hola KJ-38.2. áfangi: Borsaga*. In Icelandic. Landsvirkjun, LV-2009/104; Iceland GeoSurvey, ÍSOR-2009/053.
- Ingimarsdóttir, A., Tryggvason, H.H., Mortensen, A.K., Gautason, B., Pétursson, F., Guðmundsson, H., Jónsson, R.B., Sveinbjörnsson, S. and Haraldsson, K. (2009b). *Krafla - Víti hola KJ-38. 2. áfangi: Jarðlagagreining og mælingar*. In Icelandic. Iceland GeoSurvey, ÍSOR-2009/053, LV-2009/104.

- Johnsen, G.V. (1995). Þyngdarkort af Kröflusvæði. In: Hróarsson, B., Jónsson, D. and Jónsson, S.S. (Eds.) *Eyjar í eldhafi*, Gott nál hf., 93-100.
- Johnson, G.V., Björnsson A. and Sigurðsson, S.P. (1980). Gravity and elevation changes caused by magma movement beneath the Krafla caldera northeast Iceland. *Journal of Geophysics*, 47, 132–140.
- Jónasson, K. (1994). Rhyolite volcanism in the Krafla central volcano, north-east Iceland. *Bulletin of Volcanology*, 56, 516–528.
- Julian, B.R., Ross, A., Foulger, G.R. and Evans, J.R. (1996). Three-dimensional seismic image of a geothermal reservoir: The Geysers, California. *Geophysical Research Letters*, vol. 23 (6), 685-688.
- Júlíusson, E., Markússon, S. and Sigurdardóttir, Á. (2015). Phase-Specific and Phase-Partitioning Tracer Experiment in the Krafla Reservoir, Iceland. *World Geothermal Congress 2015*
- Karlsdóttir, R., Johnsen, G., Björnsson, A., Sigurðsson, Ó. and Hauksson, E. (1978). *Jarðhitasvæðið við Kröflu. Áfangaskýrsla um jarðeðlisfræðilegar yfirborðsrannsóknir 1976–1978*. Orkustofnun OS-JHD-7847.
- Kipp, K.L., Hsieh, P.A. and Charlton, S.C. (2008). Revised Ground-Water Flow and Heat Transport Simulator: HYDROTHERM-Version 3. USGS, [http://wwwbrr.cr.usgs.gov/projects/GW\\_Solute/hydrotherm](http://wwwbrr.cr.usgs.gov/projects/GW_Solute/hydrotherm)
- Kristinsson, S.G., Óskarsson, F., Ólafsson, M. and Óladóttir, A.A. (2014). *The high-temperature areas in Krafla, Námafjall and Theistareykir. Monitoring of surface activity and groundwater in 2014* (in Icelandic). Iceland GeoSurvey, report ÍSOR-2014/058.
- Kristmannsdóttir, H. (1978). *Alteration of bedrock in the Krafla geothermal system*. Report no. OS/JHD-7854, Orkustofnun.
- Magnúsdóttir, L. and Finsterle, S. (2015). Extending the applicability of the iTOUGH2 simulator to supercritical conditions. *World Geothermal Congress 2015*.
- Mortensen, A.K., Kjartansson, O.Ó., Jónsson, P. and Guðnason, Ó. (2007a). *Krafla - hola KJ-35 : 1. áfangi: borun fyrir 13 3/8" öryggisfóðringu frá 57 m í 270 m dýpi*. In Icelandic. Iceland GeoSurvey ÍSOR-2007/023, LV-2007/72.
- Mortensen, A.K., Gautason, B., Egilson, Þ., Kjartansson, O.Ó., Jónsson, P., Jónsson, R.B. and Guðnason, Ó. (2007b). *Krafla - hola KJ-35 : 2. áfangi: borun fyrir 9 5/8" vinnslufóðringu frá 270 m í 1296 m dýpi*. In Icelandic. Iceland GeoSurvey, ÍSOR-2007/029, LV-2007/078.
- Mortensen, A.K., Guðmundsson, Á., Júlíusson, E., Jónsson, P., Kjartansson, O.Ó. and Bjarnason, S. (2007c). *Krafla - hola KJ-35 : 3. áfangi: borun vinnsluhluta frá 1296 m í 2508 m dýpi fyrir 7" leiðara*. In Icelandic. Landsvirkjun LV-2007/088, Iceland GeoSurvey, ÍSOR-2007/044.
- Mortensen, A.K., Guðmundsson, Á., Steingrímsson, B., Sigmundsson, F., Axelsson, G., Ármannsson, H., Björnsson, H., Ágústsson, K., Sæmundsson, K., Ólafsson, M., Karlsdóttir, R., Halldórsdóttir, S. and Hauksson T. (2009a). *Jarðhitakerfið í Kröflu. Samantekt rannsókna á jarðhitakerfinu og endurskoðað hugmyndalíkan*. In Icelandic. Iceland GeoSurvey, ÍSOR-2009/057, LV-2009/111.

- Mortensen, A.K., Sigurgeirsson, M.Á., Egilson, Þ., Guðfinnsson, G.H., Tryggvason, H., Jónsson, R.B. and Sveinbjörnsson, S. (2009b). *Hola KT-40. 3. áfangi: Jarðlagagreining og mælingar*. In Icelandic. Iceland Geosurvey, ÍSOR-2009/070, LV-2009/144.
- Muskin, U. Bauer, K. and Haberland, C. (2013). Seismic Vp and Vp/Vs structure of the geothermal area around Tarutung (North Sumatra, Indonesia) derived from local earthquake tomography. *Journal of Volcanology and Geothermal Research*, 260, 27-42.
- O'Sullivan, M.J., Pruess, K. and Lippmann, M.J. (2001). State of the art of geothermal reservoir simulation. *Geothermics*, 30, 395-429.
- Pálmason, G., Johnsen, G.V., Torfason, H., Sæmundsson, K., Ragnars, K., Haraldsson, G.I. and Halldórsson, G.K. (1985). *Mat á jarðvarma Íslands*. Orkustofnun OS-85076/JHD-10.
- Pope, E.C., Bird, D.K., Arnórsson, S. and Giroud, N. (2015). Hydrogeology of the krafla geothermal system, northeast Iceland. *Geofluids*, DOI: 10.1111/gfl.12142
- Sigurgeirsson, M.Á., Mortensen, A.K. Egilson, Þ., Sveinbjörnsson, S. and Pétursson, F. (2008). *Krafla – Hola KJ-38. Borun 3. áfanga: Jarðlagagreining og mælingar*. In Icelandic. Iceland Geosurvey, ÍSOR-2008/071, LV-2008/204.
- Sigurgeirsson, M.Á., Egilson, Þ., Nielsson, S., Gautason, B., Jónsson, R.B., Sveinbjörnsson, S. and Þorsteinsson, E. (2009). *Krafla – Hola KJ-40. Forborun, 1. og 2. áfangi: Jarðlagagreining og mælingar*. In Icelandic. Iceland Geosurvey, ÍSOR-2009/020, LV-2009/027.
- Sigurðsson, Ó. and Stefánsson, V. (1994). Forðafraeðistuðlar – Mælingar á bergsýnum. Orkustofnun, OS-94049/JHD-28, 35 bls.
- Stefánsson, V. (1980). Investigation on the Krafla high temperature geothermal field. *Náttúrufræðingurinn*, 50, 333–359.
- Stefánsson, V. (1981). The Krafla geothermal field Northeast Iceland. In: Rybach, L. and Muffler, L.J.P. (Eds.), *Geothermal Systems: Principles and Case Histories*, John Wiley and Sons Ltd, 273–294.
- Stefánsson, V., Guðmundsson, Á., Steingrímsson, B., Guðmundsson, G., Friðleifsson, G.Ó., Axelsson, G., Ármannsson, H., Sigvaldason, H., Benjamínsson, J. and Sigurðsson, Ó. (1983). *Krafla, holur KJ 16, 17 og 18. Rannsóknir samhliða borun og vinnslueiginleikar*. In Icelandic. Unpublished report OS83.
- Stefánsson, V., Kristmannsdóttir, H. and Gíslason, G. (1977). *Holubrjéf nr. 7*. Orkustofnun.
- Steingrímsson, B., Friðleifsson, G.Ó. and Guðmundsson, G. (1982). Krafla, hola KJ-20. Borun í 212,5 m og steyping 13 3/8" fóðringar. Temporary report. In Icelandic. Orkustofnun OS-82115/JHD-31.
- Steingrímsson, B., Richter, B., Björnsson, G. and Birgisson, K. (1999). *Krafla. Hola KJ-33. 1. áfangi: Borun fyrir öryggisfóðringu í 321 m dýpi*. In Icelandic. Orkustofnun, OS-99053
- Sæmundsson, K. (1991). Geology of Krafla volcanic system. In: Garðarsson, A. and Einarsson Á (Eds.), *Náttúra Myávotns. Hið íslenska náttúrufræðifélag*, Reykjavík, 25–95.
- Sæmundsson, K. (2008). Krafla. Geological map, 1:25.000. Landsvirkjun and ÍSOR.

- Sæmundsson, K., Arnórsson, S., Ragnars, K., Kristmannsdóttir, H. and Gíslason, G. (1975). *Krafla. Skýrsla um niðurstöður rannsóknarborana 1974*. Orkustofnun OSJHD-7506.
- Tulinius, H. and Sigurðsson, Ó. (1988). *Jarðhitasvæðið við Hvíthóla. Hermireikningar og vinnsluspá*. Orkustofnun, OS-88007/JHD-03.
- Tulinius, H. and Sigurðsson, Ó. (1991). *Krafla. Þrívíð hermun fyrir vinnslusvæðið á Hvíthólum*. Orkustofnun OS-91046/JHD-07.
- Violay, M., Gibert, B., Mainprice, D., Evans, B., Dautria, J.-M., Azais, P. and Pezard P. (2012). An experimental study of the brittle-ductile transition of basalt at oceanic crust pressure and temperature conditions. *Journal of Geophysical Research*, 117, B03213.
- Wadati, K. (1928). Shallow and deep earthquakes. *Geophysical Magazine*, 1, 162–202.
- Walck, M.C. (1988). Three-dimensional  $V_p/V_s$  variations for the Coso Region, California. *Journal of Geophysical Research*, 93 (B3), 2047–2052.
- Weisenberger, T. and Selbekk, R.S. (2009). Multi-stage zeolite facies mineralization in the Hvalfjörður area, Iceland. *International Journal of Earth Sciences*, 98, 985–999.
- Zierenberg, R.A., Schiffman, P., Barfod, G.H., Leshner, C.E., Marks, N.E., Lowenstern, J.B., Mortensen, A.K., Pope, E.C., Fridleifsson, G.Ó. and Elders, W.A. (2013). Composition and origin of rhyolite melt intersected by drilling in the Krafla geothermal field, Iceland. *Contributions to Mineralogy and Petrology*, 165, 327–347.
- Pórarinsson, S.B., Guðmundsson, Á., Ásmundsson, R.K., Sigvaldason, H., Egilson, Þ. and Jónsson, P.H. (2006a). *Krafla - hola KV-01 : 1. áfangi : borun fyrir 13 3/8" öryggisfóðringu frá 86,5 m í 290 m dýpi*. In Icelandic. Iceland GeoSurvey, ÍSOR-2006/039.
- Pórarinsson, S.B., Guðmundsson, Á., Gautason, B., Ásmundsson, R.K., Thordarson, S. and Egilson, Þ. (2006b). *Krafla - hola KV-01. 3. áfangi: Borun vinnsluhluta frá 804 m í 2894 m dýpi*. In Icelandic. Iceland GeoSurvey, ÍSOR-2006/041.

# Appendix

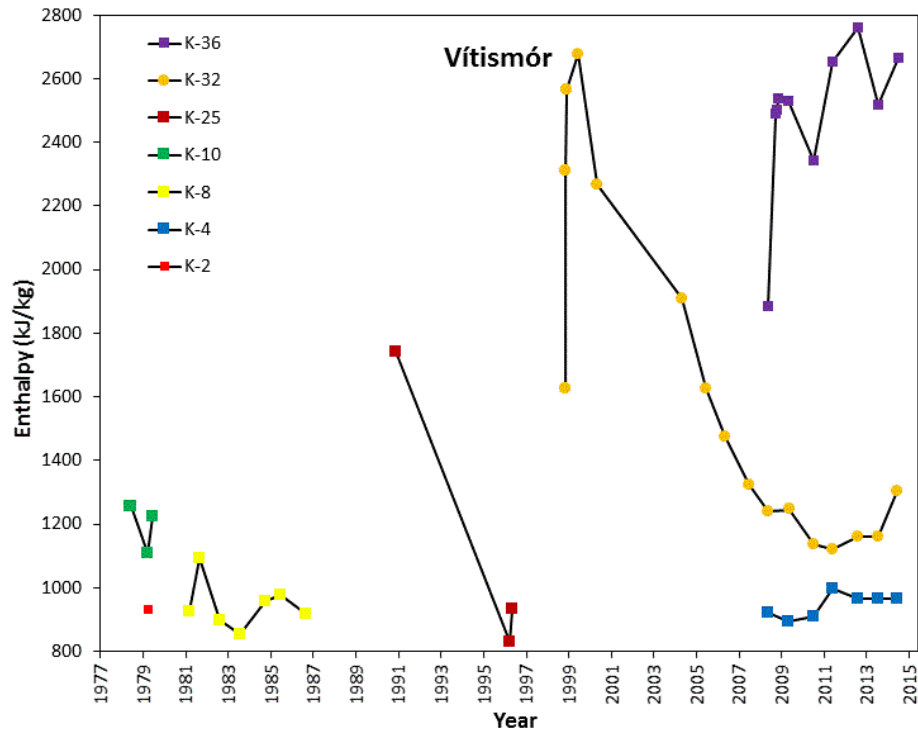


Figure A 1. Enthalpy vs. time of each well included in this study in Vítismór.

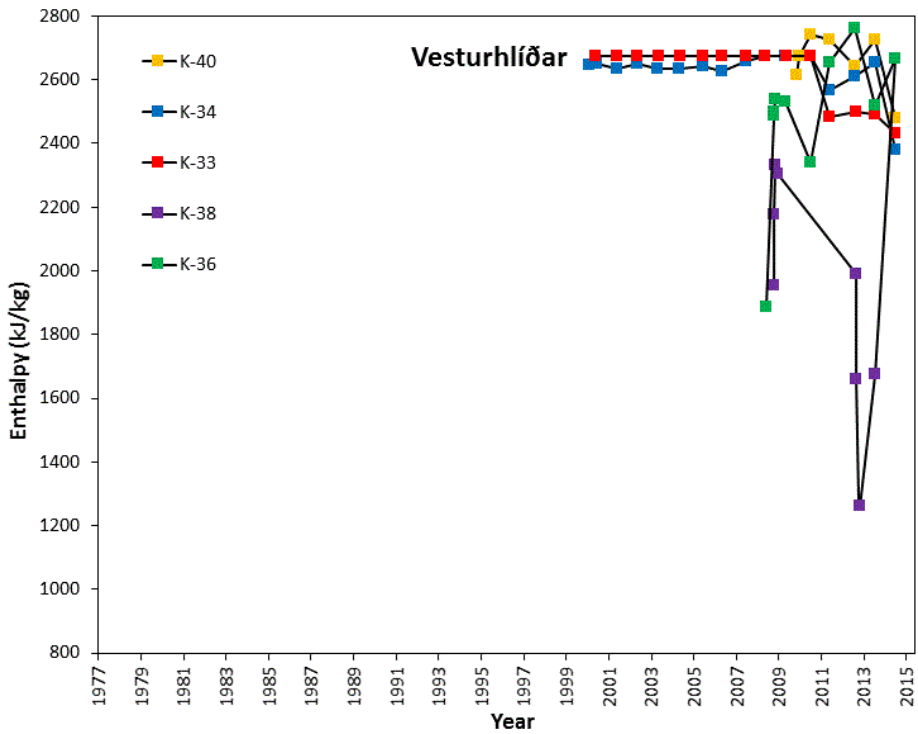
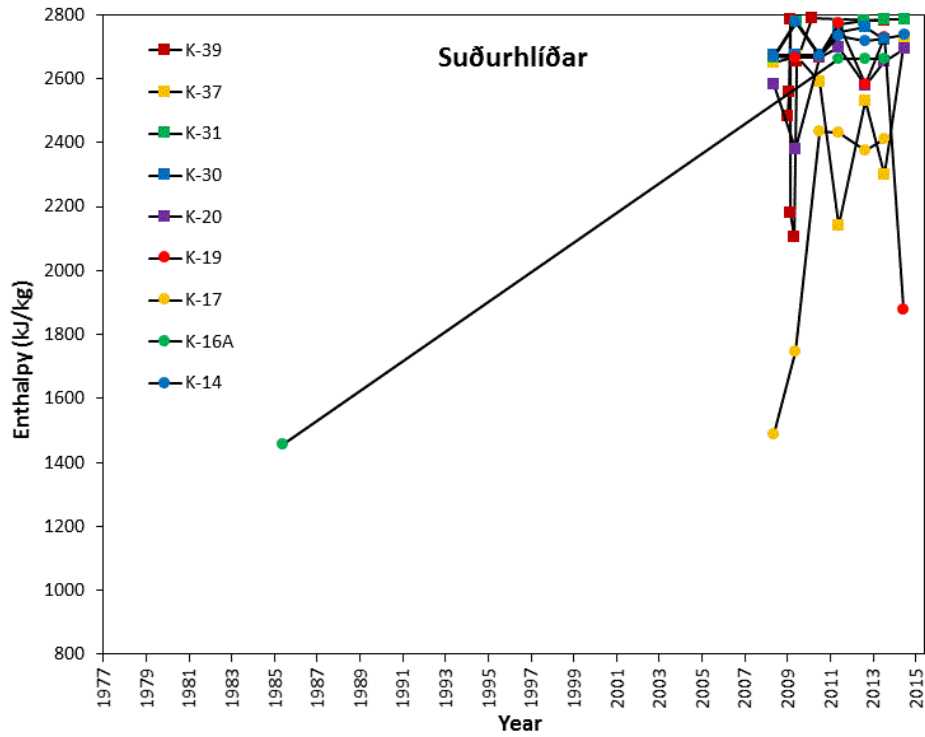
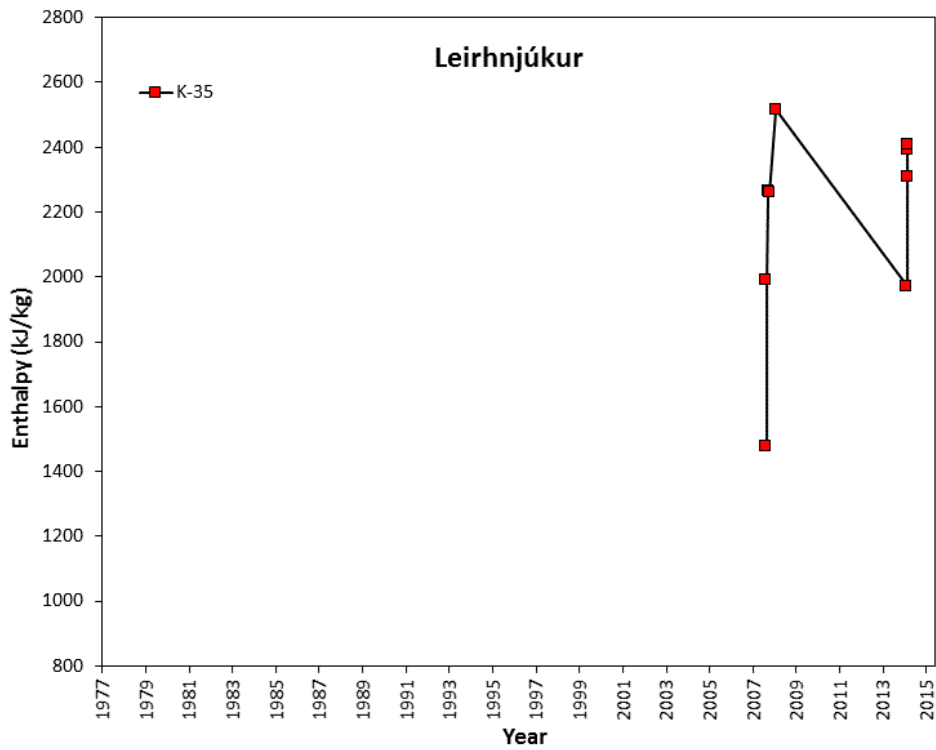


Figure A 2. Enthalpy vs. time of each well included in this study in Vesturhlíðar.



**Figure A 3.** Enthalpy vs. time of each well included in this study in Suðurhlíðar.



**Figure A 4.** Enthalpy vs. time of each well included in this study in Leirhnjúkur.

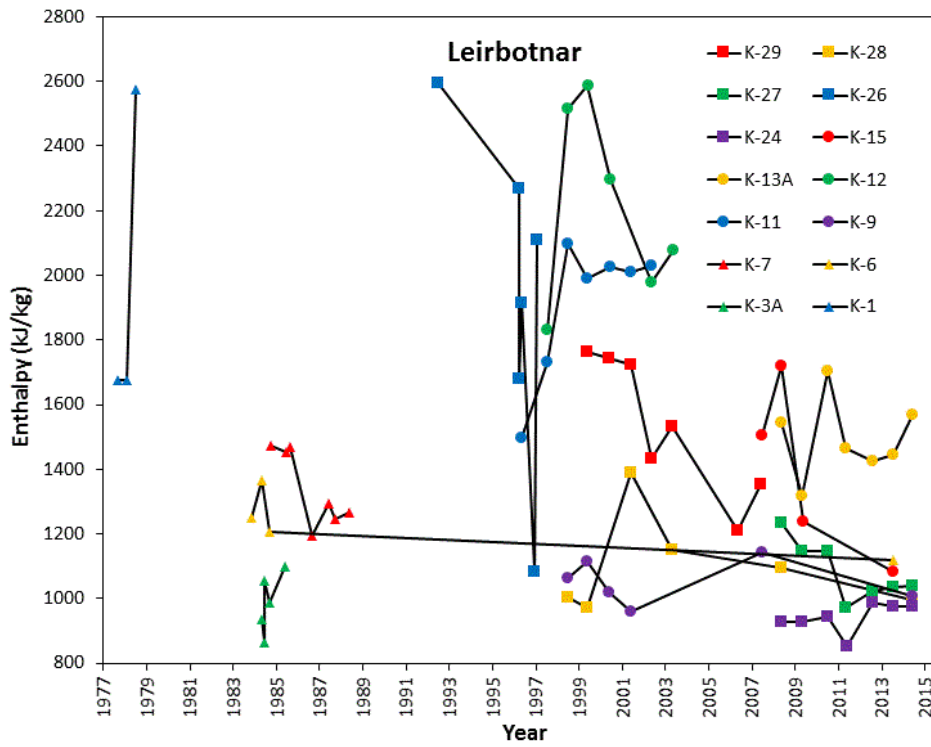


Figure A 5. Enthalpy vs. time of each well included in this study in Leirbotnar.

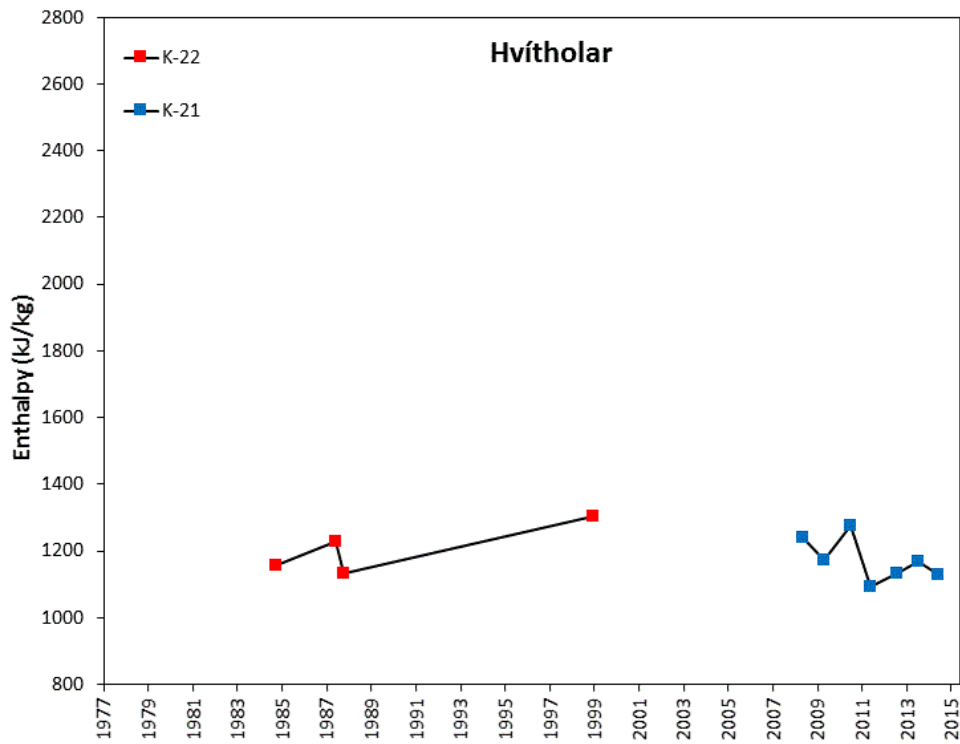


Figure A 6. Enthalpy vs. time of each well included in this study in Hvitholar.

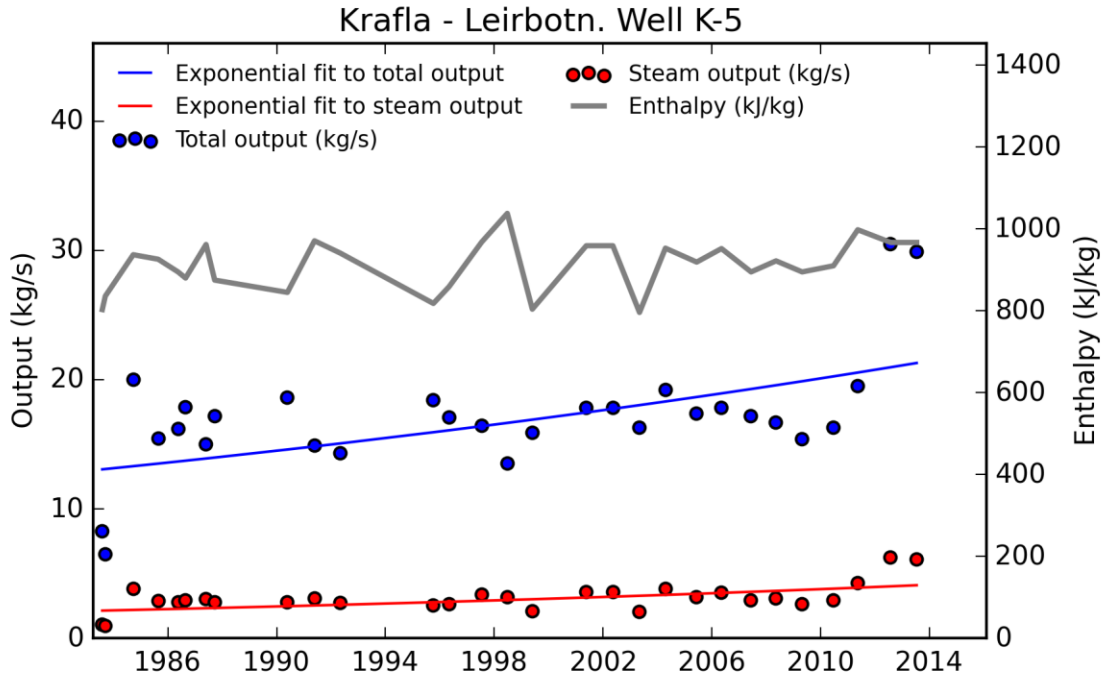


Figure A 7. Enthalpy, output and steam decay in well K-5.

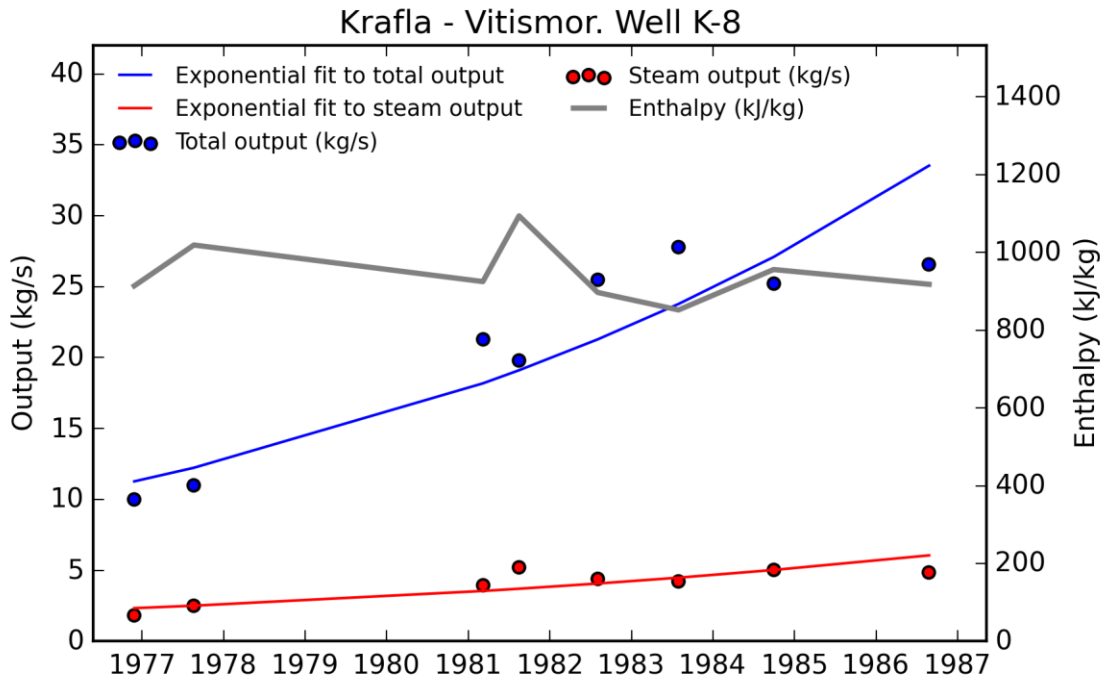


Figure A 8. Enthalpy, output and steam decay in well K-8.

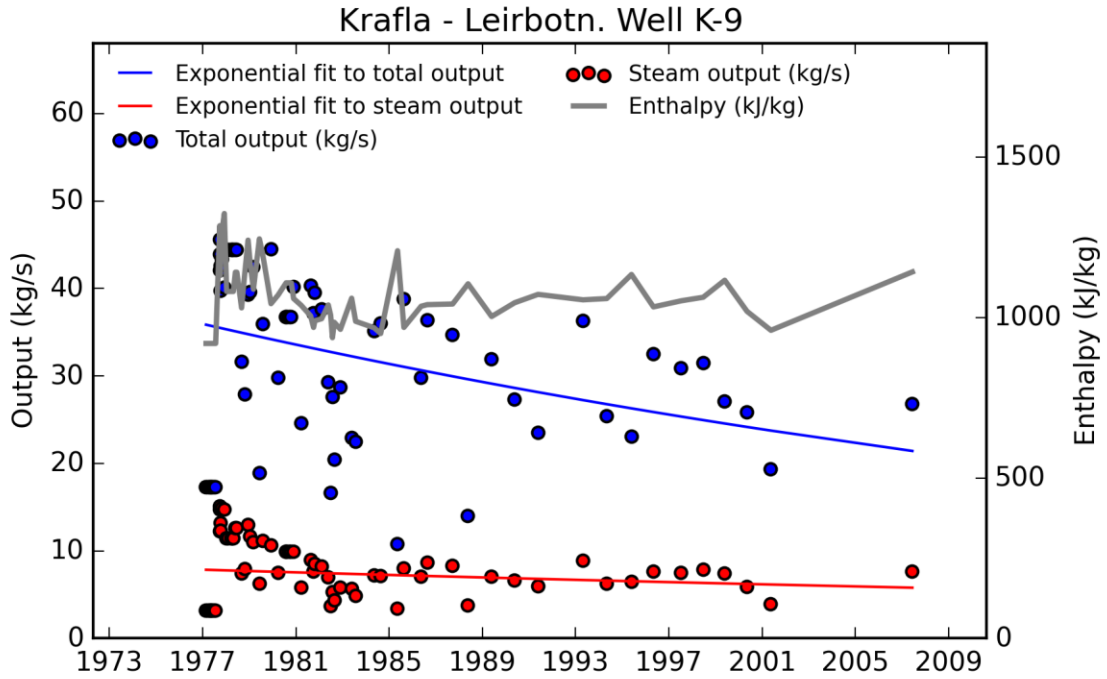


Figure A 9. Enthalpy, output and steam decay in well K-9.

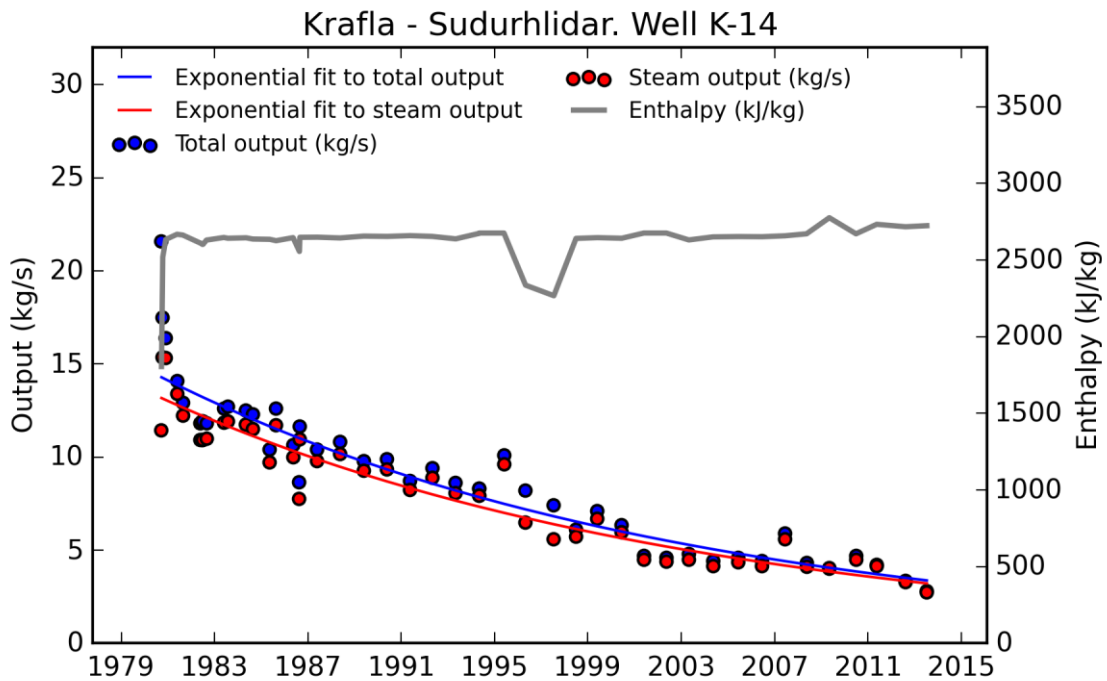


Figure A 10. Enthalpy, output and steam decay in well K-14.

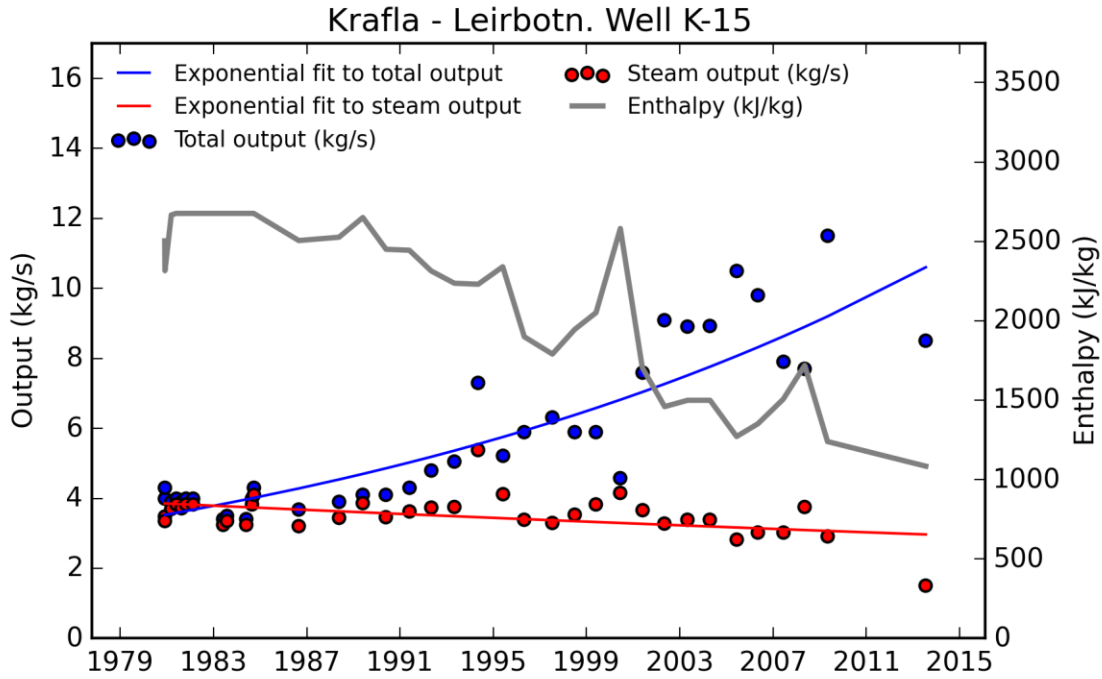


Figure A 11. Enthalpy, output and steam decay in well K-15.

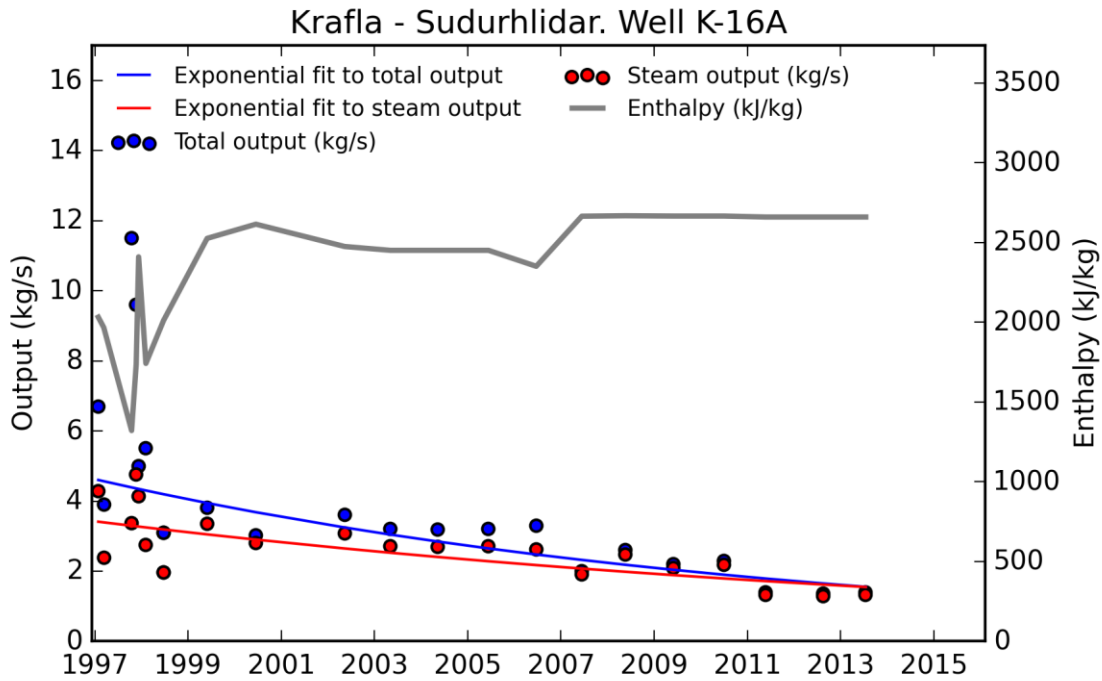


Figure A 12. Enthalpy, output and steam decay in well K-16A.

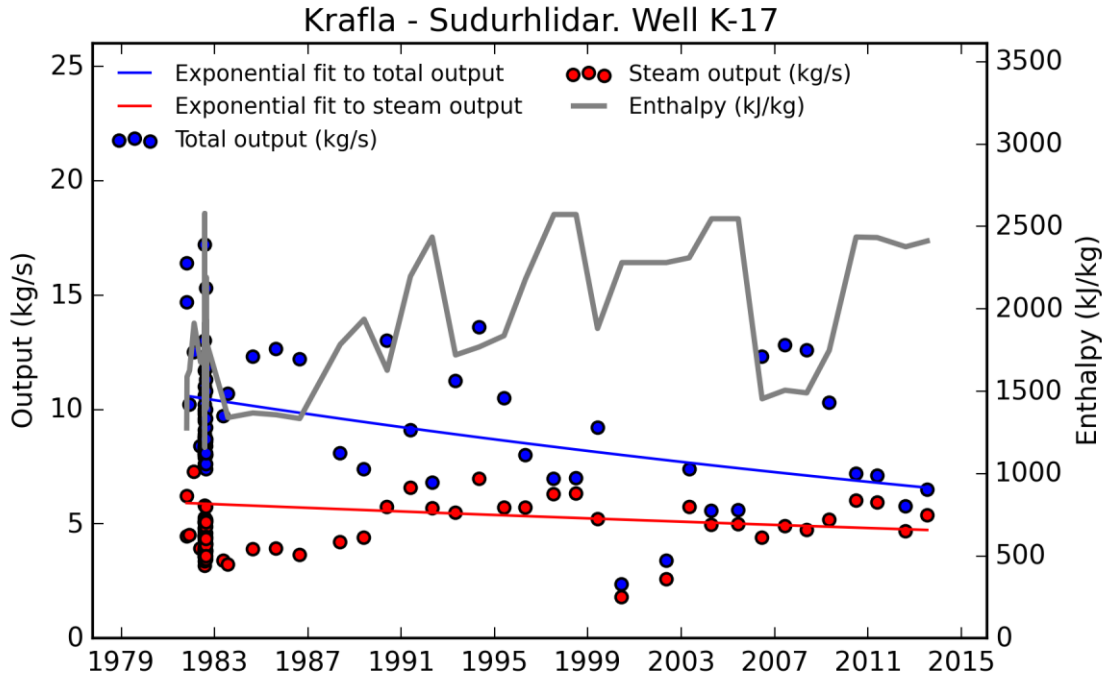


Figure A 13. Enthalpy, output and steam decay in well K-17.

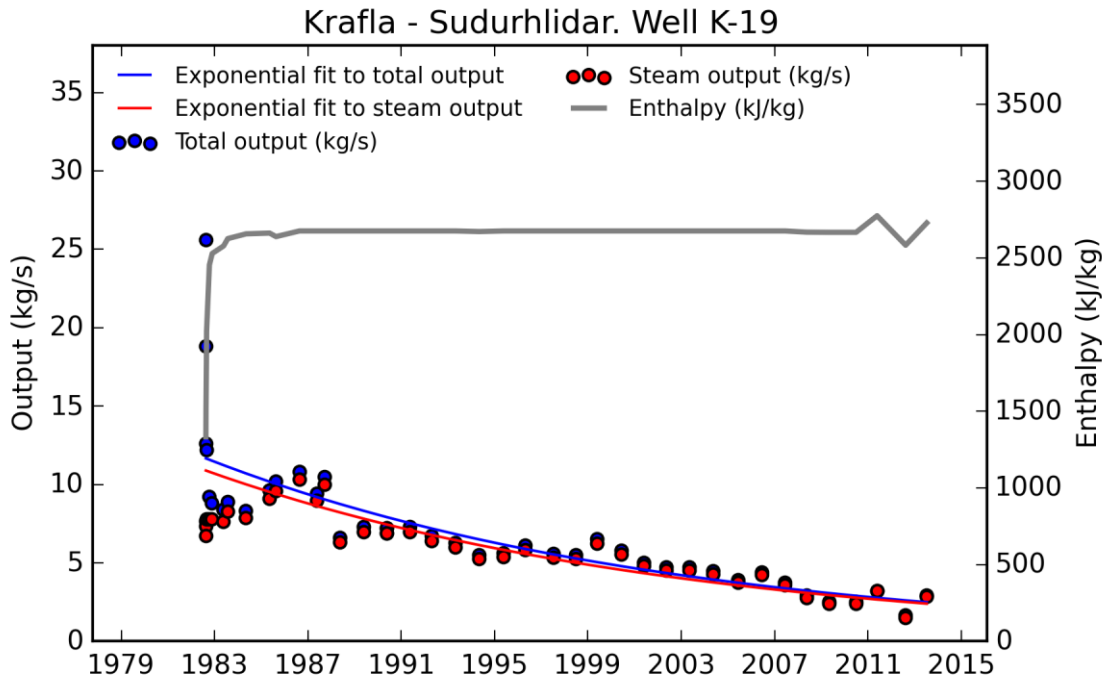


Figure A 14. Enthalpy, output and steam decay in well K-19.

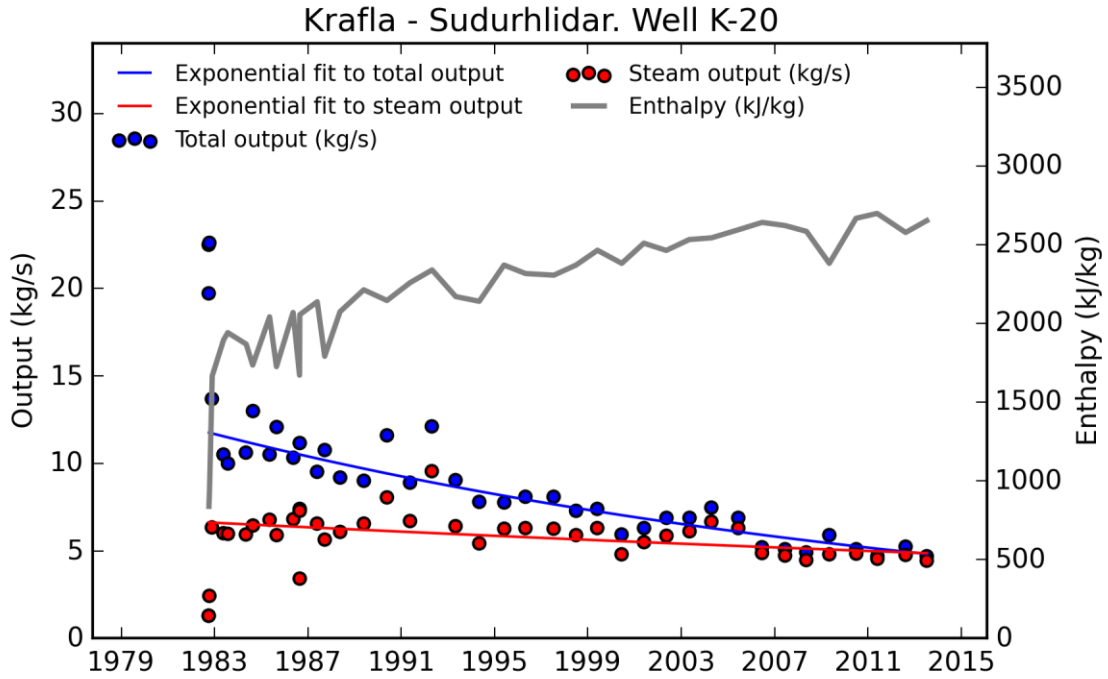


Figure A 15. Enthalpy, output and steam decay in well K-10.

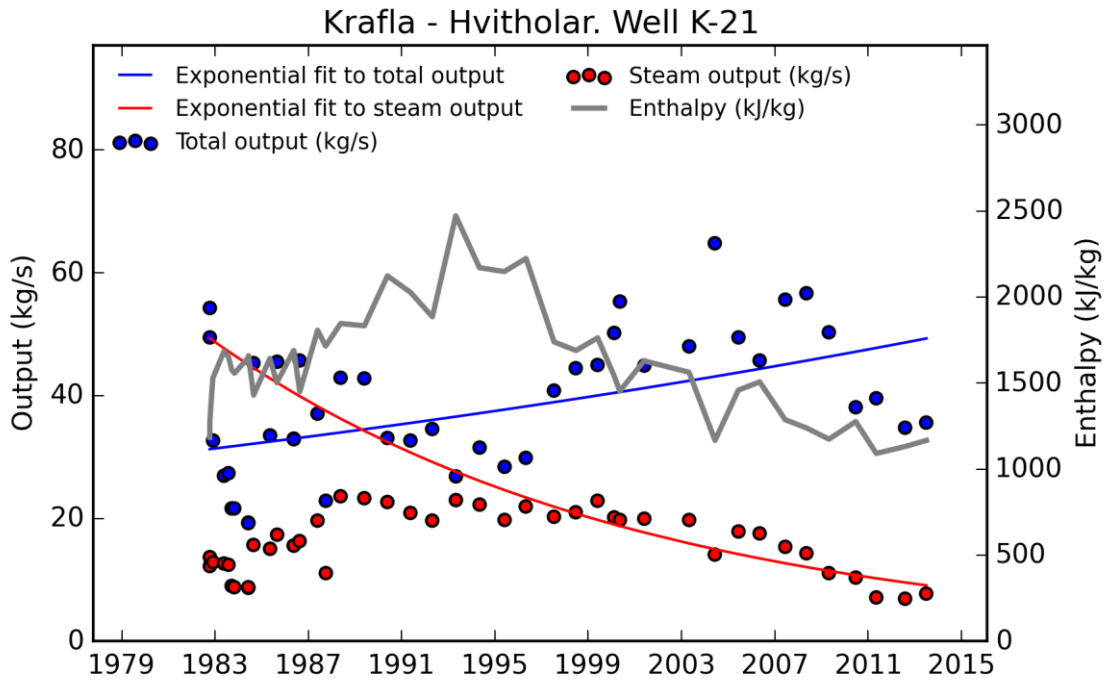


Figure A 16. Enthalpy, output and steam decay in well K-21.

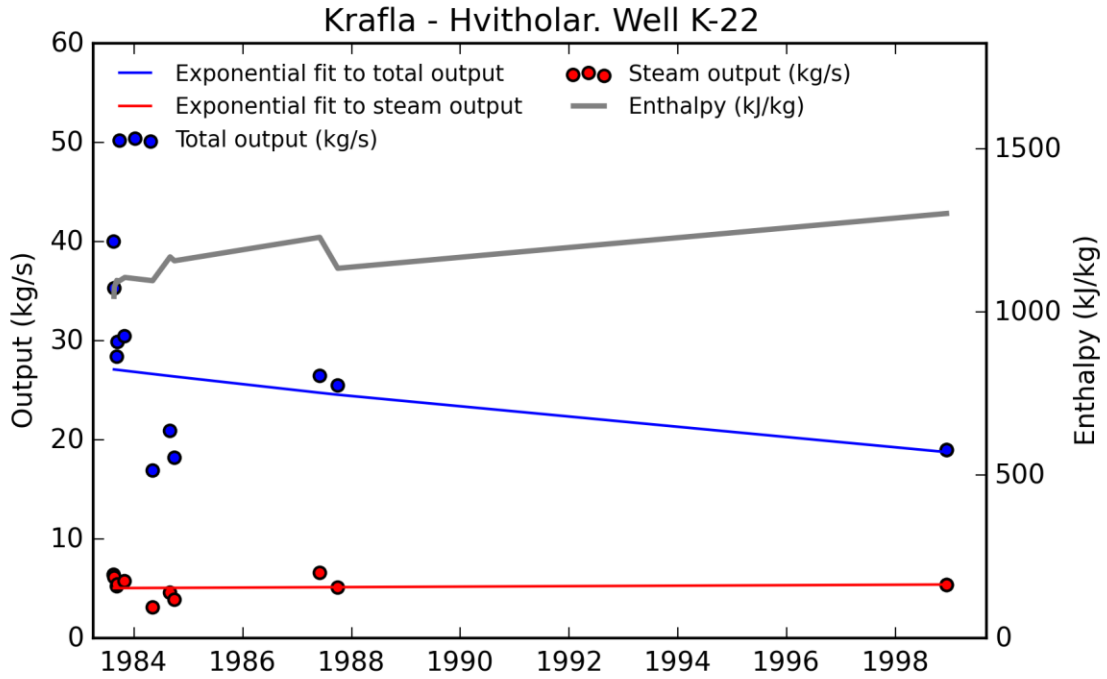


Figure A 17. Enthalpy, output and steam decay in well K-22.

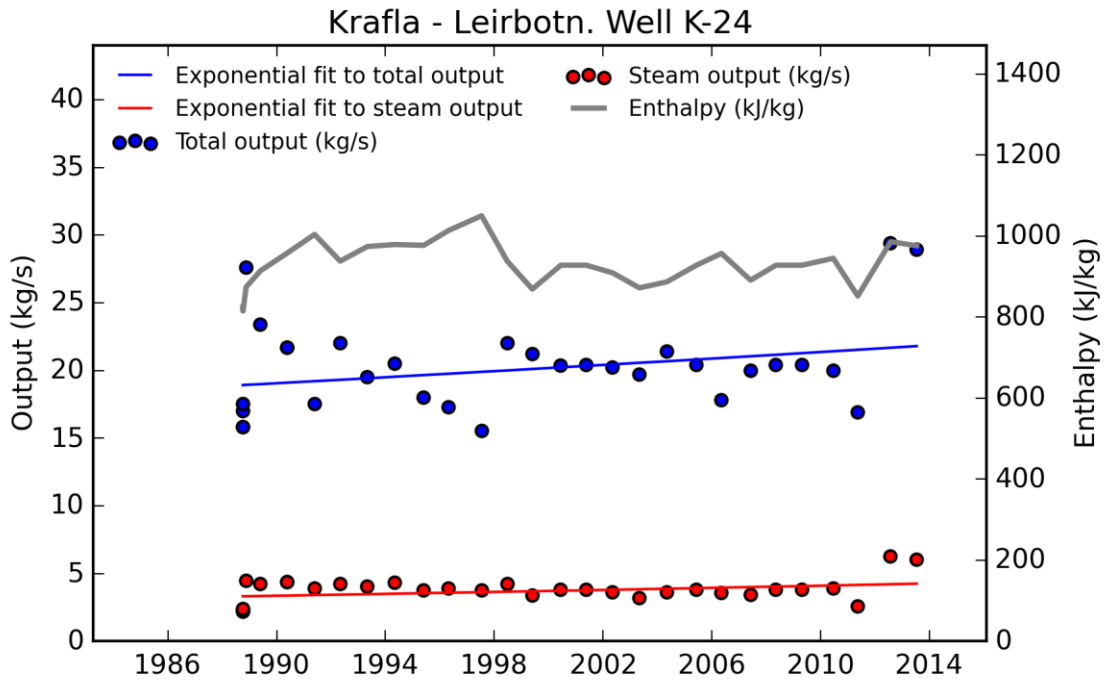


Figure A 18. Enthalpy, output and steam decay in well K-24.

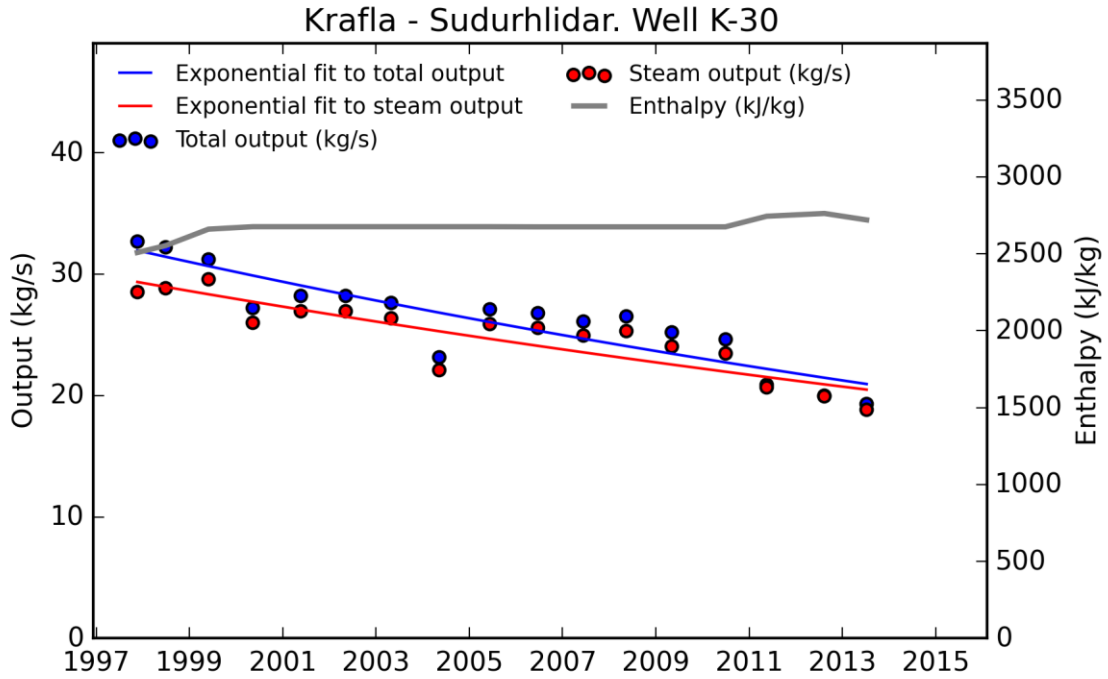


Figure A 19. Enthalpy, output and steam decay in well K-30.

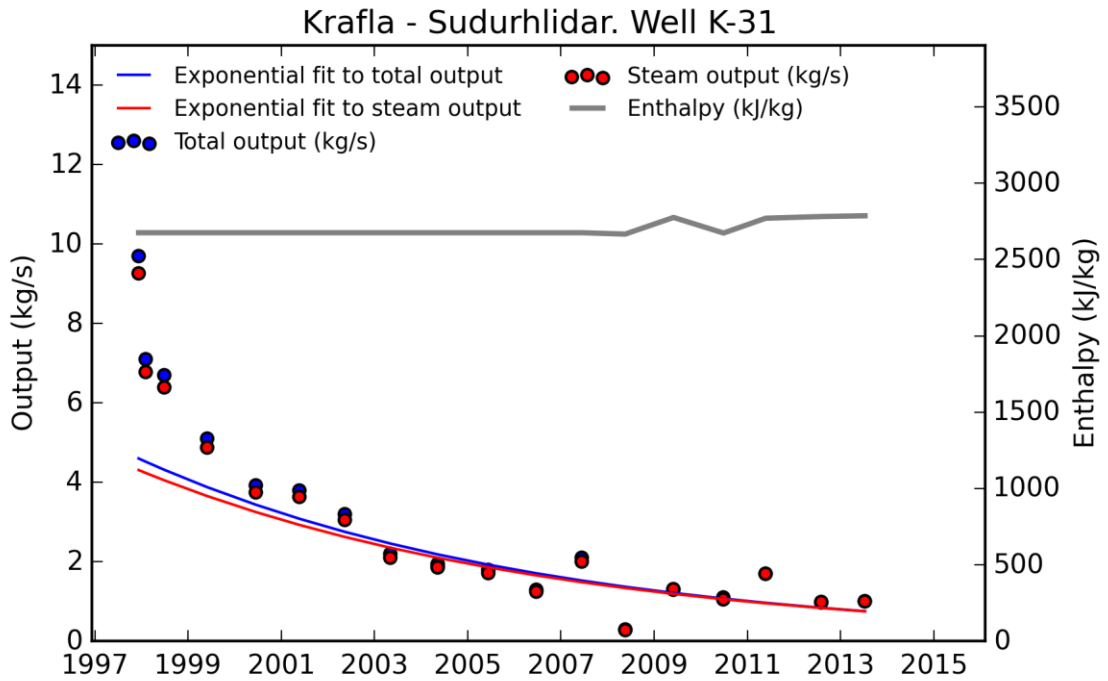


Figure A 20. Enthalpy, output and steam decay in well K-31.

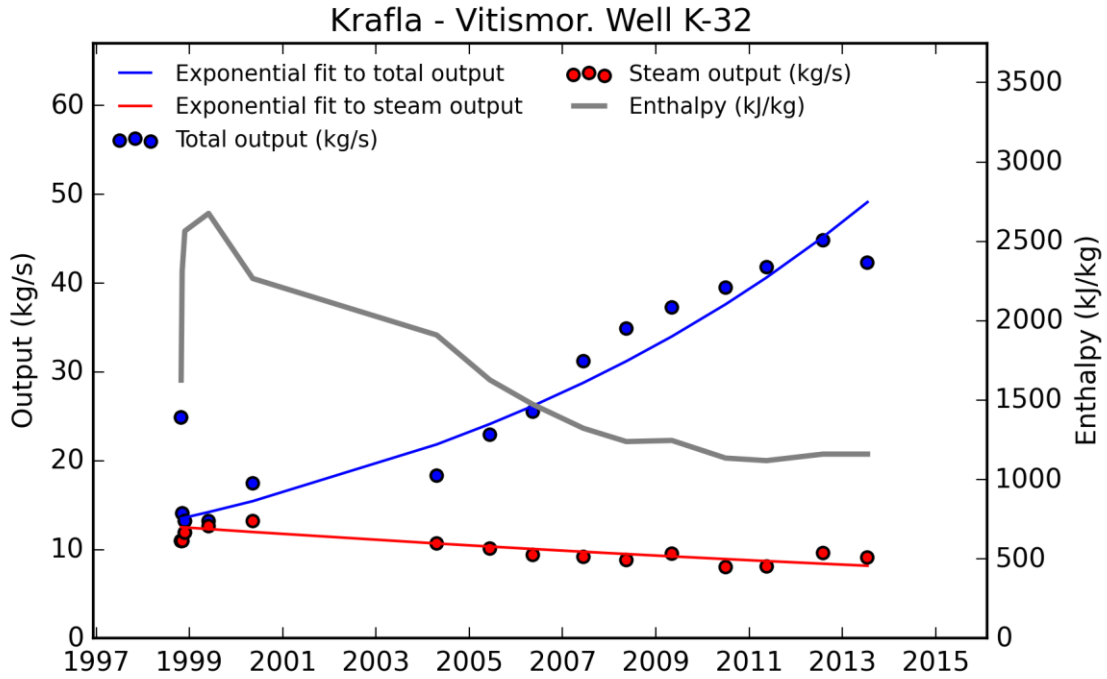


Figure A 21. Enthalpy, output and steam decay in well K-32.

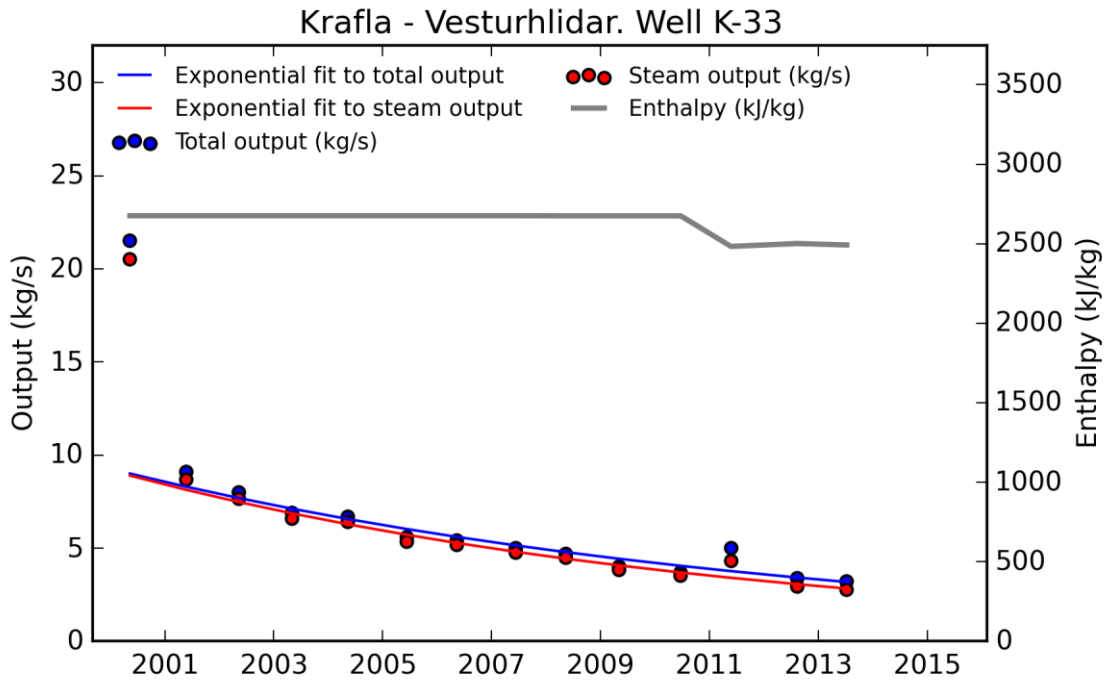


Figure A 22. Enthalpy, output and steam decay in well K-33.

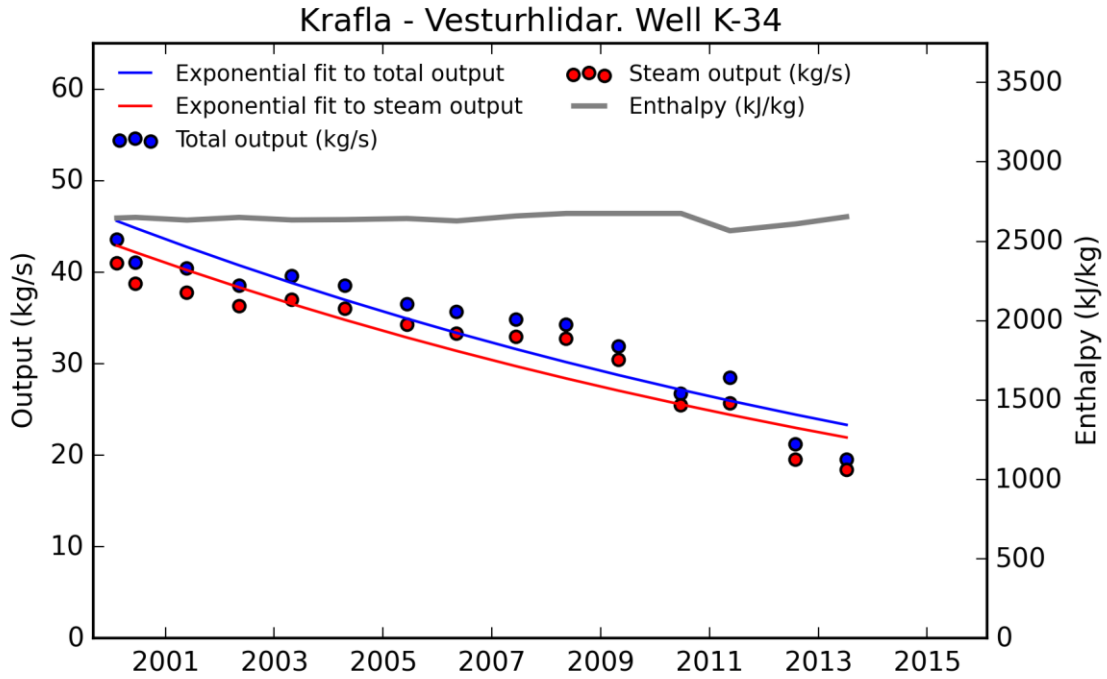


Figure A 23. Enthalpy, output and steam decay in well K-34.

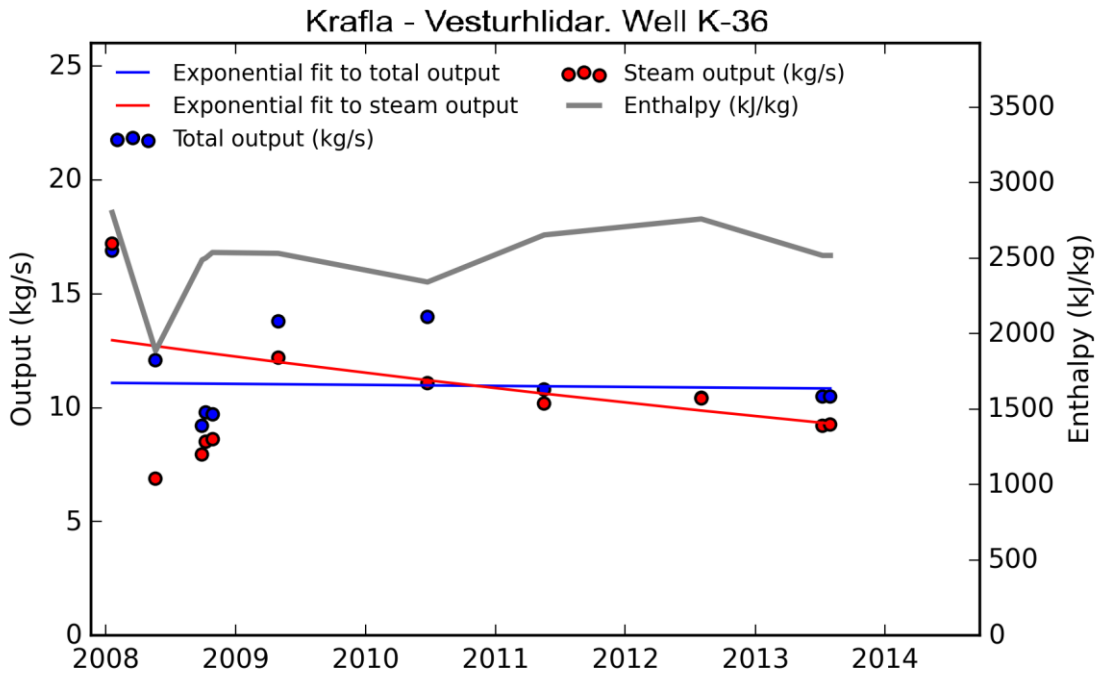


Figure A 24. Enthalpy, output and steam decay in well K-36.

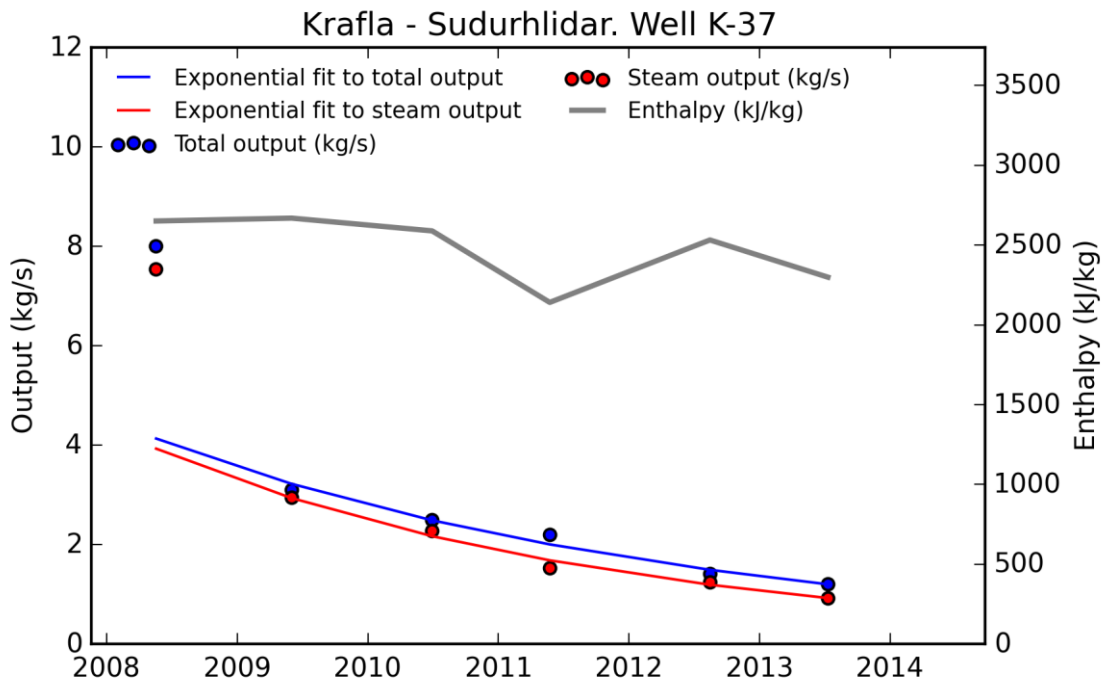


Figure A 25. Enthalpy, output and steam decay in well K-37.

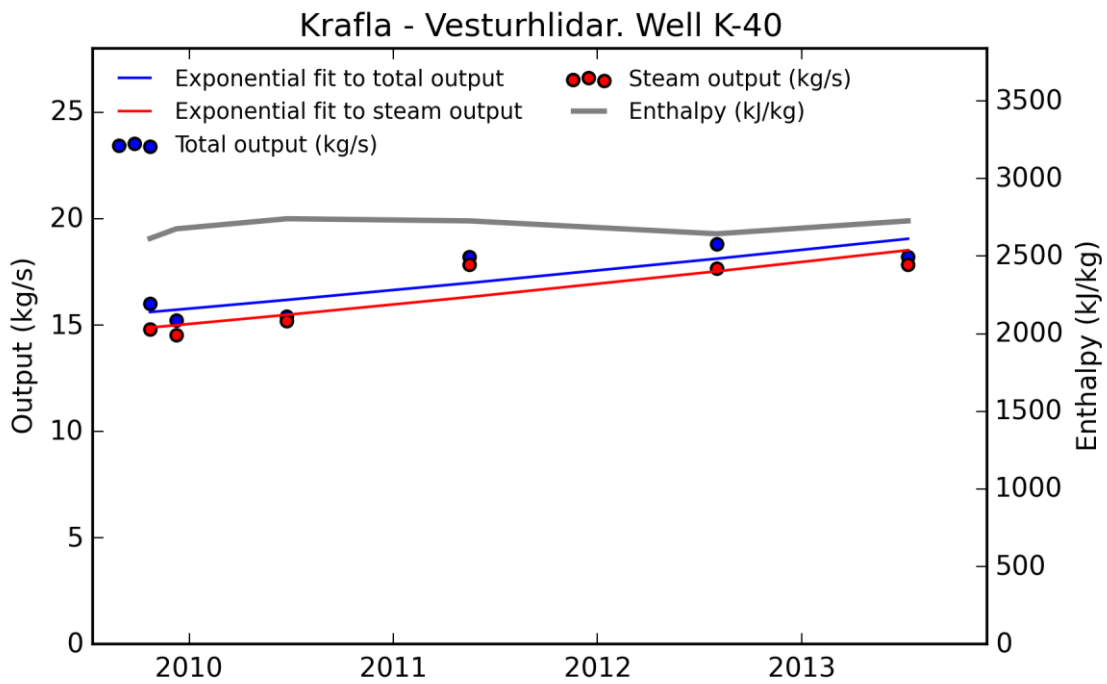


Figure A 26. Enthalpy, output and steam decay in well K-40.



Landsvirkjun

Háaleitisbraut 68  
103 Reykjavík  
landsvirkjun.is

landsvirkjun@lv.is  
Sími: 515 90 00

